

DISSERTATION

FUNCTIONAL ANALYSIS OF SMYD2 AND SMYD3 LYSINE
METHYLTRANSFERASES

Submitted by

Melissa Ashley Edwards

Graduate Degree Program in Cell and Molecular Biology

In partial fulfillment of the requirements

For the Degree of Doctor of Philosophy

Colorado State University

Fort Collins, Colorado

Fall 2016

Doctoral Committee:

Advisor: Mark Brown

Haley Tucker
Kathryn Partin
Matthew Hickey

Copyright by Melissa Ashley Edwards 2016

All Rights Reserved

ABSTRACT

FUNCTIONAL ANALYSIS OF SMYD2 AND SMYD3 LYSINE METHYLTRANSFERASES

The proteins SMYD2 and SMYD3 are two of five members of a unique family of lysine methyltransferases defined by a catalytic SET domain that is split into two segments by a MYND protein interaction domain, followed by a cysteine-rich post-SET domain. The SMYD family members have been shown to be essential for cellular development, cell cycle progression, and when dysregulated, tumorigenesis. SMYD1 has been widely studied as a pivotal component of cardiac and skeletal muscle development. Although their three dimensional structures have been solved, less is known about functional consequences of SMYD2 and SMYD3. Aberrant overexpression of SMYDs 2 and 3 have been implicated in numerous malignancies, and both have been studied as potential therapeutic targets.

The overriding aim of our research is to obtain a more thorough understanding of SMYD2 and SMYD3 function. In Chapters 1 and 2, we outline essential background regarding the SMYD family and the methods used in our studies. In Chapter 3, we address the consequences of the interaction of SMYD3 with the nuclear chaperone, HSP90. Each have been independently implicated as proto-oncogenes in several human malignancies. Loss of SMYD3-HSP90 interaction leads to SMYD3 mislocalization within the nucleus, thereby severing its association with chromatin. This results in reduction of SMYD3-mediated cell proliferation and, consequentially, impairment of SMYD3's

oncogenic activity. We suggest a novel approach for blocking HSP90-driven malignancy which may have reduced toxicity over current HSP90 inhibitors.

In Chapter 4, we turn our attention to SMYD2 and its putative role in hematopoietic carcinogenesis. In order to study the effect of SMYD2 in tumor initiation, we employed transforming oncogenes to study the consequences of SMYD2 loss in three hematopoietic models: B-Acute Lymphocytic Leukemia (B-ALL), Chronic Myeloid Leukemia (CML), and Mixed Lineage Leukemia (MLL). Loss of SMYD2 in CML and MLL, but not in B-ALL, models led to cell cycle block following by widespread apoptosis and cell death. Tumorigenicity, as assessed *in vitro* by colony formation and *in vivo* by NOD/SCID transformation, was dependent upon SMYD2. Gene expression analyses indicated that, as previously determined in multiple studies, impairment included reduction in the level of the p53 tumor suppressor. Collectively, these studies establish SMYD2 as a putative proto-oncogene in CML and MLL.

In Chapter 5, we report our efforts to extend the above findings to the living organism. SMYD2 was conditionally deleted via *cre/Lox* methodology from the germline of C57BL.6 mice exclusively in hematopoietic progenitors. SMYD2-deficient mice were born healthy and achieved normal lifespans. However, consistent with our findings of Chapter 4, we observed significant blocks in the progression of fetal and bone marrow hematopoietic stem cells to both B lymphocyte and myeloid lineages. While these blocks led to an overall reduction of mature peripheral B cells, SMYD2-deficient mice maintained a relatively normal immune response. These studies further support a model in which SMYD2 is required for normal hematopoiesis transformation.

ACKNOWLEDGEMENTS

The ensuing document is the culmination of my work, my research and my efforts but *my* body of work was only achieved by the graciousness and genius of those around me. I would first like to acknowledge my very supportive family, I love and thank you all. Especially my mother, Norma Scrutchen and my twin sister, Melony. Through three degrees and ten years of college these two women have rallied around me with their strength, prayers, funds, and unconditional love without me ever having to ask. They have been my personal champions, shoulders to cry upon and providers of laughter and levity whenever needed, they in turn, are my personal heroines.

To my University of Texas at Austin collaborators and now family, I sincerely offer thanks from the bottom of my heart. I was embraced, guided, helped and taught by the wisest and most generous scientist including June Harriss, Chhaya Das, Dr. Joseph Dekker, Maya Ghosh, Dr. Melissa Powpowski, Dr. Wei Deng, Dr. Edward Satterwhite, Catherine Rhee, and Dr. Gregory Ippolito. Thank you for helping me to grow as a research scientist and as a person. Your influence has been immeasurable and I am forever grateful.

There were several other collaborators whose work, experiments and brainstorming were instrumental in this task. I would like to specially acknowledge Dr. Mohammed Firas Sadiyah at The University of Cambridge, Dr. Kenneth Foreman at Coferon Inc., and Dr. Markus.Muschen at The University of California, San Francisco.

In regards to Dr. Haley Tucker, leader of the University of Texas at Austin lab and my co-advisor, there are hardly words to describe her impact on me. The sincerest thanks

are in order for the use of her lab, reagents, scientists, networks and for her personal investment in my academic success. Her talents and brilliance are nothing short of awe-inspiring. I am forever indebted to her and appreciative of all she has done for me.

My sincerest gratitude to the entire Williams family, not only did they help me in my time of need, but they have always been a source of encouragement and love during this massive undertaking.

Thank you to the team of young scientist I had the privilege of spending a summer with; Ryan Rykhus, Krista Henderson, Megan Hamrick, Lisbel Torres, and Michaela Stone. Each of you were instrumental in the creation and assembly of several figures which allowed me to better convey my work. Thank you for your efforts and for sharing your talents.

My committee has been amazing; Dr. Kathryn Partin and Dr. Matt Hickey are practiced in the art of mentoring. They have been incredibly patient with me and I am grateful for their help and participation while on this journey.

I must thank my advisor, Dr. Mark Brown. When I met him I told him I did not think I was smart enough to obtain my PhD, in that moment he both scolded me for the comment and assured me that I surely was. I am thankful to Dr. Brown for always believing in me; for seeing my potential when it was not obvious to me and for fostering its growth. I am thankful for his well-placed optimism, leadership and trust. He is my personal role model, a mentor, a friend, and after five years of putting up with me, family.

Lastly, thank you Leroy Mack. You reminded me that this degree and dissertation should not be seen as a challenge to burden me, but rather a challenge that I earned the right to succeed in. For your words of wisdom, truly in the time of need, thank you.

DEDICATION

This document is dedicated to my family & friends who lit up my life in my darkest moments and to my advisors who believed in me even when I did not.

TABLE OF CONTENTS

ABSTRACT	ii
ACKNOWLEDGEMENTS	iv
DEDICATION	vi
LIST OF TABLES	x
LIST OF FIGURES	xi
1. CHAPTER 1 – BACKGROUND	1
A. SMYD FAMILY PROTEINS TARGET HISTONES AS A SUBSTRATE ..1	
i. HISTONE MODIFIERS AND TYPES OF MODIFICATIONS	2
B. INTRODUCTION TO THE SMYD FAMILY PROTEINS	3
i. CHAPERONE PROTEINS	6
ii. CHAPERONE PROTEINS ENHANCE THE METHYLATION ABILITY OF THE SMYDS	8
C. THE HEMATOPOIETIC PATHWAY	9
i. GENE EXPRESSION OF SMYD2 IN HEMATOPOIESIS	11
ii. SMYD2 OVEREXPRESSION IN LEUKEMIA	11
D. INVESTIGATIONAL AIMS	13
i. AIM 1: INVESTIGATE THE STRUCTURAL AND FUNCTIONAL RELATIONSHIP BETWEEN HSP90 AND SMYD3 BOTH IN VITRO AND IN VIVO	13
ii. AIM 2: TO DETERMINE THE IMPACT SMYD2 HAS IN SPECIFIC MODELS OF HEMATOPOIETIC MALIGNANCIES	13
iii. AIM 3: TO UNDERSTAND THE ROLE OF SMYD2 IN HEMATOPOIETIC DEVELOPMENT	14
2. CHAPTER 2 – MATERIALS & METHODS	
A. MUTAGENESIS, CLONING, AND BACTERIAL EXPRESSION	24
B. BACTERIAL PROTEIN PURIFICATION	24
C. HISTONE METHYL TRANSFERASE ASSAYS	25
D. HSP90 AND GST-MEEVD BINDING ASSAYS	25
E. MAMMALIAN CELL TRANSFECTION AND WESTERN BLOTTING	26
F. PROLIFERATION ASSAYS	27
G. CELL FRACTIONATION	28
H. IN VITRO HEMATOPOIETIC TUMOR MODELS	28
I. COLONY FORMING UNIT ASSAY	29
J. IN VIVO TUMORS	29
K. CELL VIABILITY	30
L. CLONING OF THE SMYD2 CONDITIONAL TARGETING CONSTRUCT	30

M. CRE-MEDIATED DELETIONS.....	32
N. MOUSE TAIL DNA EXTRACTION.....	32
O. GENOTYPING	32
P. FLOW CYTOMETRY	33
Q. CELL CULTURE	34
R. TIMED MATINGS.....	34
S. FETAL LIVERS	35
T. MACS CELL SEPARATION.....	35
U. B CELL PROLIFERATION ASSAY	35
V. WESTEN BLOTS.....	36
W. MOUSE IMMUNIZATIONS	36
X. ELISA.....	37
3. CHAPTER 3 – C-TERMINAL DOMAIN OF SMYD3 SERVES AS A UNIQUE HSP90-REGULATED MOTIF IN ONCOGENESIS	40
A. RESULTS.....	42
i. THE CTD IS REQUIRED FOR BASAL HMTASE ACTIVITY OF SMYD3.....	42
ii. STRUCTURAL CONSERVATION OF SMYD3 CTD AND THE HSP90-BINDING TETRATRIPEPTIDE (TPR) REPEATS WITHIN FKBP52	43
iii. TPR-LIKE RESIDUES OF SMYD3 CTD ARE ESSENTIAL IN VITRO FOR HSP90 BINDING AND CATALYTIC ENHANCEMENT.....	45
iv. TPR-LIKE RESIDUES OF SMYD3 CTD ARE ESSENTIAL IN VIVO FOR NUCLEAR LOCALIZATION, HSP90 INTERACTION AND SUB-NUCLEAR SEQUESTRATION INTO CHROMATIN ...	46
v. CTD-HSP90 INTERACTION IS REQUIRED FOR MAXIMAL SMYD3 STIMULATION OF CELL PROLIFERATION	48
B. CONCLUSIONS.....	59
4. CHAPTER 4 – THE IMPACT OF SMYD2 IN SPECIFIC MODELS OF HEMATOPOIETIC MALIGNANCIES	63
A. RESULTS.....	68
B. CONCLUSIONS.....	72
5. CHAPTER 5 – THE FUNCTION OF SMYD2 IN HEMATOPOIESIS.....	73
A. RESULTS.....	74
i. LOSS OF SMYD2 REDUCES HSCS	74
ii. SMYD2 INCREASES THE POPULATION OF MYELOID AND LYMPHOID PROGENITORS	75
iii. SMYD2 DEFICIENT CMPS AND CLPS CONTRIBUTE TO INCREASED PDCS.....	75
iv. MX1 CKO REDUCES T CELL POPULATIONS	76
v. B CELL PROGENITORS MOST AFFECTED BY SMYD2 CKO...77	77

B. CONCLUSIONS.....	88
6. CHAPTER 6 – DISCUSSION	89
REFERENCES.....	95
LIST OF ABBREVIATIONS.....	104

LIST OF TABLES

TABLE 1: Types of amino acid modifications	16
TABLE 2: Hematopoietic population definitions	38
TABLE 3: Epitopes and conjugated antibodies	39
TABLE 4: Summary of HSP90 binding and histone methyltransferase activities following truncation or point mutation of residues within the SMYD3 CTD.....	53

LIST OF FIGURES

FIGURE 1: Human nucleosome	15
FIGURE 2: Histone tails and covalent modifications	16
FIGURE 3: Sites & functions of histone methylation	17
FIGURE 4: SMYD Family homology	18
FIGURE 5: SMYDs in murine development	19
FIGURE 6: Hematopoiesis	20
FIGURE 7: Migration of HSC during embryonic murine development.....	21
FIGURE 8: Lymphocytes.....	22
FIGURE 9: Expression of SMYD2 throughout hematopoiesis.....	23
FIGURE 10: Structure of SMYD3.....	49
FIGURE 11: The SMYD3 CTD is required for binding and enhanced histone methyltransferase activity (HMTase) by HSP90	50
FIGURE 12: Alignment of the carboxyl terminal (CTD) domain from SMYD3 orthologs and paralogs.....	51
FIGURE 13: Residues within a degenerate tetratricopeptide (TPR)-like domain within the SMYD3 CTD mediate HSP90 interaction	52
FIGURE 14: Enhancement of basal HMTase activity of SMYD3 requires binding of HSP90 to conserved residues within a TPR-like region of the CTD	54
FIGURE 15: TPR residues of SMYD3 CTD are essential <i>in vivo</i> for nuclear localization, HSP90 interaction and sub-nuclear sequestration into chromatin	56
FIGURE 16: CTD-HSP90 interaction is required for maximal SMYD3 stimulation of cell proliferation rate	58
FIGURE 17: The Philadelphia Chromosome.....	66
FIGURE 18: Points of transformation in various hematopoietic derived Malignancies	67
FIGURE 19: Cell death in HSC tumor models when SMYD2 is deleted	68
FIGURE 20: The effect of SMYD2 deletion on cell cycle protein expression and phases in tumor models	69
FIGURE 21: Colony formation reduced in SMYD2 depleted tumor models	70
FIGURE 22: CML-like SMYD2 deleted cells did not result in tumors	71
FIGURE 23: SMYD deficiency results in loss of HSC population.....	79
FIGURE 24: Depletion of SMYD2 affects early lineage progenitors.....	81
FIGURE 25: Increase of plasmacytoid dendritic cells (pDCs) in SMYD2 deletion...82	82
FIGURE 26: Thymic T-cell populations only impacted in adult mx1 cKO	83
FIGURE 27: Linear development of B cells.....	84
FIGURE 28: Bone marrow B cell development in the absence of SMYD2.....	85
FIGURE 29: The effect of SMYD2 deletion in mature splenic B cell populations86	86
FIGURE 30: Antibody response in B cell specific (mb1) deletion of SMYD2.....	87
FIGURE 31: In vitro deletion of SMYD2 with mx1 cre	94

CHAPTER 1 – BACKGROUND

A. SMYD FAMILY PROTEINS TARGET HISTONES AS A SUBSTRATE

Histones play a key role in compacting meters' worth of DNA into microscopic cells. The higher orders of DNA compaction are achieved by wrapping it around an octamer of core histones into a structural unit known as a nucleosome [1-3]. Each nucleosome consists of 146 base pairs of DNA wrapped 1.7 times around a histone octamer and separated by a linker region of approximately 50 base pairs of DNA (**Figure 1**) [4]. Each primary histone core is composed of eight histone subunits; two each of H2A, H2B, H3 and H4. This nucleoprotein, while highly conserved in eukaryotes, is able to form a complex not through shared sequence homology but instead through the shared domain structures of the histone components which allow interactions that ultimately form the histone octamer [5, 6]. Two heterodimers each of H3-H4 and H2A-H2B interact with each other via helical folding that not only assemble the positively charged histone core but also establish the wrapping and tight binding of the negatively charged phosphodiester backbone of DNA [4].

In addition to the folded octamer core, histones also possess unstructured N- and C-terminal tail regions which account for approximately 28% of the histone proteins' mass [7]. The tails consist of strings of amino acid residues, mostly of a basic nature. Specific residues can be modified in certain manners as indicated in (**Figure 2**). Lysine, for instance, can be subjected to many different post-translational covalent modifications, however each is mutually exclusive to another (**Table 1**). It has been proposed that a histone code exists where site specific histone tail modifications are associated with a

particular action such as transcriptional activation or repression (**Figure 3**) [8-12]. This in turn provides an extension of variations in gene expression without changing the DNA sequence. Therefore, histones prove to be crucial to the study of altered gene expression and epigenetics, factors in the development of cancer cells and various disease states [9, 13-16].

Histone modifiers and types of modifications

Histone modifiers, often referred to as “writers” such as methyltransferases and acetyltransferases, alter the nucleosomal conformation and therefore access to DNA for transcriptional activity [17]. Histone acetyltransferases or HATs, first discovered in *Tetrahymena thermophile*, catalytically add acetyl groups to the N-terminus of lysine (K) residues on histone tails utilizing acetyl CoA as an acetyl donor [18]. The activity of these primarily nuclear bound enzymes, is thought to neutralize a portion of the positively charged histone core changing its affinity to the negative DNA [19]. Due to this DNA disassociation and therefore access to it and the presence of HATs in some transcription complexes, HATs are generally associated with transcriptional activation [20]. Gene expression however is highly regulated and additional histone modifiers known as “erasers” can remove or reverse the action of a “writer”. Histone deacetylases (HDACs) catalytically remove the acetyl group from lysine residue thereby restoring its strong interaction with DNA, allowing for chromatin compaction and thereby repressing transcriptional activity [21, 22]

Unlike HATs, histone lysine methyltransferases (HKMTs) are “writers” that are commonly associated with transcriptional repression or gene silencing [23]. HKMTs utilize

an abundant co-substrate, S-adenosyl methionine (SAM), as a methyl donor to catalyze the addition of one, monomethylation (me), two, dimethylation (me²) or three, trimethylation (me³) methyl groups to a specific histone lysine residue [24]. Methylation while often pigeonholed as a gene silencing mark, can result in either activation or repression [25]. Certain modifications have been linked to specific outcomes, such as methylation of histone 3 lysine 4 (H3-K4) and H3-K36 correlating to gene transcription while methylation of H3-K9 and H3-K7 are correlated to gene silencing [26, 27]. Unlike the readily interchanging states of lysine acetylation via HATs and HDACs, most methylation marks are thought to have a more permanent nature. However, there is some turnover of histone methylation thought to be attributed to a demethylase. Lysine specific demethylase 1 (LSD1) is thought to function as an “eraser” of methyl marks at specific residues such as H3-K4 and act as a transcriptional co-repressor [28]. This dynamic process of “writing” and “erasing” marks on histone tail residues provides another layer of governing gene expression and therefore contribute to the processes of cellular development and disease states [10, 14, 29].

B. INTRODUCTION TO THE SMYD FAMILY PROTEINS

There are three classes of methyltransferases (MTs). The first, called suppressor of variegation, enhancer of zeste and trithorax, (SET) domain lysine methyltransferases were originally discovered in *Drosophila melanogaster* [30]. The second are non-SET-domain lysine methyltransferases and the third class are arginine methyltransferases [27, 31]. Regardless of their classification, these “writers” orchestrate the dynamic access and restriction of DNA for both replication and transcriptional machinery [32].

The unique structural assembly of the catalytically active SET-domain containing proteins is shared throughout eukaryotes and different from that of other enzymes that utilize the co-factor S-adenosyl-L-methionine (SAM) as a methyl donor [31]. The distinct configuration of the SAM binding pocket in SET methyltransferases causes SAM to bend when bound to the active site. SET-containing proteins are crucial in various biological processes including developmental regulation, signaling cascades, association to chaperone proteins, and proteasomal degradation to name a few [33, 34].

Due to several variations within HKMTs, including the conformation of SAM when bound, the three classes have been further categorized into subfamilies based both on sequence and structural homology as well as the specific methylation of lysine residues [5, 11, 35]. Within the SET-domain containing HKMTs is a family of proteins known as the SMYDs named as such due to possessing both a **SET** and **MYND** (Myeloid-Nervy-DEAF1) domain [36]. While the SET domain is the active region, catalyzing the addition of a methyl group to lysine residues, the MYND domain contains a zinc finger binding motif and is known for its role in protein-protein interaction particularly to proline rich regions [37, 38]. The novelty of the SMYDs continues, as in their amino acid sequence the MYND domain lies within the catalytically active SET domain, dividing the domain into pre- and posterior-SET regions (**Figure 4**) [39-41]. However, upon proper protein folding, the separated SET domains fold together to produce the active site and push the MYND domain outward [42]. There are five total SMYD proteins, (SMYDs 1-5) each highly conserved among eukaryotes and with high sequence and structural homology to each other. SMYDs 1-3 have been the most studied and have demonstrated important roles in proper development during embryogenesis (**Figure 5**) [34].

The SMYDs as HKMTs are “writers”, placing methylation marks at site specific lysine residues that allow for the recruitment of chromatin remodeling complexes to alter the access to DNA. SMYDs 1-3 have a shared methylation target at H3-K4, a site associated with transcriptional activity [39, 43]. However, each SMYD has additional unique targets that impact other processes and while they are most well-known for methylating their histone methylation targets, they have also proven to methylate non-histone proteins as well.

For instance, SMYD1 has also shown to bind to certain HDACs, resulting in targeted repression. SMYD1 also binds to a muscle-specific transcription factor skNAC (nascent polypeptide-associated complex alpha) that is required for myofibril organization [43, 44]. It has been identified as a muscle specific regulator and is essential not only to proper heart development, but also in maintaining the size of the adult heart [45, 46]. A global knockout of SMYD1 in mice led to embryonic lethality by day E9.5 as ventricular development was severely impaired [37, 47]. In addition to cardiomyocyte and myofibril development, SMYD1 also plays a vital role in cardiac diseases [45, 48].

In regard to SMYD3, in addition to its activating mark of H3-K4, in the last few years it has recently shown to also methylate H4-K5, a residue only thought to be acetylated before [49]. SMYD3 is mostly associated with triggering proliferation of cancer cells when overexpressed, most notably in such diseases as breast cancer [50], hepatocellular carcinoma [51], and cervical carcinoma [52] to name a few [53]. It is thought that cellular growth is promoted due to its interactions with RNA polymerase II, the chaperone protein HSP90 and HELZ, an RNA helicase [53, 54]. SMYD3 overexpression allows it to bind to a specific DNA motif within the promoter region of

genes such as the homeobox protein Nkx2.8 [55]. SMYD3 methylates its target H3-K4 resulting in transcriptional activation that outcompetes repressive markers for Nkx2.8. The Nkx2.8 gene has been associated with cell proliferation, tumor progression and metastasis [56-58]. Knock down of SMYD3 by inhibitors or RNAi has shown to inhibit cell growth and tumor invasion [59-62].

Recently, SMYD2 has become an interest for therapeutic cancer targets as well [63]. In addition to its histone lysine methylations at H3-K4 and H3-K36me2, SMYD2 is thought to potentially regulate the functions of tumor suppressors through its methylation of p53 at K370 and retinoblastoma (RB1) at K860 [38, 64-67]. The monomethylation on both of these well-known guardians of the genome result in the repression of their functions which are to mediate apoptosis and halt cell cycle progression, respectively [65, 68]. Developmentally, unlike SMYD1, SMYD2 is dispensable for proper heart formation however it may play a more prominent role in other cellular pathways [69, 70].

Chaperone Proteins

Molecular chaperones are highly conserved through all branches of life, including the HSP90 family [71-75]. Necessary for viability of eukaryotes, HSP90 is not required in bacteria [76, 77]. It functions as a homodimer that associates with co-chaperones to catalyze the maturation and/or activation of over 100 substrate proteins that are known to be involved in cell regulatory pathways [75]. These 'client proteins' include protein kinases, nuclear hormone receptors, transcription factors, and an array of other essential proteins [78]. While much is known regarding the ATPase-driven conformational cycling

of HSP90, the precise physical effects imparted by this chaperone that serve to activate its substrates are still poorly understood [75].

The most detailed understanding of the effects of HSP90 on its client proteins has been gleaned from its involvement with the maturation of steroid hormone receptors. Steroid receptors must be maintained in a labile conformation that allows them to be rapidly activated in the presence of their cognate ligand [79]. Hop1/Sti1, by virtue of its ability to bind Hsp70 and HSP90 in tandem, facilitates the transfer of Hsp70-bound receptors to the open form of HSP90. The HSP90 system then induces subtle alterations in the conformation of the bound steroid receptor that enhances its affinity toward its respective ligand [80]. Protein kinases comprise the most prevalent group of HSP90 client proteins. The co-chaperone Cdc37 is known to interact both with protein kinases and HSP90, thereby delivering client kinases to the HSP90 chaperone complex [81, 82]. Bound to HSP90, the client kinases are stabilized and remain in a receptive but inactive state while awaiting appropriate signals [81]. The details of the HSP90-protein kinase chaperone system are still under investigation. The essential roles that HSP90 fulfills in the normal physiology of healthy cells are even more critical for the viability of transformed cells. HSP90 is absolutely essential for the stabilization/maturation of nuclear hormone receptors, transcription factors, and protein kinases that are commonly misregulated during tumorigenesis [78]. It also serves to buffer the effects of transformation by preventing the aggregation of aberrantly expressed proteins, whose accumulation would otherwise result in toxic stress signals and progression to programmed cell death [83]. As many of the client proteins of HSP90 are linked to growth signal pathways, HSP90 is viewed as key player in the subversion of normal cells toward unrestrained proliferation.

Amplifying the corruptive potential of HSP90 is its ability to facilitate the evolution of neoplastic clones by stabilizing many of the mutated proteins that are often associated with cancerous lesions, including p53, bcr-Abl, and v-Src [74, 83]. For this reason, HSP90 is thought to be especially crucial in the development of tumors that result from the inactivation of DNA repair pathways, in which there are extensive pools of diversely mutated proteins.

Chaperone Proteins Enhance the Methylation Ability of the SMYDs

As a chaperone protein, HSP90 interacts with a vast variety of client proteins. The unique properties of any one protein in addition to the effect of HSP90s interaction, can cause a number of biological responses. Some such responses include transcriptional regulation, proteasomal degradation, apoptosis, cellular localization, chromatin remodeling, etc [84]. One way in which HSP90 is able to anchor itself to and interact with certain proteins is via TPR (tetratricopeptide repeat) domains on the protein that consist of tandem repeats of amino acids. The carboxyl terminal domain of the SMYD proteins highly resemble that of TRP domains and are thought to be able to anchor HSP90 as a result. The physical interaction has been shown to enhance the SMYD methyltransferase activity [63, 85]. Methylation assays indicated increased methylation of H3-K4 as well as other targets including chromatin remodeling complexes. [86, 87]. The interaction between HSP90 and the SMYDs is important as their aberrant expression and activity is linked to many cancers. Understanding the structure and means of interactions will better aid in therapeutic targeting the SMYD proteins.

C. THE HEMATOPOIETIC PATHWAY

Hematopoiesis is the process that gives rise to all of the immune system cells and blood components via a pluripotent hematopoietic stem cell (HSC) that can differentiate into various committed progenitors each able to further differentiate into one or more functional cell types (**Figure 6**). Many of the functional mature cells are short lived and non-dividing. Therefore, they must have a means of constant renewal. The HSC resides in the adult bone marrow. However, in vertebrates HSC precursors known as hemangioblasts are first detected during embryonic development in the yolk sac [88]. Early in development a small population of HSC precursors are responsible for generating red blood cells (RBCs) as the heart continues to develop. These RBCs play a vital role in oxygenating embryonic tissue as it rapidly expands and increases. Later in embryogenesis, the HSCs migrate to another resident area known as the aorta, gonad, mesonephros (AGM) before their colonization in the fetal liver. While there, there is a clonal expansion of HSCs in the fetal liver and eventually the fetal thymus and spleen are also populated (**Figure 7**). Upon birth and thereafter, most of the HSCs can be found and or harvested from the adult bone marrow [88].

While the initial migration and journey of the HSC precursor and HSC alone is an intricate one, that complexity continues as the single stem cell can proceed to differentiate down several pathways producing over thirty different progenitors, intermediate, and functional cells of at least ten different lineages of cells that will circulate in the blood. HSCs, therefore, exist either in a state extreme proliferation or of quiescence [89]. Their cell cycles are highly regulated by the various complexes such as cyclin dependent kinases, cytokine signaling, and relative gene expression. For instance, p21 supports

HSC quiescence. The bone marrow itself also provides a textural stromal environment filtering and relaying this information to the HSC population [90-93].

However, once undergoing cell cycling, hematopoietic stem cells rapidly proliferate and differentiate in response to stromal signals, which include but are not limited to *fms*-like tyrosine kinase 3 (Flt3), interleukin 3 (IL-3), and IL-7 [94, 95]. Immediately downstream of the HSC are two early non-lineage progenitors known as the multipotent progenitor (MPP) and the lymphoid primed multipotent progenitor (LMPP) cells. LMPPs are predominantly an immediate precursor to the common lymphoid progenitors (CLPs) which is a decisive branching point in the pathway of differentiation towards lymphocytes while the other pathway branches towards the myeloid derived cells (Figure 6). The lymphocyte pathway contains three distinct cell types (Natural Killer cells, T cells and B cells) that go through a variety of immature and intermediate stages and have a rather linear pathway of development (**Figure 8**).

Unlike the simplicity of lymphocyte lineages, the myeloid pathways are many and complex. The MPP can give rise to a common myeloid progenitor (CMP) in addition to several other committed cell precursors such as the megakaryocyte-erythroid progenitor (MEP) either of which lead to at least one other dedicated progenitor [96]. The crucial and functional cells downstream of the MEP are the megakaryocytes, erythrocytes and platelets. Developing from the CMP progenitors are the cells that function in the immune activities like pathogenesis and allergic responses and include macrophages, mast cells, dendritic cells and the basophil, eosinophil and neutrophil cells. While hematopoiesis is complex in its lineages, cells can be distinguished from one another based on their various expression of transmembrane receptors throughout development. This allows a

means to investigate precise cell populations and experiment with the impact upstream cells have on later functional cells.

Gene expression of SMYD2 in hematopoiesis

Microarray data representing the basal gene expression of SMYD2 throughout the hematopoietic pathway in mice was our initial starting point for deriving our hypotheses (**Figure 9**). In the HSC and in every lineage specific progenitor, there was a high expression of SMYD2. The highest expression of the early cells was in the precursors to the megakaryocyte-erythrocyte progenitor (pMEP), granulocyte-macrophage progenitor (gGMP), the common myeloid progenitor (sCMP) and in the granulocyte-macrophage-lymphoid progenitor (GMLP). More committed progenitors such as MEP and common lymphoid progenitor (CLP) only showed moderate expression. From the CLP where the T- and B- cells arise, there was a contrasting effect. In both the committed T- and B-cells SMYD2 expression was still present. However, it remained constant and even increasing again in T-cell development whereas it became nonexistent just past the initial precursor B cells.

SMYD2 overexpression in leukemia

Precursor-B cell acute lymphoblastic leukemia (Pre-B-ALL) is a white blood cell cancer that results in an excess of lymphoblasts; malignant, immature, malfunctioning white blood cells that rapidly develop in the bone marrow [97]. These lymphoblasts rapidly out-compete other healthy hematopoietic stem cell (HSC) derived cells such as B-lymphocytes, T-lymphocytes, erythrocytes, white blood cells and platelets. The lack of

functioning white blood cells and an overall imbalance of other HSC derived cells causes a host of systemic problems in an individual including frequent infections, muscular weakness, liver and spleen enlargement and shortness of breath. B-ALL is most commonly present in children ages one to ten and 80% of childhood leukemia is categorized as Pre-B- ALL. Due to its breadth of symptoms and effect on the immune system, ALL can be fatal if left untreated for several weeks.

Chronic myeloid leukemia (CML) is similar to ALL in that it is also a white blood cell cancer however it specifically affects cells downstream of the common myeloid progenitor which includes erythrocytes, macrophages and dendritic cells [97] whereas Pre-B-ALL affects cells downstream of the common lymphoid progenitor. In CML aberrant blood cells mature but do not function properly and slowly over time accumulate and eventually outnumber healthy cells. Because CML has a slow progression rate, damaging effects might not be observed for months or possibly even years. Therefore, this type of leukemia is most common in adults.

Both Pre-B-ALL and CML have demonstrated to generally be coupled with various chromosomal translocations that can be associated with either a favorable or poor prognosis. Pre-B-ALL cases have shown to have at least five different possible translocations including the non-favorable Philadelphia chromosome. CML however is mostly associated only with the Philadelphia chromosome translocation as it is present in 95% of cases.

Microarray data indicates that SMYD2 is upregulated in both ALL and CML [98, 99] and that SMYD2 overexpression predicts low survival in both adult and children with Pre-B-ALL [98-100]. SMYD2 has also been found to be overexpressed in some other

non-HSC derived cancers [101]. Based on these findings we sought to look for a potential developmental role of SMYD2 in the hematopoietic pathway from which all of these immunological cancers originate. Gene expression profiling of SMYD2 demonstrates that SMYD2 is highly expressed in HSCs and specifically throughout HSC lineage progenitor cells (Figure. 9) suggesting its potential for being a key factor in HSC derived malignancies including Pre-B-ALL. It has been thought that SMYD2 plays an integral part in DNA damage response due to its methylation targets including p53 and RB [64, 66] but in leukemia it may do so by directly affecting the HSC pathway.

D. INVESTIGATIONAL AIMS

Aim 1: Investigate the structural and functional relationship between HSP90 and SMYD3 both in vitro and in vivo

We have produced a series of SMYD3 CTD truncations and mutations and analyzed which residues were responsible for the binding and enhanced activity of HSP90. Methyltransferase assays were also used to determine which SMYD3 CTD regions were required to be able to methylate its substrates.

Aim 2: To determine the impact SMYD2 has in specific models of hematopoietic malignancies

We have generated *in vitro* models of three types of leukemias in which SMYD2 can be inducibly knocked out. ALL-like cells and CML-like cells were generated from SMYD2^{flox/flox} pre-B or common myeloid progenitor cells, respectively. These cells were then transduced with Bcr-Abl constructs and cre ER. MLL-like cells were generated from

SMYD2^{flox/flox} multipotent progenitor cells transduced with MLL-GAS7 constructs as well as cre ER. Control and SMYD2 deleted cells were analyzed for viability, cell cycle, colony formation and expression of tumor suppressor and related genes.

Aim 3: To understand the role of SMYD2 in hematopoietic development

We have constructed both an embryonic (vav cre) and adult inducible (mx1 cre) conditional knockout of SMYD2 at the hematopoietic stem cell. Early progenitors and stages throughout both the myeloid and the lymphoid lineage were analyzed for changes in the size of cell populations via flow cytometry. Mature B cells were later analyzed for functional production of an antibody repertoire in both control and conditional knockout (cKO) mice.

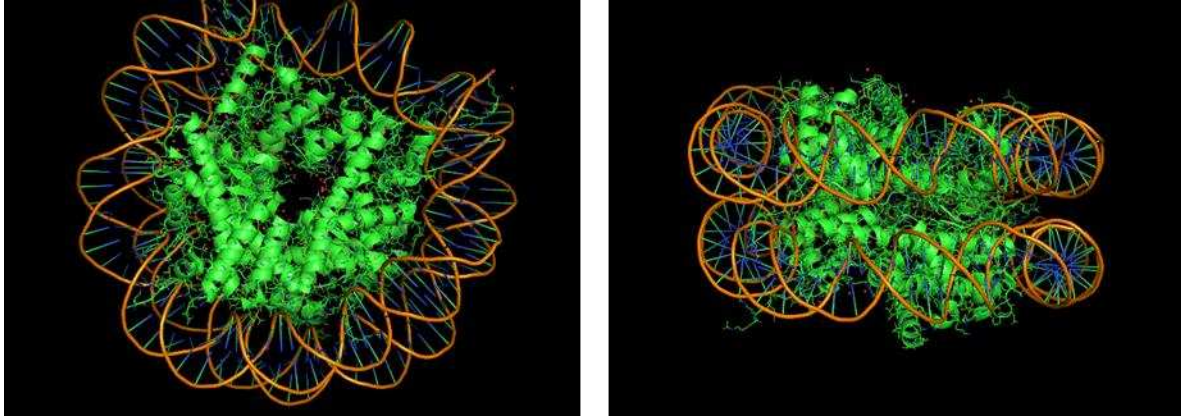


Figure 1: Human nucleosome. Structural representation of a human nucleosome showing the 146 base pairs of DNA wrapped 1.7 times around a histone octamer that consists of two each of H2A, H2B, H3 and H4. The positive histone subunits interact with each other through helical folding and with DNA via its negatively charged phosphodiester backbone (PDB 5AV5).

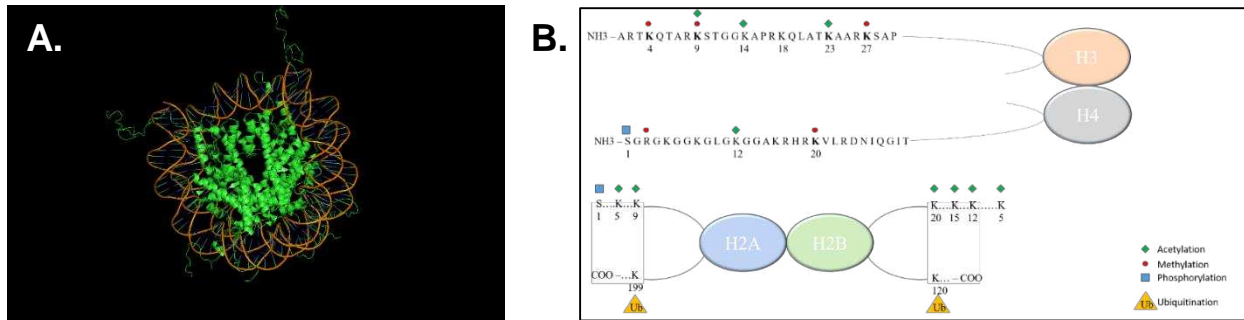


Figure 2. Histone tails and covalent modification. **(A)** A cartoon diagram of the unstructured histone tails protruding outward from the core nucleosome. **(B)** Select sites of post-translational modifications on the histone tails. The modifications shown include acetylation (green diamonds), methylation (red circles), phosphorylation (blue squares), and ubiquitination (orange triangle). Note that Lys 9 in the H3 tail can be either acetylated or methylated. (Adapted from Zhang et al. *Genes Dev.* 2001) [25].

Table 1. Types of amino acid modifications. A table indicating the manner in which various histone residues can be differentially post-translationally modified. Lysine residues can be subjected to several types of modification

Histone Tail Amino Acid Residue (Abbreviation)	Post-translational Modifications				
	Methylation	Acetylation	Phosphorylation	Ubiquitination	Sumoylation
Lysine (K)	X	X		X	X
Arginine (R)	X				
Serine (S)			X		
Threonine (T)			X		
Tyrosine (Y)			X		

Histone lysine	Function(s)	Histone lysine methyltransferases
H1 K26	Transcriptional silencing	 EZH2 (catalytic subunit of Polycomb repressive complex 3)
H3 K4	Transcriptional activation and elongation Transcriptional activation	 SET1  SET7/9
H3 K9	Euchromatic silencing; DNA methylation Euchromatic silencing	 and  G9a; Hs GLP1 (EuHMT1) and  ESET (SETDB1)
H3 K27	Euchromatic silencing	 and  G9a
H3 K36	Transcriptional regulation	 NSD1
H3 K79	Demarcation of euchromatin	 DOT1 (a non-SET domain histone lysine methyltransferase)
H4 K20	Cell cycle-dependent silencing, mitosis and cytokinesis Heterochromatic silencing Transcriptional regulation	 SET8  SUV4-20H1 and SUV4-20H2  NSD1

Figure 3: Sites & functions of histone methylation. Site specific methylation of histone tail residues are associated with one or more functions. Methylation can result in either transcriptional repression or activation. Select known methyltransferases responsible for methylating the specific residue in either human or mouse genomes are indicated on the right (Adapted from Dillon et al. Genome Biology. 2005) [34].

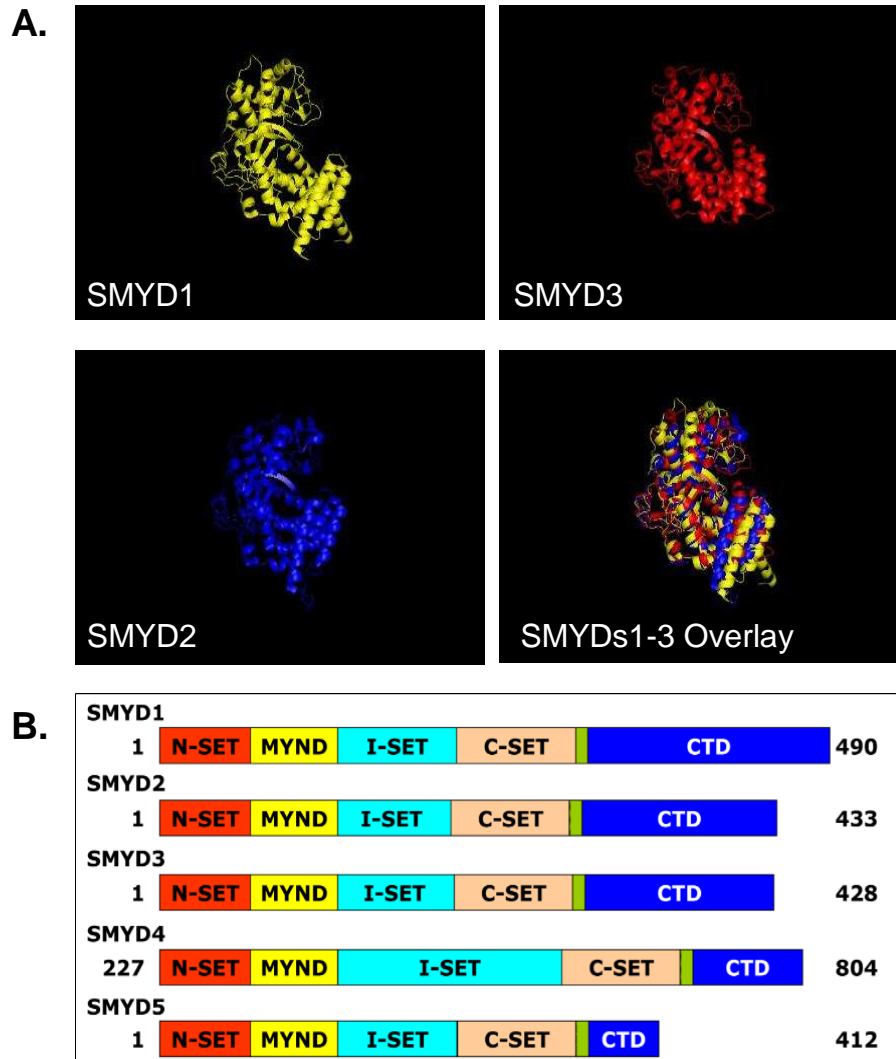


Figure 4: SMYD Family homology. Both the **(A)** cartoon diagram overlay and **(B)** the amino acid alignment display the sequence and structural identity of the familial proteins (PDB: SMYD1; 3n71, SMYD2; 3tg4, SMYD3; 3mek).

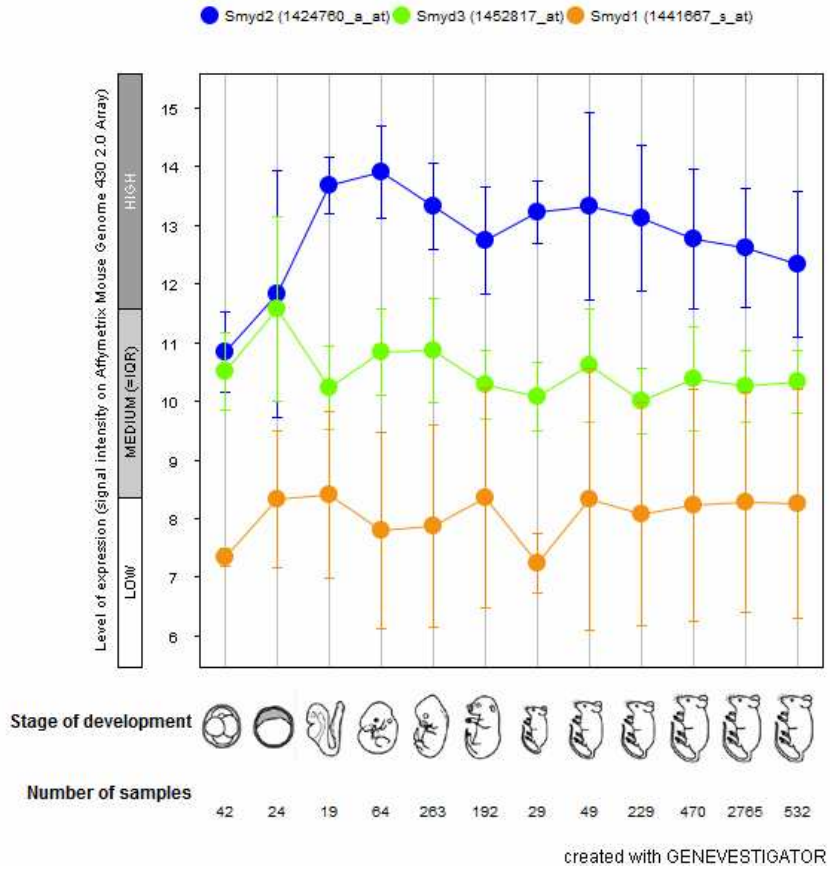
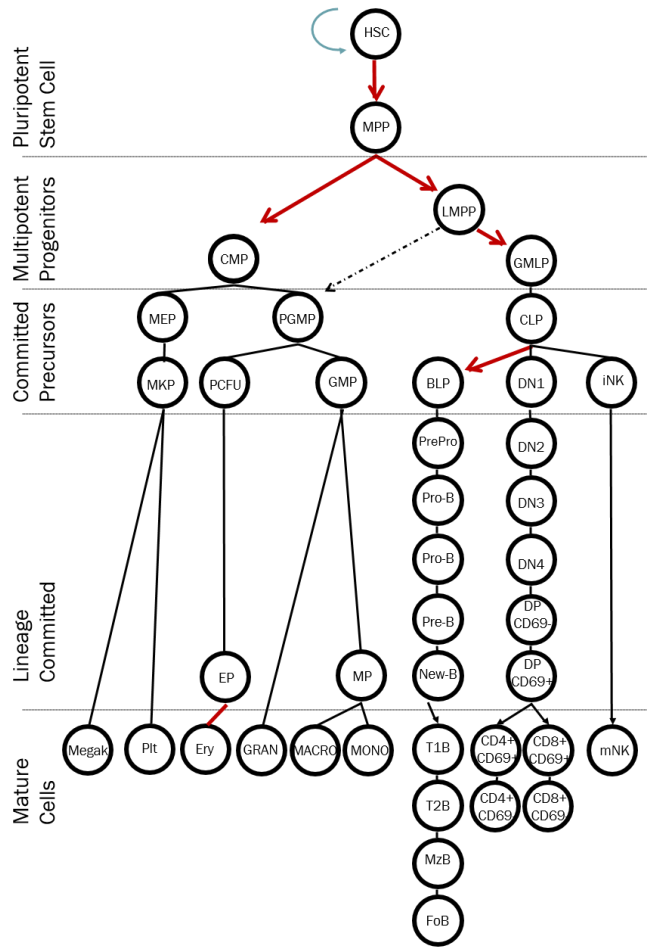


Figure 5: SMYDs in murine development. SMYDs 1-3 have demonstrated roles in cellular development and differentiation. The murine stages of development indicate where each of the first three SMYDs are expressed. All of SMYDs 1-3 are at their highest expression during the earlier stages.



Abbr	Name	Abbr	Name
HSC	Hematopoietic Stem Cell	iNK	Immature Natural Killer
MPP	Multipluripotent Progenitor	DN	Double Negative
CMP	Common Myeloid Progenitor	DP	Double Positive
GMLP	Granulocyte/Macrophage Lymphoid Progenitor	Pit	Platelete
MEP	Megakaryocyte/Erythrocyte Progenitor	Ery	Erythrocyte
pGMP	pre Granulocyte/Macrophage Progenitor	GRA	Granulocyte
CLP	Common Lymphoid Progenitor	MONO	Monocyte
MKP	Megakaryocyte Progenitor	T 1/2 B	Transitional 1/2 B-cell
pCFU	pre Colony Forming Unit	MzB	Marginal Zone B-cell
GMP	Granulocyte/Macrophage Progenitor	FoB	Follicular B-cell
BLP	B-Cell Lymphoid Progenitor	mNK	Mature Natural Killer

Figure 6: Hematopoiesis. A simplified version of the cells derived from a single self-renewing hematopoietic stem cell. Two main branches, the myeloid lineage and the lymphocyte lineage give rise to the above noted cells.

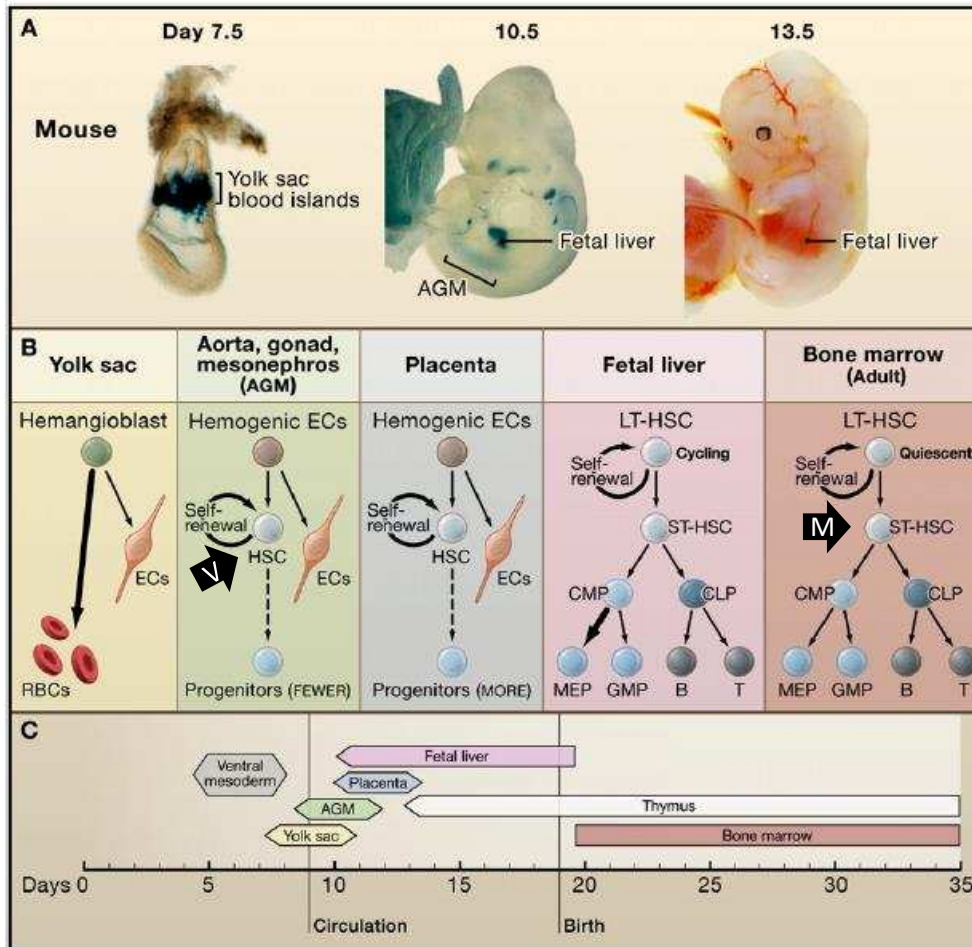


Figure 7: Migration of progenitor HSC and HSC through resident organs in embryonic mouse development. Precursors to HSC's began in the yolk sac to provide RBCs needed to oxygenate new tissues. Those cells migrate through the AGM to the fetal liver before permanent residence in the bone marrow after birth [88]. Arrows indicate the stage at which each the *vav cre* (V) and the *mx1 cre* (M) delete *SMYD2* in HSCs.

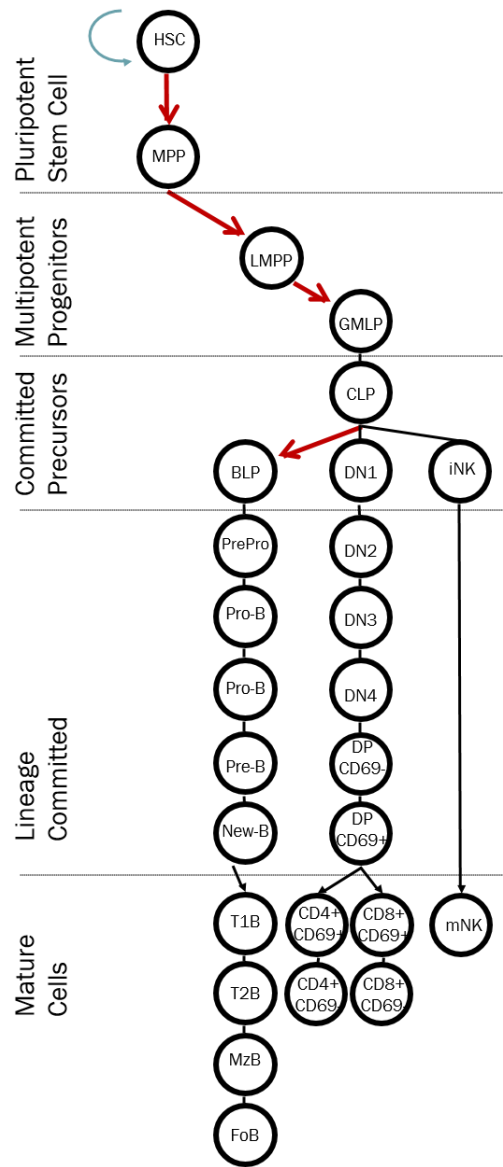


Figure 8: Lymphocytes. Downstream of the common lymphoid progenitor are the B cell, T cell and Natural killer cells that mature in a linear fashion through several different stages.

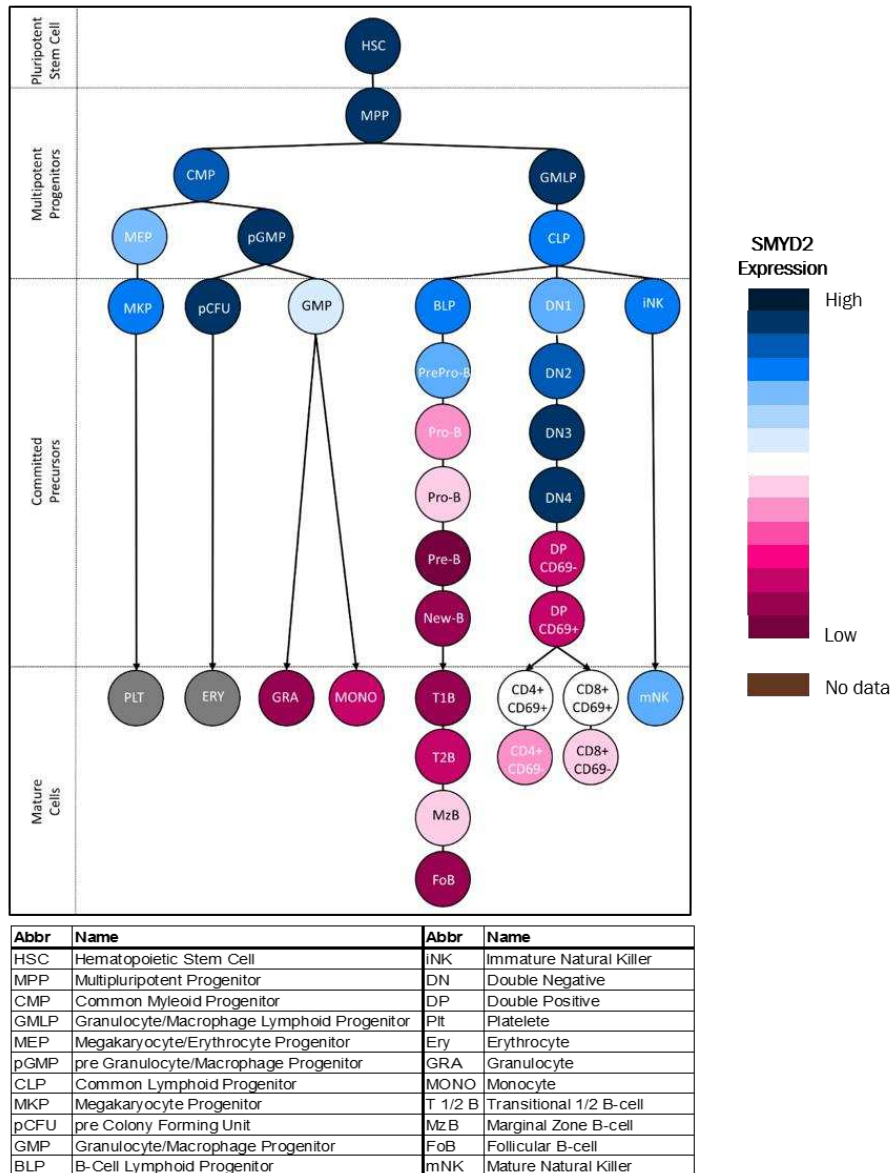


Figure 9: Expression of SMYD2 throughout hematopoiesis. SMYD2 is most highly expressed in the HSC and in the early progenitor in both the myeloid and lymphoid lineages. Throughout T cell development, SMYD2 expression remains high through most of the maturation process whereas there is little expression beyond early B cell stages. The myeloid lineage has varied expression of SMYD2 in its committed progenitors and very low expression onward [102, 103].

CHAPTER 2 - MATERIALS & METHODS

A. MUTAGENESIS, CLONING, AND BACTERIAL EXPRESSION

Point mutants were generated using GeneEditor *in vitro* Site-Directed Mutagenesis System (Promega) according to manufacturer's instructions using as template full length human SMYD3 cloned into Gateway pENTR vector (Invitrogen). For PCR, samples were heated to 94°C for 5 min, subjected to amplification for 16 cycles of 0.5 min at 94°C, 0.5 min at 55°C, and 0.5 min at 68°C and extended after the last cycle at 72°C for 7 min.

B. BACTERIAL PROTEIN PURIFICATION

Polyhistidine (6xHis)-tagged SMYD3 wildtype, truncation and substitution mutants were shuttled using directional TOPO cloning into Gateway (Invitrogen) pET™-DEST42. High level expression was induced by IPTG in *E. coli* strains MG232 (Scarab LTM) or HSP90Plus™ (Expression Technologies Inc). Cells were lysed in buffer A [50 mM Tris-HCl pH7.7, 250 mM NaCl with protease inhibitors (Roche Applied Science, Cat. #11-873-580-001)] and centrifuged to remove cell debris. The soluble fraction was purified over an IMAC column charged with nickel (GE Healthcare, NJ), and eluted under native conditions with a step gradient of 10 mM, then 500 mM imidazole. Proteins were then further purified by gel filtration using a Superdex 200 column (GE Healthcare, NJ), into 25 mM Tris-HCl pH7.6, 150 mM NaCl, and 1 mM TCEP. Protein was pooled based on SDS-PAGE and concentrated to 1–10 mg/ml.

C. HISTONE METHYL TRANSFERASE ASSAYS

For *in vitro* HMTase assays, SMYD3 proteins (0.1–1 µg) +/- equivalent amt. of human HSP90α (Assay Designs, Ann Arbor, MI, USA, cat. no SPP-776D) were incubated with 1 µg of mixed histones from calf thymus (Sigma) or recombinant core histones (Upstate). Two µCi S-adenosyl-L-[methyl-3H] methionine (SAM; Amersham Biosciences) was included as a methyl donor. All reactions were carried out in 40 µl HMT reaction buffer (10 mM dithiothreitol, 100 mM NaCl, 4 mM MgCl₂, and 50 mM Tris-HCl at pH 8.8) at 30°C for 3 hours. An 18% SDS-PAGE gel was used to resolve samples and fluorography was used to visualize isotope incorporation. Substrate loading was visualized by Coomassie blue staining.

D. HSP90 AND GST-MEEVD BINDING ASSAYS

Determination of apparent dissociation constants (K_d) values for wildtype or mutant 6X-His-SMYD3 with either HSP90α or GST-MEEVD (plasmid provided by Dr. Lynne Regan, Yale Univ.) complex formation was carried out as follows: 1.5 µM of each purified 6X-His-SMYD3 protein was mixed with various amounts of HSP90α or GST-MEEVD (0.25, 0.5, 1, 2, 4, 8, 16, and 32 µM) in 130 µl of buffer B (20 mM Tris-HCl (pH 8.0), 300 mM NaCl, 20 mM imidazole, 5 mM β-mercaptoethanol, and 5% glycerol) in the presence or absence of 1 mM ATP plus 5 mM MgCl₂ and incubated at 25°C for 30 min. Ni-NTA-agarose (15 µl of a 50% slurry in buffer B, Qiagen) was added to each reaction mixture, and incubation was carried out at 4°C with constant shaking for 40 min. Mixtures were transferred to an Ultrafree- MC centrifugal filter device (UFC30HV00, Millipore) and centrifuged at 6000 rpm for 10s. After 3 washes with Buffer B, the Ni-NTA-agarose was

pelleted at 6000 rpm for 10 s. Resin was then mixed with 10 μ l of elution buffer [20 mM Tris-HCl (pH 8.0), 300 mM NaCl, 5 mM β -mercaptoethanol, 250 mM imidazole, and 5% glycerol] and incubated at room temperature for 10 min. Following centrifugation at 6000 rpm for 1 min, elution step was repeated and combined eluates were fractionated on SDS-PAGE. For input controls, 10% of the amounts of HSP90 α and GST-MEEVD used for binding reactions were processed identically but in the absence of 6X-His-SMYD3 proteins. After staining with Coomassie Blue, protein amounts were quantitatively estimated with a densitometer (GS-800TM, Bio-Rad). Ratio of densities of HSP90 or GST-MEEVD to 6X-His-SMYD3 represents the percentage of 6X-His-SMYD3 bound. Concentration of 6X-His-SMYD3 /HSP90 and 6X-His-SMYD3/ GST-MEEVD complexes were derived from the ratio of their densities multiplied by total 6X-His-SMYD3 concentration (1.5 μ M). Concentrations of respective complexes were plotted against total concentrations of HSP90 or GST-MEEVD. Kd values were obtained by non-linear least square curve fitting using the Sigmaplot program (SSPS Inc.) using the following equation:

$ER = (Kd + Et + Rt) - \sqrt{(Kd + Et + Rt)^2 - 4 \times Et \times Rt} / 2$, where ER is the concentration of the 6X-His-SMYD3-HSP90 or GST-MEEVD complex; Et, total HSP90 or GST-MEEVD concentration; and Rt, total SMYD3 concentration.

E. MAMMALIAN CELL TRANSFECTION AND WESTERN BLOTTING

Wildtype and mutant SMYD3 cDNAs were transferred from Gateway pENTR into pEF-DEST51 (N-terminal V5-tagged) by TOPO cloning. NIH3T3 cells were transiently transfected, harvested 48 hours later, and then lysed in RIPA buffer (150 mM NaCl, 1%

NP- 40, 0.5% DOC, 50 mM Tris pH 8, 0.1% SDS) containing protease inhibitors (Roche Molecular Biochemicals, Indianapolis, IN). Expression levels were determined by Western blotting. Proteins were resolved on 8–15% SDS-PAGE, transferred to nitrocellulose (Protran BA, Schleicher and Schuell, NH), and blocked using 5% nonfat milk (10g nonfat milk, 150 mM NaCl, 10 mM Tris pH 8, 0.05% Tween-20) overnight at 4°C. Membranes were incubated with anti-SMYD3 polyclonal antibody [19] for 1 hour at room temperature, extensively washed, then incubated with ECL Plex Goat anti-Rabbit IgG-Cy5 Secondary Antibody (GE Healthcare) for 1 hour at room temperature. Blots were exposed and developed using ECL blot detection reagent (Amersham Pharmacia Biotech) according to manufacturer's instructions.

F. PROLIFERATION ASSAYS

Mouse embryonic fibroblasts (MEFs) were isolated from E13.5 C57Bl/6 embryos as previously described [49]. Cells were plated at $\sim 5 \times 10^6$ /ml in RPMI (supplemented with 10% heat-inactivated fetal calf serum, 100 U/ml penicillin, 100 μ g/ml streptomycin, 5×10^{-5} M β -mercaptoethanol, and 1 mM sodium pyruvate) transfected) and transfected by lipofection (Fugene) with ~ 6 ug of either SMYD3 wildtype, mutants or empty vector. To determine the rates of cell proliferation, transfected MEFs were plated in triplicate 1 d after infection at a density of 10^4 cells/cm² and counted every 24 h using a Z1 Coulter Particle Counter (Beckman Coulter) with elimination of dead cells calculated by trypan blue exclusion.

G. CELL FRACTIONATION

Cells were separated into cytoplasmic (C), soluble nuclear protein (NP), chromatin (CH), and nuclear matrix (NM) fractions as follows. Approximately 1×10^8 cells were washed twice in PBS and the pellet was resuspended in 2ml HNB buffer (500 mM sucrose/15 mM Tris-HCL pH 7.5/60 mM KCL/.25 mM EDTA/.125 mM EGTA/.5 mM spermidine). Then 1ml HNB buffer was added dropwise (HNB buffer+ 1% NP-40) and incubated at 4°C for 5 minutes before centrifugation at 6,000g for 3 min at 4°C; the supernatant of this is the C fraction. The pellet was then resuspended in 1ml CSKT buffer (CSK buffer + 1% Triton-X), incubated at 4°C for 5 minutes before centrifugation at 3,000g for 3 min at 4°C; the supernatant of this is the NP fraction. The pellet was then resuspended in 720 μ l CSK buffer (10 mM Pipes pH 6.8/300 mM sucrose/3 mM MgCl₂/2 mM EGTA) and 30 μ l RNase-free DNase, incubated at 37°C for 15 minutes then added 250 μ l 1M AmSO₄/CSK and incubate at 4°C for 5 minutes, before centrifugation at 3,000g for 3 min at 4°C; the supernatant of this is the CH fraction. The pellet was resuspended in 1ml 8M Urea and centrifuged at 13,000g for 5 minutes; the supernatant is the NM fraction. Purity of the subfractions was assessed by western blotting with antibodies noted in Figure 15C as previously described [50].

H. *IN VITRO* HEMATOPOIETIC TUMOR MODELS

Bone marrow was extracted from femurs of SMYD2^{flox/flox} mice. Cells were then depleted of erythrocytes, cultured and selected for preB, common myeloid progenitor or multipotent progenitor cells for ALL, CML and MLL tumors, respectively. FACS analysis of lineage markers was performed to confirm cell stages: For ALL, SMYD2 IL-7 cells were

B220+CD19+, for CML FcyR^{int}CD34^{int} and for MLL, Lin-Sca1+cKit+Flt3^{int}. These cells were then transduced with MSCV-based retroviral p210 bcr-Abl constructs to generate ALL and CML-like cells and with MLL-GAS7 constructs to generate MLL-like cells.

To induce cre to delete SMYD2, tumor-like cells were transduced with cre-ERT2 pyromycin construct or empty vector. After, cells were treated with tamoxifen (4OHT) to activate cre and subsequently delete SMYD2 alleles in B cell precursor ALL, CMP cell for CML and in MPP cell for MLL. Samples collected over 4 days and WB.

I. COLONY FORMING UNIT ASSAY

Either 100,000 CML or MLL cells, or 10,000 ALL cells with or without treatment with 4-OHT to initiate deletion of SMYD2 *in vitro*, were plated on a semi-solid methylcellulose-based medium in a colony forming unit (CFU) assay. Cells were cultured in a 5% CO₂ incubator at 37°C. Cells were left to grow in a 3D culture for 21 days and the media were changed every 2 days. The CFU formation was monitored weekly.

J. IN VIVO TUMORS

NOD-SCID mice were purchased from the Jackson Laboratory (JAX Mice & Services Bar Harbor, ME USA). For tumor formation, 10³, 10⁴, 10⁵ or 10⁶ of non-treated (control) cre-ER^{T2} (n=65) or cre-ER^{T2} treated with 4-OHT to initiate deletion of SMYD2 (n= 60) cells were injected intrafemorally into 6 to 8-week old male NOD/SCID mice. Tumor size was measured by caliper weekly for at least 3 months or until the presence of a tumor diameter >17mm, tumor ulceration or bleeding, when in those cases mice were sacrificed earlier. For examining tumor growth and/or detecting metastasis by bioluminescence imaging, mice were injected with luciferin (1 mg/ml, Promega

Corporation). Mice were then anesthetized using Ketamine HCl, xylazine, NaCl, 0.9% (GE Healthcare, UK). The in vivo bioluminescence monitoring was performed in a Xenogen IVIS Lumina II System (Advanced Molecular Vision, Inc.). Animals were then sacrificed.

K. CELL VIABILITY

CML, MLL, and ALL cells were seeded in 6-well plates and cultured for up to 60 days. Cells were harvested at 2 day intervals to detect cells undergoing apoptosis. Apoptosis was detected using an Annexin V-FITC apoptosis detection kit (Keygen, Nanjing, China). Briefly, 2×10^6 cells were digested into cell suspension with EDTA-free trypsin and resuspended in cold binding buffer and incubated for 15 min in the dark at room temperature following addition of 5 μ l of Annexin V-FITC and 5 μ l of propidium iodide (PI, Keygen, Nanjing, China) solutions. Flow cytometry analysis was performed using an LSR II Fortessa cytometer. For 4',6-diamidino-2-phenylindole (DAPI) staining, slides were incubated for 30 min at room temperature in the dark with mounting medium for fluorescence containing DAPI (Vectoer Laboratories, Inc., Burlingame, CA, USA). The cells were then observed through a fluorescence microscope.

L. CLONING OF THE SMYD2 CONDITIONAL TARGETING CONSTRUCT

To construct the SMYD2 conditional targeting construct, two genomic fragments were first subcloned from the C57BL/6 murine Bac clone-RPC124288J3. A 2.2kb KpnI fragment containing exon 1 and a KpnI fragment containing 5.2kb of intronic sequence between exons 1 and 2 was subcloned into pBluescript (Stratagene). Fragment 1 (5.2kb)

was excised with KpnI, blunt ended, and ligated into the unique blunt ended Sall site of pDELBOY [118]. The resulting clones were screened for correct orientation and for the regeneration of the Sall site. Fragment 2 (2.2kb) was excised with KpnI and ligated into the unique KpnI site of pDELBOY containing fragment 1. This was subsequently screened for correct orientation. Fragment 3, containing 0.6kb upstream of exon 1, was generated using Platinum Pfx DNA Polymerase (Invitrogen), C57BL/6 genomic DNA as template, and the following primer pair:

5'-GTCGACATTGAGCTAATGTGCTTA-3'; 5'-CTCGAGGTAACACTCAACCTCTGC-3'.

The resulting PCR product was treated with TAQ Polymerase, ligated into pGEMTEASY (Promega), and excised with Sall and XhoI. This product was ligated into the unique XhoI site of pDELBOY containing fragments 1 and 2 and subsequently screened for correct orientation. The completed targeting construct was linearized at the short arm of homology using XhoI. C57BL/6 ES cells were then transfected and selected with G418 and gancyclovir. Targeted ES cell colonies were screened by Southern hybridization analysis using probes specific for the genomic sequence external to the arms of homology. The 5' Southern used a 0.8kb PCR fragment using the following primer pair:

5'-GGCTGGAGTTAGAGGTGGTTATGA-3'; 5'-ACAGCTCTGGGCTCGGAAATAAAG-3'.

The 3' Southern used a 0.9 kb PCR fragment using the following primer pair:

5'-AACTCCATGTGGTGGGAATTCTGTGGT-3'; 5'-
GCAGCCTGAAAGAATCCCTTAGACT-3'.

M. CRE-MEDIATED DELETIONS

Mice were from a C57BL/6 (CD45.1) background. To generate the SMYD2 conditional knockout mice, we mated cre (vav or mx1) and SMYD2^{fl^{ox}/fl^{ox}} YFP+ mice. To activate mx1-cre *in vivo*, 100 µg of plpC (Sigma-Aldrich) was injected every other day for 5 days and samples taken at least two days after the final injection. PCR genotyping from tail DNA was used to confirm genetic profiles and determine mates. Fluorescent microscope and flow cytometry were also used to determine presence of YFP.

Mice were bred in specific pathogen-free environment and caged in groups less than five. During housing, animals were cleaned twice a week. All animal protocols and experiments were approved by the local Institutional Animal Care and Use Committee (IACUC). Protocol ID AUP-2012-00169

N. MOUSE TAIL DNA EXTRACTION

A crude DNA extraction was made from 2mm mouse tail clippings dissolved in 200ul of 1x PBDN buffer. 10mg/ml Proteinase K was added to each sample and placed at 55° C for 3hrs to overnight. Samples were then boiled for 5 minutes and centrifuged. The supernatant was then used as the DNA template in the genotyping PCR experiments.

O. GENOTYPING

A PCR master mix of reagents was made to ensure each sample of 1ul mouse tail DNA template received 5ul 10x PCR buffer, 1ul 10mM dNTPs, .2ul Taq polymerase, 0.5ul each of 100um forward and reverse primers and 2.8ul of water. The samples were run

through a thermocycler on the following programs per each set of primers to generate a PCR product:

SMYD2:

5'GGTCTGGCTTTGGAGTTGAGCC3'; 5'GAGCTTCGTGGAGTGCAGGAC3'

Ran at: 94°C x 5' (94°C x 30", 62°C x 30", 72°C x 30") x 35 cycles, 72°C x 7'

Mx1 cre:

5'GCGGTCTGGCAGTAAAACTATC3'; 5'GTGAAACAGCATTGCTGTCACTT3'

Ran at: 94°C x 2' (94° C x 20", 60° C x 20", 72° C x 20") x 35 cycles, 72° C x 2'

Vav cre:

5'AGATGCCAGGACATCAGGAACCTG3'; 5'ATCAGCCACACCAGACACAGAGATC3'

Ran at: 94° C x 5' (94° C x 30", 64° C x 45", 72° C x 45") x 35 cycles, 72° C x 7'

YFP:

5'GGAGCGGGAGAAATGGATATG3'; 5'AAAGTCGCTCTGAGTTGTTAT3';

5'AAGACCGCGAAGAGTTTGTC3'

Ran at: 94° C x 5' (94° C x 30", 58° C x 1', 72° C x 1') x 35 cycles, 72° C x 7'

All PCR products were analyzed via gel electrophoresis. 15ul of each sample and loading dye was run on a 2.0% agarose gel with the addition of ethidium bromide. Electrophoresis was ran at 100v for approximately 30minutes before visualization in a UV light box.

P. FLOW CYTOMETRY

Bone marrow from femurs, spleen, thymus and peripheral blood cells were harvested from experimental and control mice and kept on ice and in RPMI media. Cell

suspensions were washed, strained through 70um mesh filters and counted. At least 1.5×10^6 cells were aliquoted into 1.5mL Eppendorf tubes, pelleted and incubated for 30mins at room temperature in the dark or for one hour at 4° C in the dark with a 1% concentration of fluorescently labeled antibody (BioLegend, BD Biosciences and eBiosciences) stains for each tissue type in 100ul of sterile 1x PBS buffer. Cells were then washed of their stains, transferred to 5ml polystyrene tubes in 2ml of sterile 1x PBS buffer. Arc compensation beads stained for each color used per assay were used as controls. Definitions of each cell population were defined as denoted in **Table 2** and antibody conjugates are listed in **Table 3**. All samples and controls were collected on the BD Bioscience LSR II Fortessa. Analysis of flow data was conducted using FlowJo software.

Q. CELL CULTURE

Cell lines were grown in appropriate media; alpha-MEM for OP9 cells, RPMI for primary bone marrow cells and DMEM for 293T cells without any antibiotic supplements. Cells were cultured at 37°C in a humidified atmosphere of 5% CO₂.

R. TIMED MATINGS

Female mice (n = 1 or 2) of 6wks old were placed in a cage overnight with a single male mouse. Putative pregnancy was determined by the presence of a copulation plug the following morning (approximately 0800), which was designated as GD0.5. Female mice were group-housed (n = 1 to 5 mice per cage) according to their copulation-plug status,. Pregnancy was confirmed by the birth of a litter.

S. FETAL LIVERS

We conducted timed matings of SMYD2 F/F Vav cre+ YFP+/+ males with a SMYD2 F/F YFP +/- female and harvested the embryos at day E15.5. Fetal livers were removed, pushed through a 70 um mesh screen to obtain a single cell suspension and red blood cell lysed. These cells were then labeled with fluorescently conjugated antibodies and analyzed by flow cytometry.

T. MACS CELL SEPARATION

Magnetic cell sorting was performed using the Miltenyi Biotec lineage depletion kit and according to the manufacturer's instructions in order to separate earlier bone marrow progenitor cells from later lineage specific cells. The bone marrow of both control and experimental mice were harvested by flushing mouse femurs with MACS Buffer on ice. The cell suspension was then strained through 70um mesh filters, washed, counted and labeled with CD43 magnetic beads. The labeled cells were run through the magnetic fields of the MACS separator columns and the effluents collected for analysis.

U. B CELL PROLIFERATION ASSAY

The proliferation assays were conducted and adapted from the Cold Spring Harbor Protocol for the OP9-DL1 System, doi: 10.1101/pdb.prot5156. Early primary progenitor cells from 4-8 week old experimental and control mouse bone marrow, previously separated by MACS cell separation, were strained, washed and counted. 5×10^5 cells were plated on top of a culture of 80-90% confluent OP9 cells in alpha-MEM media with the addition of the cytokines Flt3 and IL-7 at a concentration of 5mg/mL and 1ng/mL

respectively. The co-culture was maintained for up to twenty days during which time cells were harvested for counting, detection of YFP, and flow cytometry analysis around days 0, 5, 8, 12 and 16. Cells were re-plated with or without trypsin mediated passage to fresh confluent OP9 cultures every four to five days.

V. WESTERN BLOTS

Proteins were resolved in SDS PAGE gel at 200V for 35min and electrotransferred by tank method to membranes at 30V for 1hour. The blots were blocked in 5% BSA with TBS-T buffer for 1hour, then rinsed five times for ten minutes each with TBS-T. Blots were incubated with primary antibody diluted in TBS-T 1:1000 overnight, washed five times for ten minutes each with TBS-T, and then incubated with secondary antibody 1:1000 for 1hour. Blots were washed five times in TBS-T before visualization on Storm Imaging System.

W. MOUSE IMMUNIZATIONS

Mice were SMYD2^{flox/flox} mb1 cre⁺ YFP or SMYD2^{flox/flox} mb1 cre⁻ YFP. All mice were maintained on a C57BL/6 background in specific pathogen-free facilities. Mice were immunized with NP-KLH at a molar ratio ~17:1 (NP/KLH). Antigen was precipitated on alum at a concentration of 1 mg/ml and delivered by intraperitoneal (100 µg) or subcutaneous (50 µg) injection. Blood serum was collected at 0, 14, and 28 days after inoculation and analyzed via ELISA.

X. ELISA

For measuring the levels of serum IgG isotypes, ELISA plates were coated with goat–anti-mouse Ig(M+G+A), incubated with serially diluted sera (1:50, 1:150, 1:450, 1:1,350, 1:4,050, 1:12,150, and 1:36,450), and developed with horseradish peroxidase (HRP)-conjugated goat Ab specific for each mouse IgG isotype (Southern Biotechnology Associates). Plates were developed with HRP-conjugated goat Abs specific for mouse IgM and IgG isotypes and Dako TMB One-Step substrate. Antibody concentrations were calculated by using the linear ranges of the dilution and standard curves generated with purified mouse monoclonal IgG antibodies.

Table 2. Hematopoietic population definitions. Each stage of differentiation is unique in its expression of extracellular surface markers. Cells were distinguished from each other according to the listed definitions.

Tissue	Population	Population Abbr	Marker	Lineage
B o n e M a r r o w	Hematopoietic stem cell	HSC	Lin ⁻ Sca1 ⁺ ckit ⁺ Flt3 ⁻	B220, CD19, CD3e, CD4,
	Multipotent progenitor	MPP	Lin ⁻ Sca1 ⁺ ckit ⁺ Flt3 ^{int}	CD8a, CD11b, Gr1, NK1.1,
	Lymphoid primed multipotent progenitor	LMPP	Lin ⁻ Sca1 ⁺ ckit ⁺ Flt3 ^{hi}	Ter119
	Common lymphoid progenitor	CLP	Lin ⁻ Flt3 ⁺ IL-7 ⁺ Sca1 ^{low} +ckit ^{low}	
	Common myeloid progenitor	CMP	Lin ⁻ Sca1 ⁻ ckit ⁺ FcyR ^{int} CD34 ^{int}	
	Granulocyte/macrophage progenitor	GMP	Lin ⁻ Sca1 ⁻ ckit ⁺ FcyR ^{hi} CD34 ^{hi}	
	Megakaryocyte/erythroid progenitor	MEP	Lin ⁻ Sca1 ⁻ ckit ⁺ FcyR ^{low} CD34 ^{low}	
	Progenitor B cell	Pro-B	B220 ⁺ CD19 ⁻ CD43 ⁺ ckit ⁺ IgM ⁻	
	Pre B cell	Pre-B	B220 ⁺ CD19 ⁺ CD43 ⁻ IgM ⁻	
	Large Pre-B	Large Pre-B	B220 ⁺ CD19 ⁺ CD43 ⁺ IgM ⁻ BP1 ⁺	
	Small Pre-B	Small Pre-B	B220 ⁺ CD19 ⁺ CD43 ⁻ IgM ⁻ CD2 ⁺	
	Immature B cell	Imm B	B220 ⁺ CD19 ⁺ CD43 ⁺ IgM ^{hi} IgD ⁻	
	Mature B cell or Recirculating B cell	Mat B or Recirc	B220 ⁺ CD19 ⁺ IgM ^{hi} IgD ⁺	
	Macrophage	Macro	Mac1 ⁺ Gr1 ^{low} CD115 ⁺	
Granulocytes	Gran	Mac1 ⁺ Gr1 ^{hi} CD115 ⁻		
Plasmacytoid dendritic cell	pDC	CD11b ⁻ CD11c ^{low} B220 ⁺ PDCA1 ⁺		
T h y m u s	Double negative	DN	CD4 ⁻ CD8 ⁻	B220, CD19, CD3e, CD8a
	Double positive	DP	CD4 ⁺ CD8 ⁺	TCRB, TCRyΔ, CD11b, NK1.1,
	Helper T cells	CD4+	CD4 ⁺ CD8 ⁻	Ly-6G, CD11b, CD11c, Ter119
	Cytotoxic T cells	CD8+	CD4 ⁻ CD8 ⁺	
S p l e e n	Immature B cell	Imm B	B220 ⁺ CD19 ⁺ IgM ^{hi} IgD ⁻	
	Transitional B cell 1	Trans B 1	B220 ⁺ CD19 ⁺ IgM ^{hi} IgD ⁻ CD21 ⁻ CD23 ⁻	
	Transitional B cell 2	Trans B 2	B220 ⁺ CD19 ⁺ IgM ^{hi} IgD ⁺ CD21 ⁺ CD23 ⁺	
	Mature B cell or Recirculating B cell	Mat B or Recirc	B220 ⁺ CD19 ⁺ IgM ^{hi} IgD ^{hi}	
	Follicular B cell	FO B	B220 ⁺ CD19 ⁺ CD21 ^{int} CD23 ^{hi}	
Marginal zone B cell	MZ B	B220 ⁺ CD19 ⁺ CD21 ^{hi} CD23 ^{low}		

Table 3. Epitopes and conjugated antibodies. Stains utilizing the listed fluorescently labeled antibodies were used to define cells as mentioned in Table 2.

Epitope	Conjugate	Epitope	Conjugate
B220	qDot605 Alexa700	CD71	PE
BP1	PE	ckit	PE-CY7
CD2	APC	F4/80	PE-CY7
CD3e	APC-CY7 PerCP-CY5.5	FCyR	PE
CD4	PerCP-CY5.5	Flt3	APC
CD8a	APC PerCP-CY5.5	Gr1	APC PerCP-CY5.5
CD8b.2	Pacific Blue	IgD	Pacific Blue
CD11b	PE-CY7 Pacific Blue PerCP-CY5.5	IgM	APC-CY7 PerCP-CY5.5
CD11c	APC-CY7	IL-7Ra	V21 PerCP-CY5.5
CD115	qDot605	MHCII	Pacific Blue
CD19	APC Alexa700	NK1.1	PerCP-CY5.5
CD21/35	PE-CY7	PDCA1	PE
CD22	PE	Sca1	APC-CY7 Alexa700
CD23	PE	TCRB	APC
CD34	Alexa700	TCR γ Δ	PE
CD43	APC PE	Ter119	PerCP-CY5.5

CHAPTER 3 – C-TERMINAL DOMAIN OF SMYD3 SERVES AS A UNIQUE HSP90-REGULATED MOTIF IN ONCOGENESIS

The histone code of post-translational modifications determines the level of chromatin accessibility to both transcription factors and polymerase complexes [11, 104, 105]. In this way, the SMYD family of histone methyltransferases (HMTases) plays critical roles in the modulation of transcriptional activity to impart normal cellular differentiation as well as oncogenic transformation. SMYD3 catalyzes trimethylation (me₃) of H4-K20 [106], H4-K5 [49] and H3-K4 [54] and monomethylation of vascular endothelial growth factor receptor 1 [107]. These various histone methylation marks lead to altered expression levels of genes physically associated with the methylated histone. Indeed, SMYD3 has been strongly implicated as a proto-oncogene in hepatocellular, colorectal and breast carcinomas [40, 50, 108-110] by virtue of its high over-expression and promoter-associated polymorphisms specific to malignant cells.

HSP90 is a key chaperone involved in the proper folding of many cellular proteins and its deregulation is strongly implicated in a broad array of malignancies [78, 111]. At the same time, HSP90 has been implicated as a driver of evolution, either as a stabilizer of particular polymorphisms in coding and regulatory sequences of key proteins [84, 112] or as an inducer of heritably altered chromatin states [113], suggesting it has a significant role in epigenetic modification. This later role is more surprising, as HSP90's primary role is traditionally seen as a folding chaperone to a vast number of client proteins, including a myriad of epigenetic regulators. It remains an open question as to whether HSP90 has specific interactions with a select few epigenetic proteins through which the heritably altered chromatin states are cooperatively induced.

HSP90 has been the target of many novel cancer therapeutics. The most advanced of these function by occupying the ATP binding site, thus blocking the release of HSP90 substrates. Unfortunately, adverse side effects are the unintended consequence of eliminating the molecular chaperone activity of this broadly expressed and essential protein [114]. Altering the association of HSP90 with specific partners is seen as a potential, but challenging and as yet unsolved, approach toward mitigating these side effects. One line of thought is that altering the epigenetic functions of HSP90 without significantly altering its molecular chaperone function might lead to a better tolerated therapeutic outcome.

SMYD3 and HSP90 can physically interact, with HSP90 stimulating the basal HMTase activity of SMYD3 [40]. The relevance of this association in a cellular milieu and its association with the epigenetic roles of either of these proteins is, however, poorly characterized. The potential to connect both the physical associations and the epigenetic functions of SMYD3 and HSP90 has increased significantly with the almost concurrent publication of three independent crystal complexes of SMYD3 [39, 115, 116]. The SMYD3 structures revealed an overall compact architecture in which the N- and C-terminal portions of the “split-SET” domain (N-SET and C-SET) adopt a canonical SET domain fold and closely assemble with the MYND (Myeloid translocation protein 8, Nery, and DEAF-1) zinc-binding and protein-protein interaction domain [117-119]. The structures also feature a previously uncharacterized, ~150 residue C-terminal domain (CTD) which is conserved in all SMYD paralogs except SMYD5. The CTD forms a superhelical 9 α -helical bundle which constricts the floor of the substrate binding site to a variable degree among the SMYDs [42, 67]. Based on structural overlays, the superhelical bundle

appears to be a second protein-protein interaction domain, termed the tetratricopeptide repeat (TPR). TPRs facilitate a wide range of diverse functions and are composed of ~34 amino acids of roughly conserved sequence that invariably assemble into characteristic helix-turn-helix structures [120]. A previously documented interaction of HSP90 with the TPR of the cyclophilin FKBP52 [121, 122] implicates the CTD as the HSP90 binding motif for most human SMYDs [123, 124]. This model was suggested for SMYDs 2, 3, and 5 [85], but the cellular consequences of potential HSP90-SMYD interactions have not been addressed.

Herein, we investigate the structural and functional relationship between HSP90 and SMYD3 both *in vitro* and *in vivo*. We show that the CTD is essential for basal SMYD3 methyltransferase activity and establish a unique interfacial interaction for maximal HMTase induction by HSP90. We suggest that disruption of the association between SMYD3 and HSP90 may impact cellular differentiation and oncogenic transformation, providing a potential avenue for blocking HSP90- enabled malignancy with a reduced toxicity profile in SMYD3-overexpressing cells.

A. RESULTS

The CTD is required for basal HMTase activity of SMYD3

Inspection of the SMYD3 structure (**Figure 10A**) revealed that a relatively large space near the post-SET domain and N-terminal portion of the CTD along the inner wall of the pocket is decorated by polar residues from the CTD (mainly residues from N324-C333 of helix 4) (**Figure 10B**). Sirinupong et al. [125] had identified residue K329 as a key linchpin residue, helping maintain the spacing between the CTD and the rest of the protein. In

addition, residues T277 and N327 form multiple hydrogen bonds which help stabilize the assembly of helices 1–4 of the CTD. The remaining residues (E294, E295, D332, and C333) all align in roughly linear fashion in close succession, except for Q287. This conserved clustering suggests that these polar residues might cooperate with the post-SET residues to restrict the histone substrate on both sides of the methyl-lysine. In this context, the CTD could function as a cap necessary to bind substrates effectively and selectively. Consistent with this hypothesis, deletion of CTD helices 1–9 [SMYD3(1–279)] eliminated basal HMTase activity of SMYD3 for histone H4 (**Figure 11A**).

This loss in basal HMTase is also associated with significantly reduced binding of SMYD3 to HSP90 (**Figure 11B**). The C-terminal five residues (MEEVD) of HSP90 are putatively sufficient to recognize TPR motifs [122]. While this pentapeptide bound WT SMYD3, it failed to interact significantly with SMYD3(1–279). This indicated that not only is the CTD required for the basal HMTase activity of SMYD3, but that recognition of HSP90 via its last five C-terminal residues may also be required. Unexpectedly, deletion of helices 7–9 [SMYD3(1–364)], which neither contains nor interacts with any of the polar residues mentioned above, also led to loss of basal HMTase activity and to loss of binding to HSP90 and its derivative MEEVD peptide (**Figure 11**).

Structural conservation of SMYD3 CTD and the HSP90-binding tetratricopeptide (TPR) repeats within FKBP52

To reconcile the above results for SMYD3(1–364), a model of the binding of HSP90 to the CTD of SMYD3 proved extremely helpful. The CTDs are significantly conserved among SMYDs 1–3 and their orthologs after position 364 of SMYD3 (**Figure 12**). Others

[42, 116, 125] have posited that the CTD of various SMYDs may be associated with HSP90 binding and have even generated overlays predicting the orientation of the MEEVD peptide in the TPR-like motif. Recapitulation of this overlay (**Figure 13A, 13B**) using FKBP52, which was solved in a complex with the terminal 5 amino acids (MEEVD) of HSP90 [122], indicated that the overlay may be incorrect.

First, the HSP90 pentapeptide is inserted deep into the pocket, leading to a potential steric conflict between HSP90 and substrates of SMYD3. The HSP90 CTD is almost certainly not a disordered domain nor is it a purely linear chain. But in this model, the CTD must be positioned somewhere near the lip of the SMYD3 protein, thereby reducing access. Second, the residues in that region are incompatible with the HSP90 peptide (**Figure 13B**). Several of the residues of the MEEVD peptide model are in steric clash with the CTD residues, where a loop from the I-SET domain occupies a similar space. This clash was rationalized away by hypothesizing an autoinhibitory mode [42], which we grant is possible. Yet, even if the SMYD3 side chains were adjusted so as to relieve steric clashes, the acidic residues of the HSP90 C-terminal tail sit in a neutral to acidic portion of the pocket, suggesting a lack of electrostatic complementarity as well. Third, deletion of helices 7–9 should not significantly perturb the MEEVD peptide binding which is inconsistent with our data (**Figure 11B**). Thus, an alternative binding mode must be considered.

TPR-like residues of SMYD3 CTD are essential in vitro for HSP90 binding and catalytic enhancement

In order to reconcile our data with a TPR-like motif which could bind HSP90, we aligned helices 7–9 with the HSP90 binding region of FKBP52 [121, 122] (**Figure 13C**). Helices 4–9 in SMYD3 align with the first 3 helices of the TPR motif from FKBP52 (**Figure 13D**), which features the C-terminal pentapeptide MEEVD. Several SMYD3 residues between CTD helices 4 and 5, 7 and 8, and at the end of helix 9 were predicted from the FKBP52 structure [122] to be within contact distance (6Å) of the modeled HSP90 pentapeptide. All are conserved among closest SMYD3 orthologs and, to varying degrees, among SMYD3 paralogs and with FKBP52 (**Figure 12; Table 4**). Mutation of several of these residues led to diminished SMYD3 binding to both HSP90 and MEEVD, including I339 and K375, structural anchors between N- and C-terminal components of the CTD, or to complete loss of binding on mutation of H382, a potential HSP90 interfacial residue, or C421, an anchor for helix 9 to the rest of the CTD (**Figure 14A**). Dissociation constant (K_d) measurements averaged from 5 biologic replicas with density measurements within linear range (Materials and Methods) indicated that HSP90 and MEEVD binding losses ranged from ~10-fold for I339A at the low end to ~40-fold for C421A at the high end (**Table 4**). The same point mutations lost up to 8-fold enhancement of HSP90 stimulation of HMTase activity toward histone H4 (representative data in **Figure 14B; Table 4**).

To ensure that these mutations are specific, we mutated nearby residues, such as N340 and E420. These mutations had no effect on HSP90 binding or enhancement (**Table 4**). Taken with the data of Figure 12, these results indicate that the more N-terminal

helices of the SMYD3 CTD are required for its constitutive HMTase activity, whereas the TPR-like C-terminal helices are required for the enhanced activity afforded by HSP90.

TPR-like residues of SMYD3 CTD are essential in vivo for nuclear localization, HSP90 interaction and sub-nuclear sequestration into chromatin

To establish the cellular effects of the deletion and point mutants which impaired HSP90 binding in vitro, nuclear (N) and cytoplasmic (C) distributions of their overexpressed FLAG-tagged constructs were evaluated in NIH3T3 fibroblasts. As shown in Figure 15A, deletion of the 9 helices of the CTD in SMYD3(1–279) eliminated nuclear localization (compare lanes 5 and 6), whereas deletion of helices 7–9 in SMYD3(1–364) (lanes 3 and 4) showed no difference with wildtype (WT, lanes 1 and 2). Thus, nuclear entry function resides within helices 1–6 of the CTD. Potentially relevant is the previous observation that the predictive general nuclear localization sequence (NLS) for Kap β 2 transporter recognition (Φ G Φ X13RX3 PY; Φ , any hydrophobic residue) [126] matches the SMYD3 sequence from L341 to Y358. This sequence and, particularly the P357Y358 essential for Kap β 2-NLS recognition, are not exposed, but buried by helices 7–9 of the CTD of SMYD3, suggesting HSP90 C-terminal binding may serve to expose the putative NLS.

Next we tested whether the HSP90 binding requirements established in vitro were observed in cells. Following over-expression of the indicated SMYD3 constructs of Figure 15B, ~5% of the protein was reserved for Input (lane 1) and the remainder was subjected to antiSMYD3 or anti-HSP90 immunoprecipitation (IP; lanes 2 and 3) with pre-immune sera (α -Ig) serving as a control (lane 4). Complexes were resolved on SDS-PAGE, and

interactions of over-expressed SMYD3 with endogenous levels of HSP90 were assessed by anti-HSP90 and anti-FLAG western blotting. Strong, reciprocal interaction was observed for SMYD3 WT, whereas no interaction was detectable if helices 7–9 were truncated [SMYD3(1–364), Figure 15B]. Each of the SYMD3 point mutants which had reduced or no interaction with HSP90 in vitro (**Figure 14B**) showed highly reduced interactions in NIH3T3 cells (**Figure 15B**).

The lack of association between HSP90 and SMYD3 mutants raised the possibility that HSP90 interaction with SMYD3 CTD, and particularly helices 7–9, is essential for SMYD3 nuclear transport. To address this, we overexpressed select SMYD3 substitution mutants (**Figure 15C**), fractionated the NIH3T3 cells into cytoplasmic (C), soluble nuclear (N), chromatin (Ch) and nuclear matrix (NM) components and then carried out semi-quantitative antiFLAG Western analysis. Established markers (bottom 3 panels) validated purity of the sub-fractions. As previously shown [74, 127], HSP90 accumulates in the cytoplasm (C) and within the soluble and chromatin sub-fractions (**Figure 15C**, lanes 1 and 3). WT SMYD3 accumulated in a similar pattern as HSP90. While nuclear localization was achieved with SMYD3(1–364) and each of the nonHSP90 interacting point mutants, they were mislocated to various extents, with virtually complete loss of K375A and H382A from chromatin into the nuclear matrix (compare lanes 3 and 4). Hence, association of the SMYD3 CTD with HSP90 is not required for nuclear transport per se but is required to distribute SMYD3 to its site of functional catalysis-nuclear chromatin.

CTD-HSP90 interaction is required for maximal SMYD3 stimulation of cell proliferation

Although maximal nuclear activity of SMYD3 requires HSP90 association, its activity against cytoplasmic targets may be uncompromised and hence may not require HSP90 interaction for its oncogenicity. Numerous studies [50, 54, 128-130] demonstrated proto-oncogene-type actions of SMYD3 under conditions of genetic-based promoter mutations leading to gain-of-function in malignant tumors or following enforced ectopic over-expression in non-transformed cells. HSP90 assists in the folding and function of numerous proto-oncogenes, as its inhibition by small molecules or siRNA leads to their destabilization and subsequent suppression of malignancy. As shown in **Figure 16**, stable over-expression of wildtype SMYD3 in mouse embryonic fibroblasts (MEFs) leads to a statistically significant ($p < .001$) approximately 3-fold enhancement in proliferation relative to vector control. This enhancement is significantly abrogated to varying extents in SMYD3 CTD mutants impaired in HSP90 interaction. Specifically, we observed low statistical difference ($p < 0.10$) between vector-only and all CTD mutants which lose HSP90 association, whereas the I339A mutation which retains HSP90 association trends much more closely to that of WT SMYD3 ($p < 0.10$). We did not observe significant changes in morphology, adhesion or cell migration following enforced expression of SMYD3, as was observed in some previous reports [50, 54, 128-132]. That these previous enforced expression studies were performed in transformed cell lines, which quite probably express higher levels of endogenous SMYD3 than did our diploid MEF transfectants, may account for this difference.

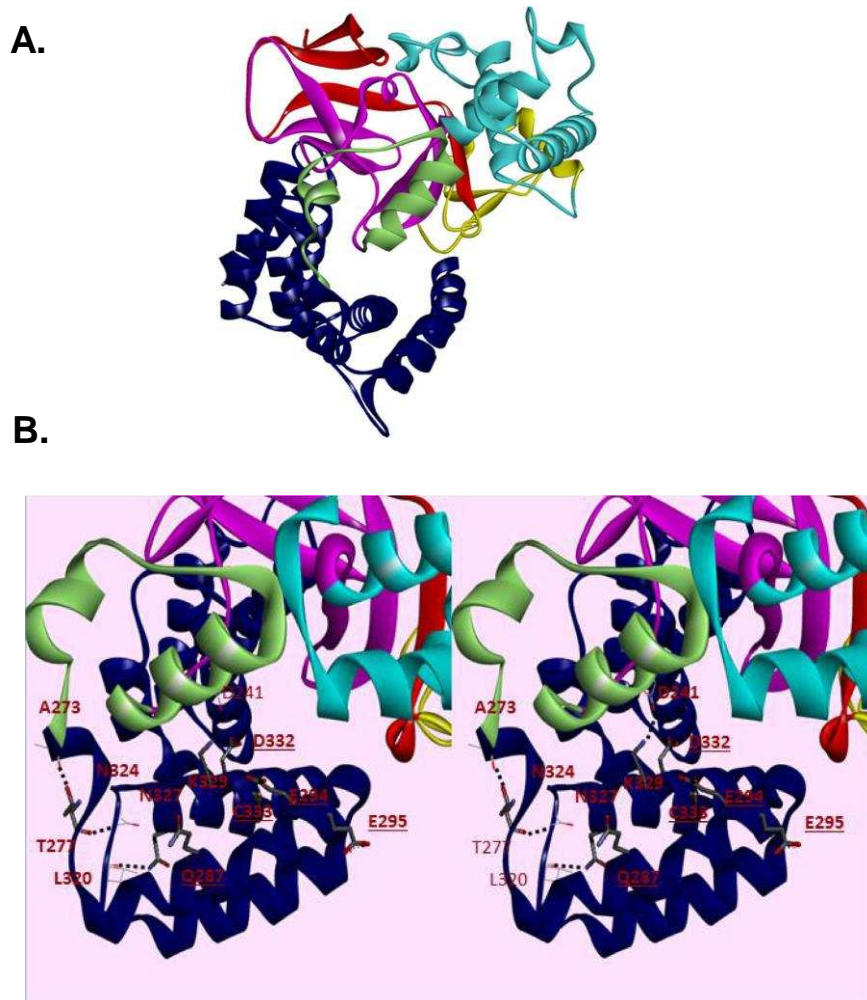


Figure 10: Structure of SMYD3. (A) Structure of SMYD3 colored by domain components. SMYD3 has 6 domain components: N-SET (red), MYND (Yellow), I-SET (cyan), C-SET (magenta), post-SET (pale green), and the CTD (blue). (B) **Cross-eye Stereo view of helices 1–6 of the CTD of SMYD3.** SMYD3 domains are colored separately, with the CTD colored blue. Residues conserved in SMYD3 orthologs but not paralogs are displayed in thick bonds. Dashed lines indicate hydrogen bonds. Underlined residues are available on the surface for interactions. Other domains include the N-SET (red), MYND (yellow), I-SET (cyan), C-SET (magenta) and the post-SET domain (pale green).

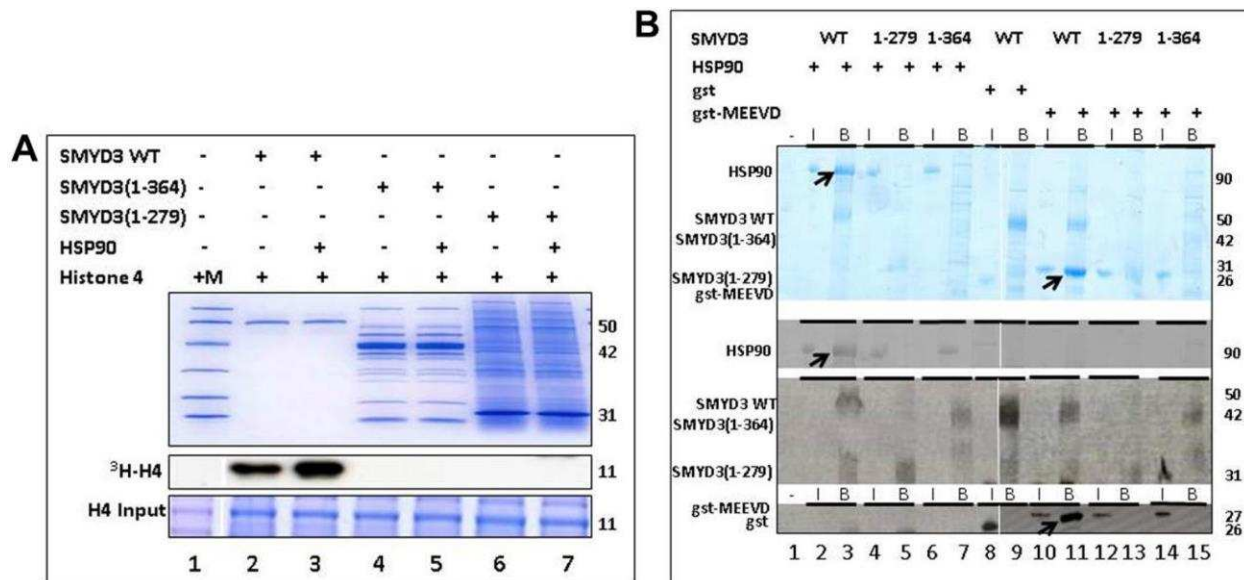


Figure 11: The SMYD3 CTD is required for binding and enhanced Histone Methyltransferase Activity (HMTase) by HSP90. (A) Truncation mutants were expressed in *E. coli* and validated for purity on 10% SDS-PAGE stained with Coomassie Blue (Upper panel). Equal amounts of truncated and wildtype (WT) SMYD3 were then compared for *in vitro* HMTase activities in the presence or absence of HSP90 by ³H-S-adenylmethionine incorporation into histone H4 (3H-H4) followed by gel fractionation and autoradiography after loading onto a separate 20% SDS-PAGE (lower and middle panels). The SMYD3(1–279) truncation eliminates the entire CTD, while SMYD3(1–364) lacks the final 3 helices of the CTD. Molecular weights in kD indicated to the right of each panel were determined from marker mix (M, included in Lane 1 with H4 only) which, as indicated by the blue vertical line was run on parallel 10% and 20% gels. (B) The SMYD3 CTD is required for binding of HSP90 and for binding to a pentapeptide MEEVD previously shown [29] to be sufficient for the interaction of HSP90 and a TPR domain within the immunophilin, FKBP52. Nickel-NTA beads were mixed with ~1 μg wildtype (WT) 6X-His-SMYD3 or ~1 μg 6X-His-mutants in which the entire CTD (1–279) or its C-terminal 3 helices (1–364) were truncated. The slurries were incubated with either HSP90α or GST-MEEVD and bound protein (B lanes) was eluted from the beads and analyzed on 12.5% SDS-PAGE. For input controls (I lanes), 10% of the amounts of HSP90α and GST-MEEVD used for binding reactions were processed identically but in the absence of 6X-His-SMYD3. Band assignments (left) were made by sizes of Coomassie stained bands (upper panel) as judged by migration of a standard molecular weight marker mix (not shown). These assignments were confirmed (lower panels) by western blotting using antibodies (indicated on the left) specific for SMYD3, HSP90 and GST. Arrows denote positions of WT bound HSP90 or GST-MEEVD. Molecular weights are indicated on the right in kD. Blue vertical lines denote composites of lanes run on parallel gels repositioned to emphasize outcomes.

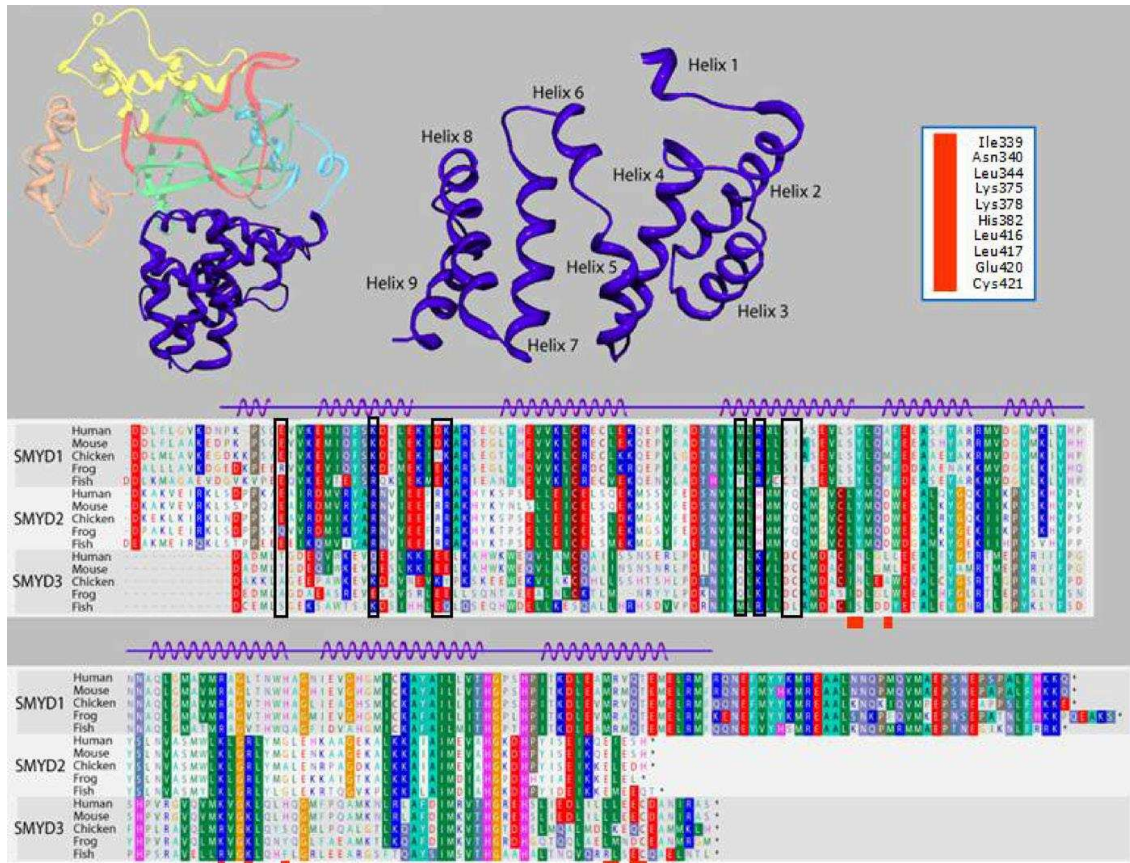


Figure 12: Alignment of the carboxyl terminal (CTD) domain from SMYD3 orthologs and paralog. Structure of the 9-helix bundle SMYD3 CTD (right upper panel, blue). The primary human sequence of SMYD3 CTD is aligned (lower panel) with corresponding CTDs of closest paralogs, SMYDs1 and 2, in multiple species. Residues are colored according to their physical properties. For example, all shades of red represent acidic residues, all shades of blue represent basic residues, and all shades of green represent hydrophobic residues. Black boxes in the alignment indicate residues conserved among orthologous SMYD subfamilies but not among paralogs in the same species. Red boxes below the alignments correspond to the SMYD3 residue labels in the upper right hand corner. These residues are modeled as being within 6Å of the MEEVD C-terminal peptide from HSP90 in human SMYD3 (see Figure 13B) or were mutated (see Table 4).

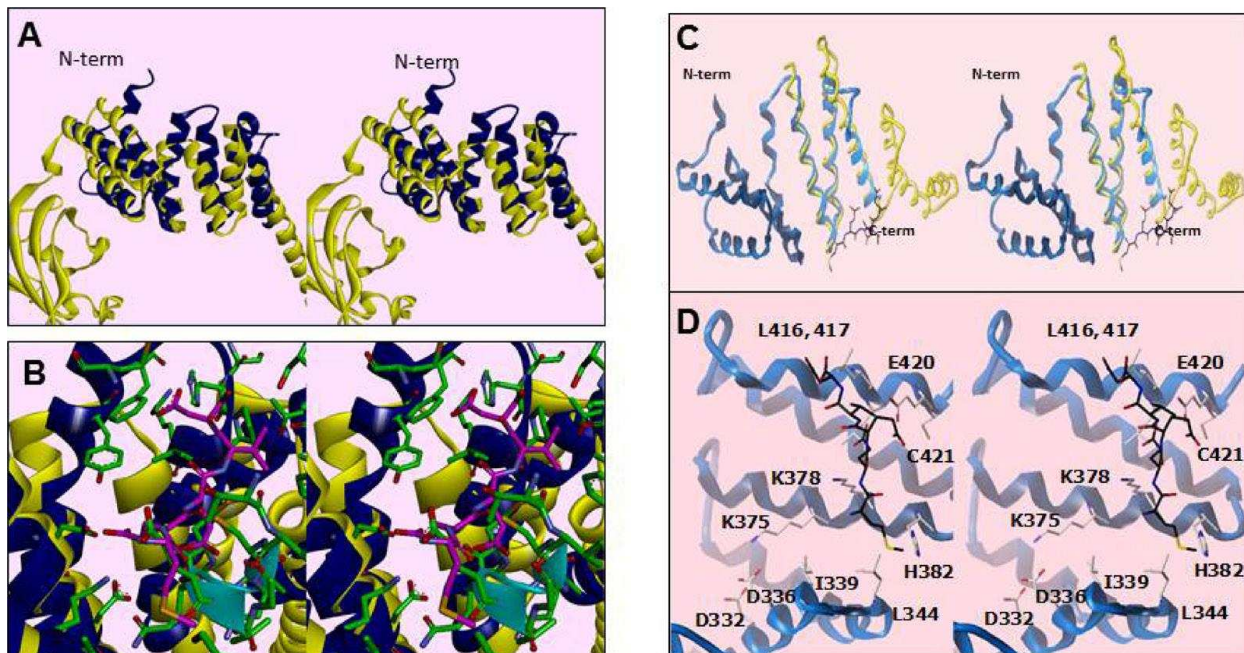


Figure 13: Residues within a degenerate tetratricopeptide (TPR)-like domain within the SMYD3 CTD mediate HSP90 interaction. (A) Cross-eye stereo recapitulation of the modeled overlay of SMYD3 CTD (blue) with the TPR motif from FKBP52 (yellow) as in [20, 21, 26]. The N-terminal of the CTD is labeled for clarity of orientation. **(B)** Stereo close-up of the overlay in Figure 13A, with ribbon coloring retained. Residues from SMYD3 are in green while the MEEVD pentapeptide from the C-terminus of HSP90 in the FKBP52-bound structure is in magenta. The residues from the I-SET domain are marked by the cyan ribbon. **(C)** Stereo depiction of the current publication's modeled overlay of helices 7–9 of the SMYD3 CTD (blue) with the HSP90-binding region of FKBP52 (yellow). **(D)** Stereo close-up of the overlay in Figure 13C, with ribbon coloring retained. Residues from HSP90 are in black, while those from SMYD3 are in off-white. Residues in the vicinity of the modeled HSP90 peptide are labelled.

Table 4: Summary of HSP90 binding and histone methyltransferase activities following truncation or point mutation of residues within the SMYD3 CTD. §Mutated residues conserved among SMYDs 1, 2, 3 and/or FKBP52 (F); #ratio of HSP90-induced to basal- *in vitro* SMYD3 HMTase activities for the indicated construct (Methods and Materials). A minimal number of 4 biological replicates were measured to determine ratios, standard deviations, and statistical significance. Basal levels were eliminated by the two CTD deletions [SMYD3 (1-364) and (1-279)] but remained essentially unchanged for any of the point mutations listed here. **SMYD3 side chain predicted to be within 6Å of bound HSP90 pentapeptide, MEEVD; ***SMYD3 surface residue; †Critical SMYD3 structural element.

SMYD3	conserved in SMYDs/FKBP52§	induced/basal HMTase#	K _d (μm) HSP90	K _d (μm) MEEVD	p value
WT		4.8 ± 0.7	18 ± 4	55 ± 12	< .001
1-279		< 0.1	>1000	>1000	< .001
1-364		< 0.1	>1000	>1000	< .001
I339/A†	1, 2, 3, F	2.4 ± 0.5	352 ± 29	544 ± 88	< .05
N340/A***	1	3.0 ± 0.4	39 ± 14	78 ± 14	
L344/A**,***	1	3.8 ± 0.7	14 ± 7	85 ± 19	
K375/A†	1,2,3	1.1 ± 0.2	526 ± 90	670 ± 122	< .01
K378/A**,***	2,3,F	3.3 ± 0.6	31 ± 4	33 ± 13	
H382/A**,***	1,3,F	0.6 ± 0.4	777 ± 63	868 ± 94	< .01
L417/A**,†	2,3,F	3.2 ± 0.5	96 ± 19	40 ± 10	
E420/A**,***	1,3,F	3.9 ± 0.6	48 ± 16	30 ± 8	
C421/A†	1	1.0 ± 0.2	710 ± 132	850 ± 77	< .01
C421/S†	1	0.6 ± 0.3	622 ± 111	932 ± 205	< .005

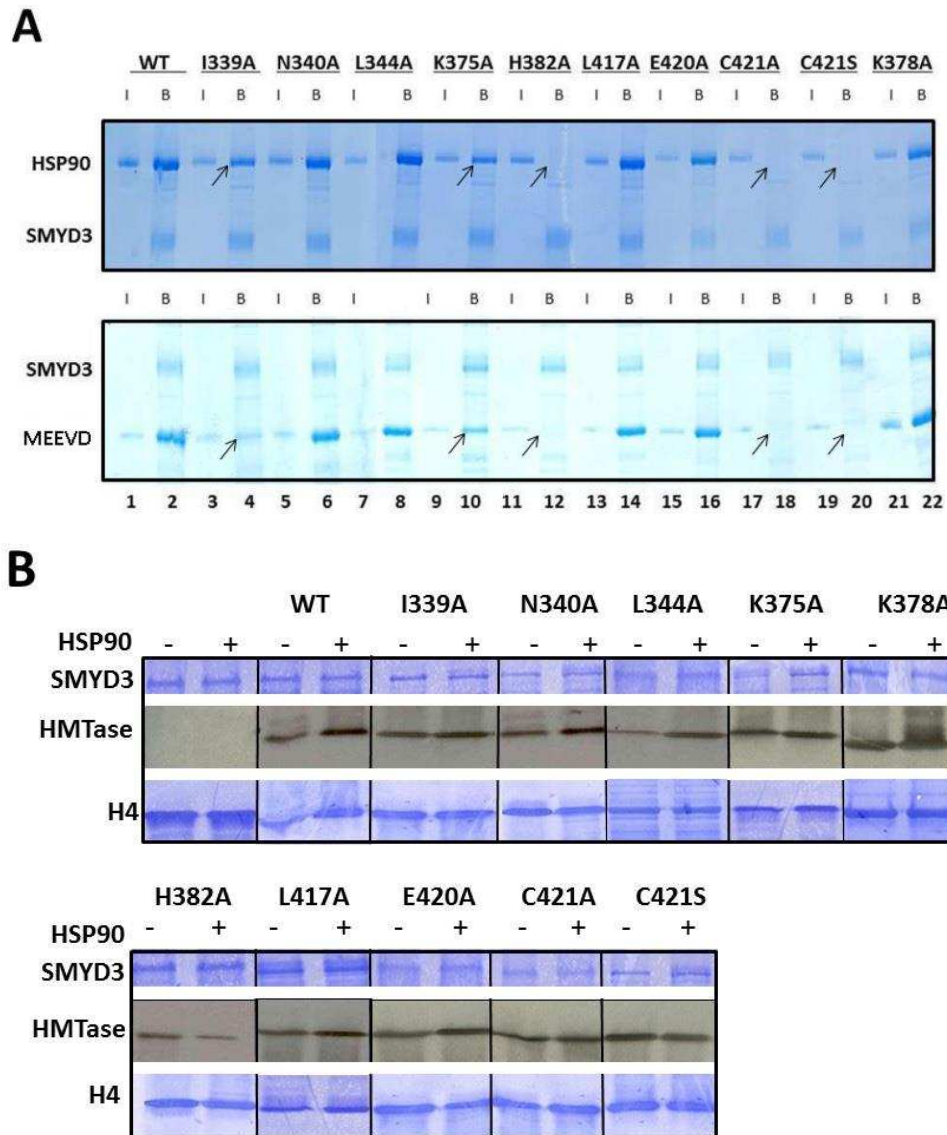


Figure 14: Enhancement of basal HMTase activity of SMYD3 requires binding of HSP90 to conserved residues within a TPR-like region of the CTD. (A) Conserved residues within a TPR-like region of SMYD3 CTD are required for HSP90 and MEEVD binding. Residues mutated (detailed in Materials and Methods) were predicted to interact with the HSP90 peptide or to be critical for CTD integrity. Nickel-NTA beads were mixed with ~1 μ g wildtype (WT) 6X-His-SMYD3 or ~1 μ g 6X-His-mutants. The slurries were incubated with either HSP90 α or GST-MEEVD and bound protein was eluted from the beads and analyzed on 12.5% SDS-PAGE. Arrows denote loss of SMYD3-mutant interaction. Blue vertical lines denote repositioning of lanes run on the same gel repositioned to emphasize outcomes. **(B)** CTD residues required for HSP90 binding are required for HSP90-mediated enhancement of SMYD3 HMTase activity. *In vitro* 3H-SAM HMTase assays (autoradiographs, center panels) were performed as described in Materials and Methods and in the legend to Figure 11A. Inputs are shown by Coomassie stains in upper (SMYD3 WT and mutants) and lower (recombinant histone H4) panels.

Blue vertical lines denote repositioning of lanes run on the same gel repositioned to emphasize outcomes.

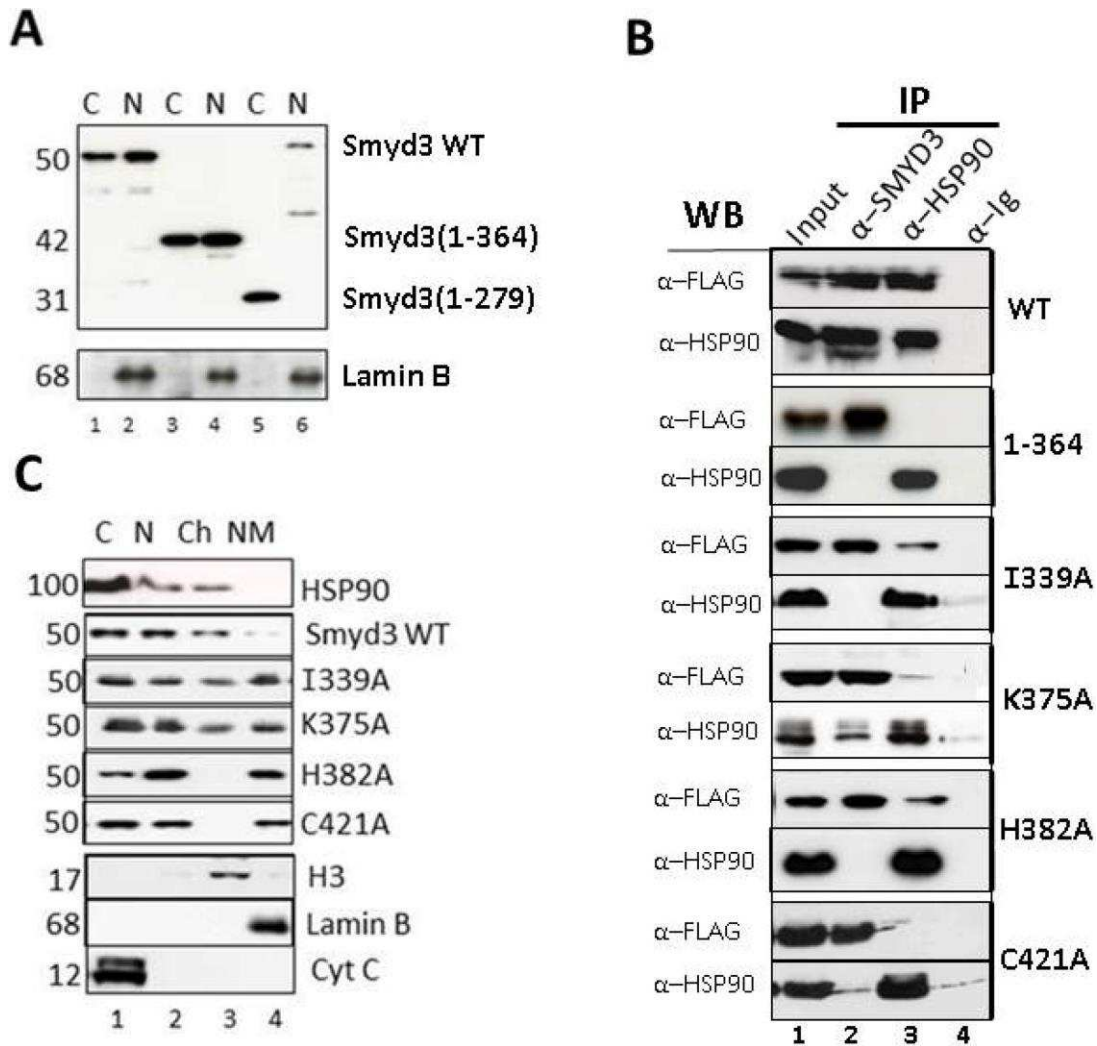


Figure 15: TPR residues of SMYD3 CTD are essential *in vivo* for nuclear localization, HSP90 interaction and sub-nuclear sequestration into chromatin. (A) Deletion of the 9 helices of the CTD eliminates nuclear localization. Upper panel: NIH3T3 cells were transiently transfected with the indicated FLAG-tagged SMYD3 WT or deletion mutants, separated into nuclear (N) and cytoplasmic (C) fractions, and protein lysates were analyzed by SDS-PAGE/anti-FLAG western blotting. Purity of the fractions and confirmation of equal protein inputs was confirmed by anti-Lamin B western (lower panel). **(B)** Confirmation *in vivo* of SMYD3-HSP90 interactions established *in vitro*. Following transient transfection of the indicated FLAG-tagged wildtype (WT) and CTD point mutants into NIH3T3 cells, ~5% of the whole cell lysate was reserved for Input (lanes 1) and the remainder was subjected to immunoprecipitation with antibodies (α) specific for SMYD3 or HSP90 (IP; lanes 2 and 3) with pre-immune sera (anti-Ig, lanes 4) serving as negative control. Complexes were resolved on SDS-PAGE, and interactions of over-expressed SMYD3 with endogenous levels of HSP90 were assessed by anti-HSP90 and anti-FLAG western blotting. **(C)** CTD mutation perturbs distribution of SMYD3 within sub-nuclear compartments. Following over-expression of the indicated FLAG-tagged constructs,

NIH3T3 cells were fractionated into cytoplasmic (C), soluble nuclear (N), chromatin (Ch) and nuclear matrix (NM) and following resolution on SDS-PAGE, protein subcellular localization was assessed by semi-quantitative anti-FLAG Western analysis. Western blotting with established markers (indicated in bottom 3 panels) validated purity of the sub-fractions.

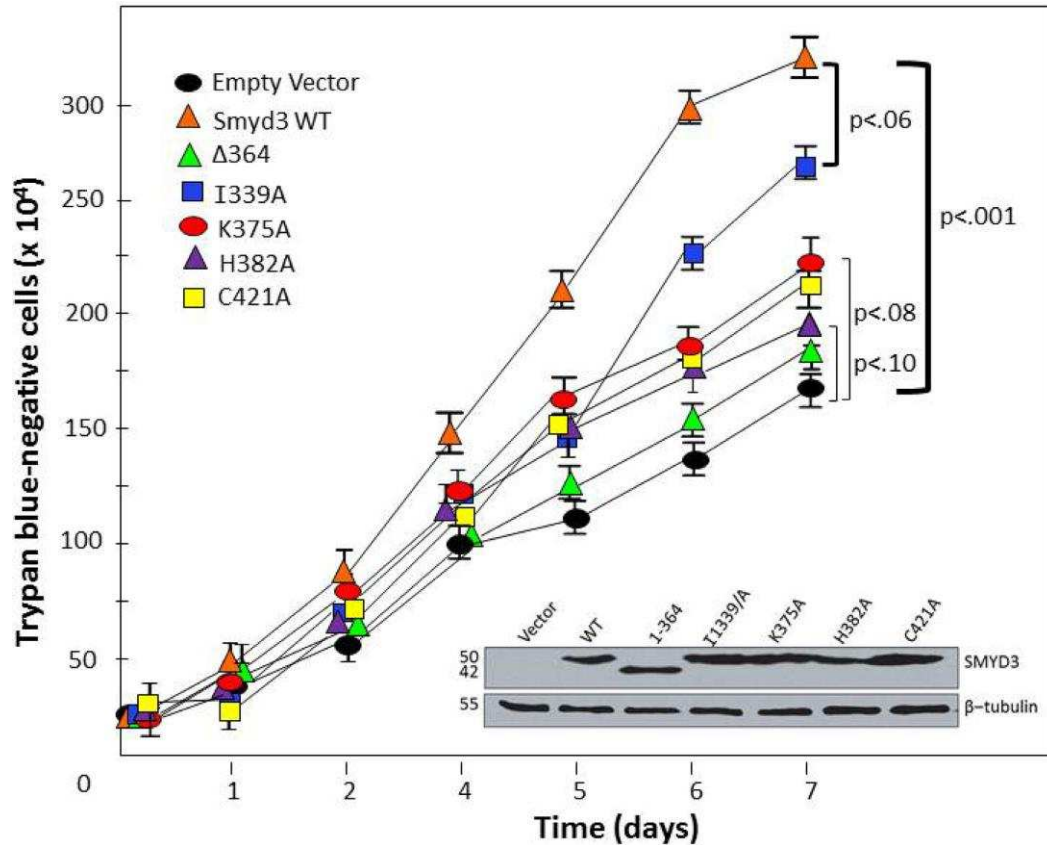


Figure 16: CTD-HSP90 interaction is required for maximal SMYD3 stimulation of cell proliferation rate. The indicated WT and mutant constructs (top left) were transiently transfected into mouse embryonic fibroblasts. Relatively equal levels of expression were confirmed by Western blot of total cell lysates at day 1 (inset). Proliferation rates were assessed at the indicated time-points following transfection by counting trypan blue-negative (living) cells. Growth curves are shown as averages of 4 independent experiments with standard deviations (I) Brackets denote paired *t*-test-derived mean-difference probabilities (*p*) with width of the bracket representing magnitude. Δ364 stands for SMYD3 (1–364).

B. CONCLUSION

SMYD3 is overexpressed in a variety of tumor types, including hepatocellular carcinomas and breast cancers, with poor prognosis commonly observed [41]. It is an important epigenetic regulator, known to methylate histones at several sites, including H4-K20. We demonstrate that the C-terminal domain (CTD) is essential for SMYD3's histone methyltransferase (HMTase) activity, as truncates of either the whole CTD or even just the three C-terminal helices of the CTD suffice to eliminate basal methylation of H4, both *in vitro* and *in vivo*. A central hypothesis proposed in the analysis of SMYD1 as applied to SMYD3 [20] conflicts with our results. Based on the differential geometries adopted by the CTDs of SMYD1 and SMYD3, those authors speculated that the SMYD3 CTD must undergo a hinge-like movement to relieve its inherent auto-inhibition of substrate entry and/or release, suggesting that the CTD serves mainly a regulatory role. In contrast, we directly demonstrated that CTD deletion greatly reduced enzymatic activity (Figure 11A and Table 4), suggesting that, at least for basal histone catalysis, the CTD stabilizes the SMYD3 active site.

To further understand the binding determinants of this regulatory site, we hypothesized that HSP90, which is known to stimulate SMYD family HMTase activity upon binding, interacts with the final three helices of the CTD. This proposal stands in contrast to earlier predictions which suggested that the entire CTD should interact with HSP90, based on overlays between the CTD and the HSP90-interacting tetratricopeptide repeat (TPR) domain of FKBP52. Detailed analysis of the HSP90 binding site modeled onto SMYD3 suggested several residues important for binding. These residues are conserved among both SMYD3 paralogs and orthologs, indicating potential functional

significance. Our data establish a strong correlation between modification of these terminal helices, either through truncation or through point mutations, and sensitivity to HSP90 activation. Most strikingly, the side chain of H384 points out into solvent and is not expected to play a role in SMYD3 CTD conformational integrity but is predicted in our model to play an important role in HSP90 C-terminal recognition. As predicted, the H384A substitution mutant suffers near complete loss of HSP90 activation of SMYD3 both in *in vitro* and cellular contexts, suggesting the modeled binding model is indeed predictive. Only the last 5 C-terminal residues of HSP90 (MEEVD) play a significant role in SMYD3 activation, as association and activation patterns are nearly identical between the full length HSP90 and the 5-mer (Table 1).

The TPR-like CTD of SMYD3 also appears necessary for cell localization and for nuclear trafficking. Indeed, the TPR motif has been well documented for its role in HSP90-dependent protein localization [42]. For example, mitochondrial localization of the immunophilin FKBP51 is dependent upon HSP90 via the TPR motif of FKBP51 [43]. Without a TPR motif and/or in the absence of HSP90, FKBP51 translocates to the nucleus where it has been shown to prevent oxidative stress [43]. Conversely, the association of many nuclear hormone receptors with TPR-motif containing proteins is known to facilitate their transport into the nucleus via association with HSP90 complexes [42]. Such is the case with the mineralocorticoid receptor which is transported into the nucleus by way of its association with TPR-containing FKBP52 in an HSP90 complex [44].

Our results indicate that a substantial, if not exclusive, component of SMYD3-driven proliferation derives from its CTD interaction with HSP90. HSP90 facilitates SMYD3 localization with chromatin and generically prevents SMYD3 destabilization. While we

cannot exclude HSP90 catalyzed stabilization of SMYD3 as the primary driver of the proliferation results, the fact that MEEVD suffices to activate SMYD3 *in vitro* but is not considered relevant to HSP90's chaperone function suggests HSP90 most likely serves to relieve the regulatory components on SMYD3 to enable SMYD3's epigenetic function. Nevertheless, sorting out the relative importance of these multiple HSP90 interaction with SMYD3 in native and oncogenic environments warrants further exploration. Based, then, on our data, a model of SMYD3- HSP90 cooperatively in heritably altering chromatin states emerges, with HSP90 interactions with the CTD of SMYD3 proceeding via a two-component regulatory motif. The terminal helices 7–9 in this motif serve as a regulator of both the nuclear localization and compartmentalization sequences, with regulation of the latter facilitated through the enhanced accessibility of histone substrates. Relief of this HSP90-dependent regulatory feature permits a conformation in SMYD3 that supports efficient substrate binding. The remainder of the CTD (helices 1–6) serves as a binding enhancer and specificity determinant for SMYD3 substrates. Increasing levels of SMYD3 in the presence of HSP90 effectively allows HSP90 to transform into an epigenetic agent.

Given the general nature of HSP90 as a stress sensor, the connection between HSP90 and SMYD3 offers a unique opportunity for insight into oncogenesis and possibly evolution. Since most cancerous cells are in a perpetually stressed state, teetering on the brink of apoptosis, they face continual selection pressure, much like evolving organisms do. Activation of epigenetic stress response pathways should permit those cells to access survival mechanisms that might not otherwise be accessible under lower stress conditions. Generically, oncogenesis and metastasis require the manipulation of several processes, such as metabolic and cell cycle checkpoints, apoptosis,

expression/repression of cell adhesion and motility factors, and recruitment of angiogenic factors. The scope of this process is analogous to measures that are required for resetting a differentiated cell to a state of pluripotency, followed by selection of another differentiated state, and favors the conditions required for rapid mutagenesis and microevolution. HSP90, also termed the 'cancer chaperone', has a central role in these processes by maintaining the stability and activity of many client proteins which are essential for each process [13]. SMYD3 appears to place suppressive marks in normal cells, but may inappropriately place activating marks on other residues over time when continually overexpressed. This role reversal may occur because, even though SMYD3 has greater affinity for the H3-K4 site than for other histone peptide sequences, the specificity of its MYND domain partners prevent it from interacting significantly with those sites in normal cells. Overexpression may lead to saturation of those partner binding sites which would then permit SMYD3 recognition of these alternate high affinity sites. HSP90 putatively helps stabilize, localize, and activate the excess SMYD3, allowing continuous methylation of its targets. Such expression levels would be permanently achieved by the types of malignancy-associated SMYD3 promoter polymorphisms previously observed [11, 12, 45], leading to rapidly proliferative clonal expansion well beyond what we observed in our data of Figure 16. Clearly, the ability to prevent reversion to a more pluripotent state in the first place may suffice to significantly reduce the short term threat from cancers, suggesting the interaction between HSP90 and epigenetic proteins such as SMYD3 needs a closer inspection.

CHAPTER 4 – THE IMPACT OF SMYD2 IN SPECIFIC MODELS OF HEMATOPOIETIC MALIGNANCIES

Hematopoiesis is the pathway of cellular development that produces all of the cells that circulate in the blood [88, 96]. These cells include red blood cells and platelets in addition to immune cells such as macrophages, B cells and T cells. The process of hematopoiesis starts with a pluripotent, self-renewing hematopoietic stem cell (HSC). The HSC differentiates into early progenitor cells, which will develop into one of two distinct lineages, the myeloid and the lymphoid lines. These two lineages have committed precursors which further generate the multiple cells in the HSC pathway. Hematopoiesis occurs in the adult bone marrow and is triggered by a series of signals transported through the stromal environment. Many cells in this pathway undergo maturation via a progression of stages and selection. Aberrations in the hematopoietic cells result in a multitude of leukemias and lymphomas defined and named by the cell in which the transformation occurred (**Figure 18**). Many of these cellular transformations possess chromosomal translocations which cause activation through transgene expression.

Chromosomal rearrangements generally occur at a specific stage in somatic cell types. These cells, such as those in hematopoiesis and during gametogenesis, undergo rearrangements in order to generate diversity. This process, though, can result in mutations as there is an exchange of genetic material between two non-homologous chromosomes. Each chromosome would have undergone double stranded DNA breaks through genetic instability or enzymatic activity. The exchange and joining of the double stranded breaks cause an aberrant exchange of genetic material between the

chromosomes called a translocation (Figure 17). One or more oncogenic translocations are found in most cancers.

In hematopoietic malignancies, there are several well studied oncogenic translocations. The Philadelphia chromosome, a translocation between chromosomes 9 and 22, causes the production of a fusion genes known as BCR-Abl. This transgene remains constitutively active as a kinase, inducing cell signaling, deregulating proliferation, and prevention of apoptosis. The Philadelphia chromosome, or t(9:22), is present in 95% of chronic myeloid leukemia (CML) incidents.

Current treatment options include a hematopoietic stem cell transplant to repopulate healthy, non-transformed cells in addition to a drug Imatinib by Gleevec, that inhibits the kinase activity of the transgene. Unfortunately, compatible bone marrow donors are not always available and the effect of the drug is short lived.

Translocations involving the mixed lineage leukemia gene are also present in the hematopoietic pathway. Much like the SMYD proteins, the MLL gene produces a protein that methylates H3-K4. MLL fusion proteins have demonstrated the ability to transform hematopoietic cells into leukemic stem cells.

Here we turn our attention to SMYD2 and its putative role in hematopoietic carcinogenesis. In order to study the effect of SMYD2 in tumor initiation, we employed transforming oncogenes to study the consequences of SMYD2 loss in three hematopoietic models: B-Acute Lymphocytic Leukemia (ALL), Chronic Myeloid Leukemia (CML), and Mixed Lineage Leukemia (MLL). Loss of SMYD2 in CML and MLL, but not in B-ALL, models led to cell cycle block following by rampant apoptosis and cell death. Tumorigenicity, as assessed *in vitro* by colony formation and *in vivo* by NOD/SCID

transformation, was dependent upon SMYD2. Gene expression analyses indicated that, as previously determined in multiple studies, impairment included reduction in the level of the p53 tumor suppressor. Collectively, these studies establish SMYD2 as a putative proto-oncogene in CML and MLL.

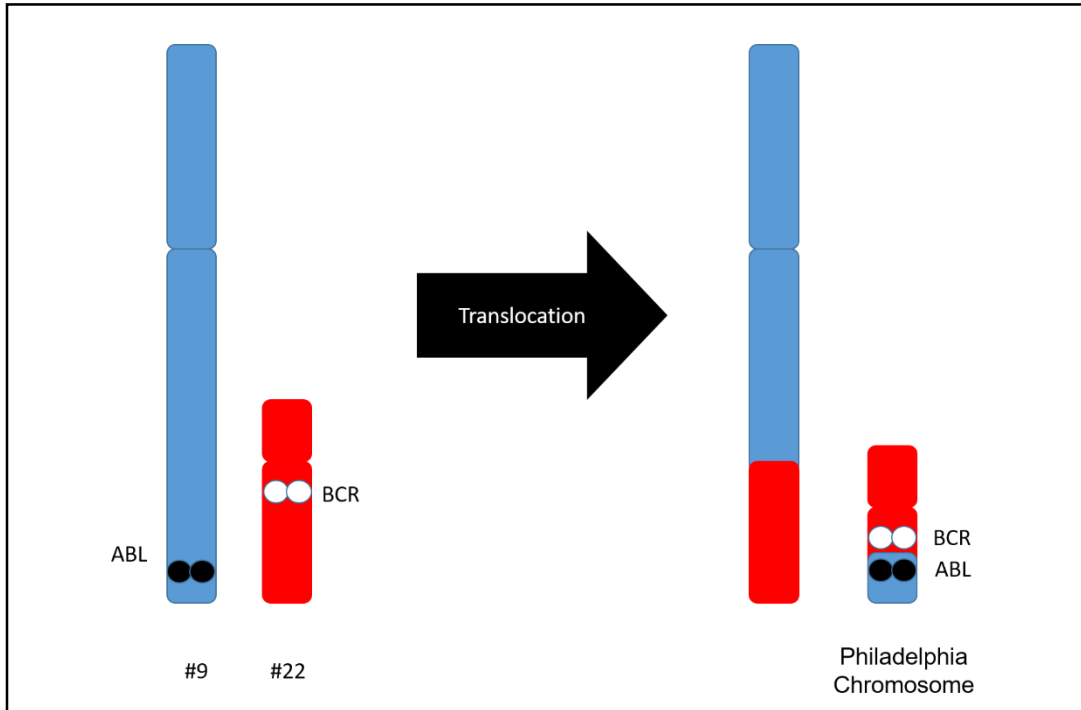


Figure 17: The Philadelphia Chromosome. A depiction of the translocation between chromosomes 9 and 22 resulting in the fusion gene Bcr-Abl also known as the Philadelphia Chromosome [133].

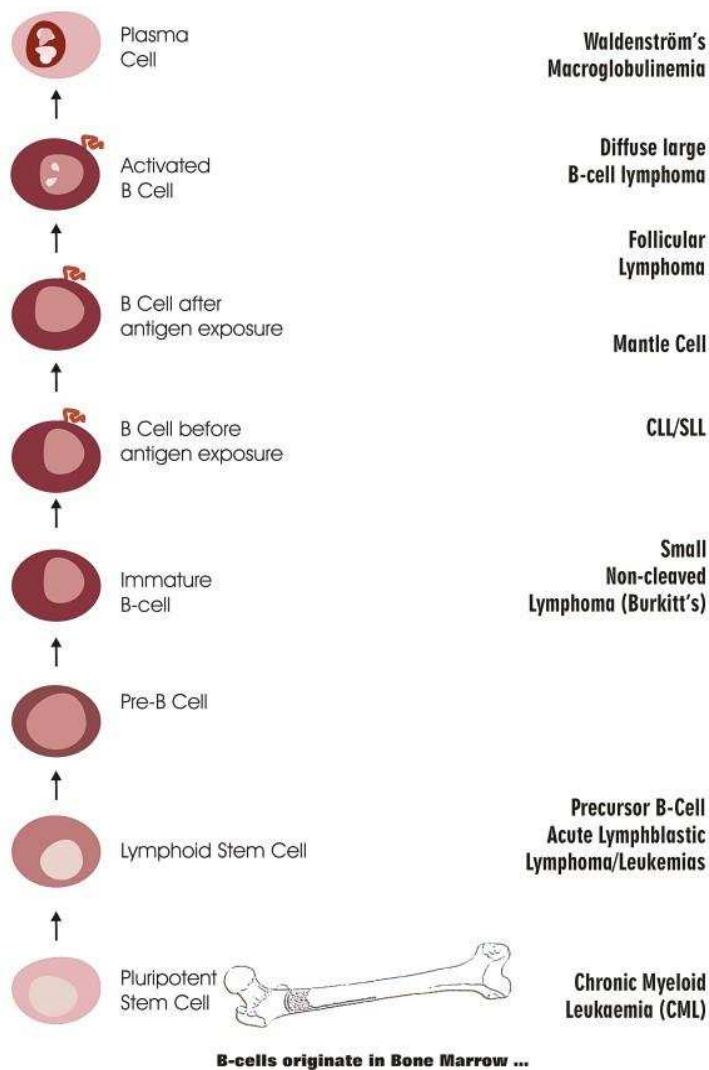
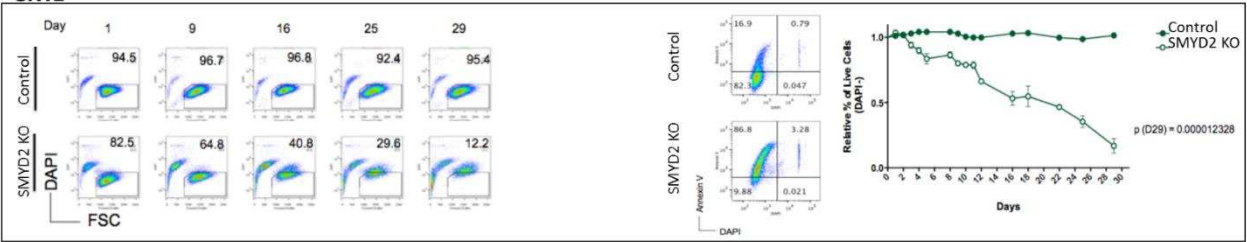


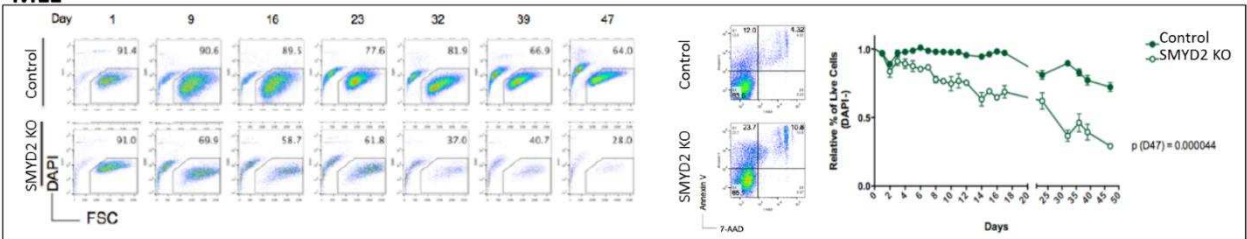
Figure 18: Points of transformation in various hematopoietic derived malignancies. An illustration of select cells in the hematopoietic pathways during maturation and associated tumorigenic states. Some of these cancer phenotypes are also connected to transgene expression caused by chromosomal translocations.

A. RESULTS

CML



MLL



ALL

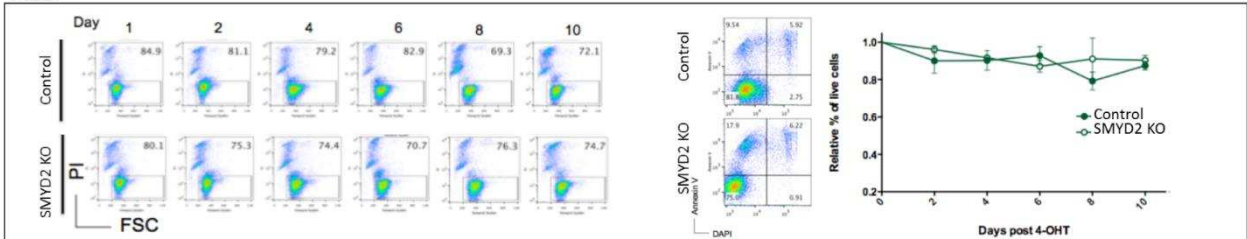


Figure 19: Cell death in HSC tumor models of CML, MLL and ALL when SMYD2 is deleted. Deletion of SMYD2 in MLL and CML cells reduced their viability to 30% on day 47 (MLL) and to 16% on day 29 (CML). The viability of ALL cells, upon SMYD2 deletion, was comparable to the control cells. CML SMYD2 cKO cells have a higher percentage of about 80% of pre-apoptotic cells (Annexin V⁺, DAPI⁻), while MLL and ALL cells showed an increase of about 45% and 52% respectively.

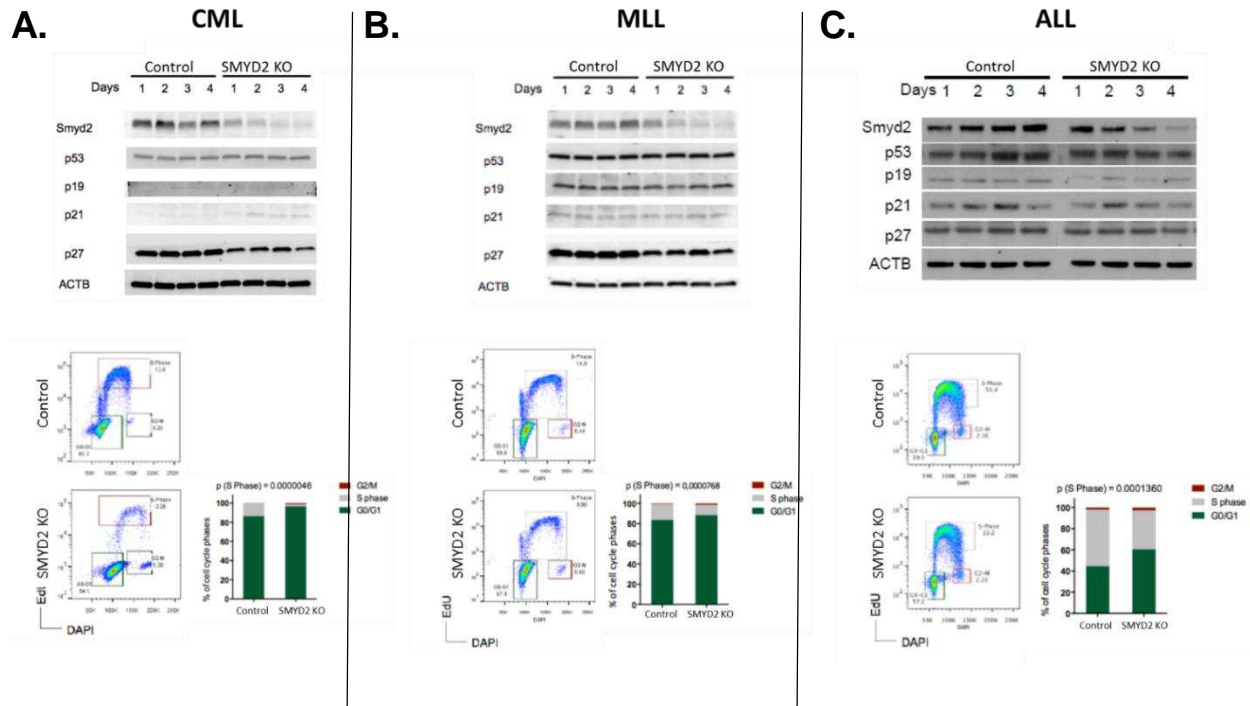


Figure 20: The effect of SMYD2 deletion on cell cycle protein expression and phases in tumor models. Cell-cycle proteins such as p53, p21, Arf and p27 showed no significant changes after the deletion of SMYD2 in the **(A)** CML, **(B)** MLL and **(C)** ALL *in vitro* tumor models. A measurement of 5-ethynyl-2-deoxyuridine (EdU) incorporation by flow cytometry was conducted. CML cells showed a severe block in their cell cycle where an increased percentage of cells were present in G0-G1 phase (about 13% more in CML and 9% more in MLL), accompanied with a reduction in the percentage of cells entering the S phase (82% less in CML and about 33% less in MLL) in comparison to the control. ALL cells also showed an increase in their G0-G1 phase of about 31% and a decrease in their S phase of about 31%.

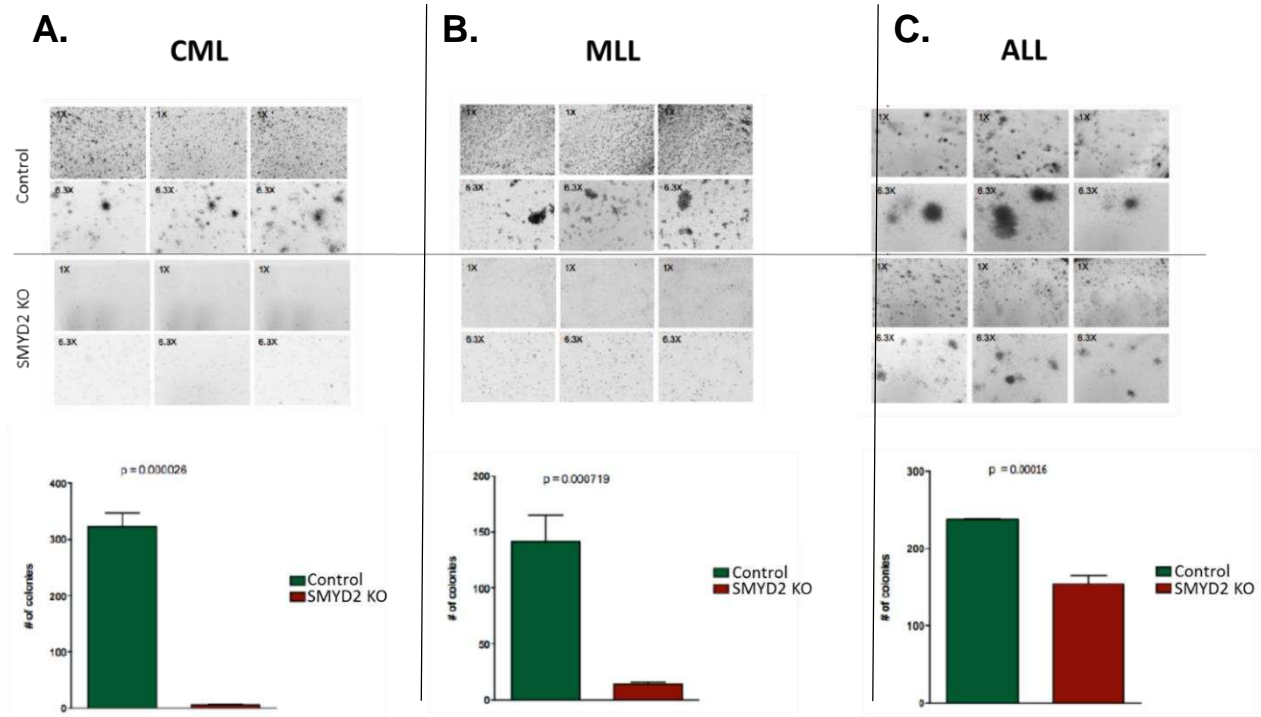


Figure 21: Colony formation reduced in SMYD2 depleted tumor models. After 21 days, in case of **(A)** CML and **(B)** MPP cells, or 14 days, in case of **(C)** ALL cells, CML cells transduced with SMYD2 cKO showed a complete absence of colonies, while MPP and ALL cells transduced SMYD2 cKO showed a reduction in their number of colonies of about 85% and 35% respectively.

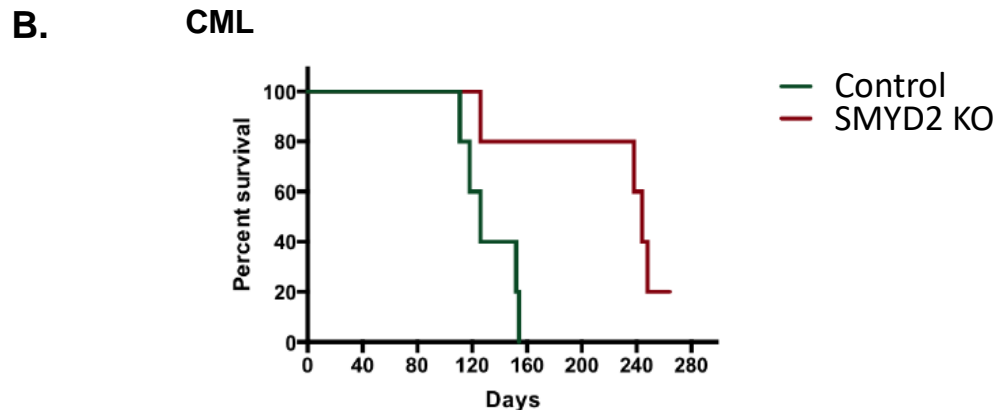
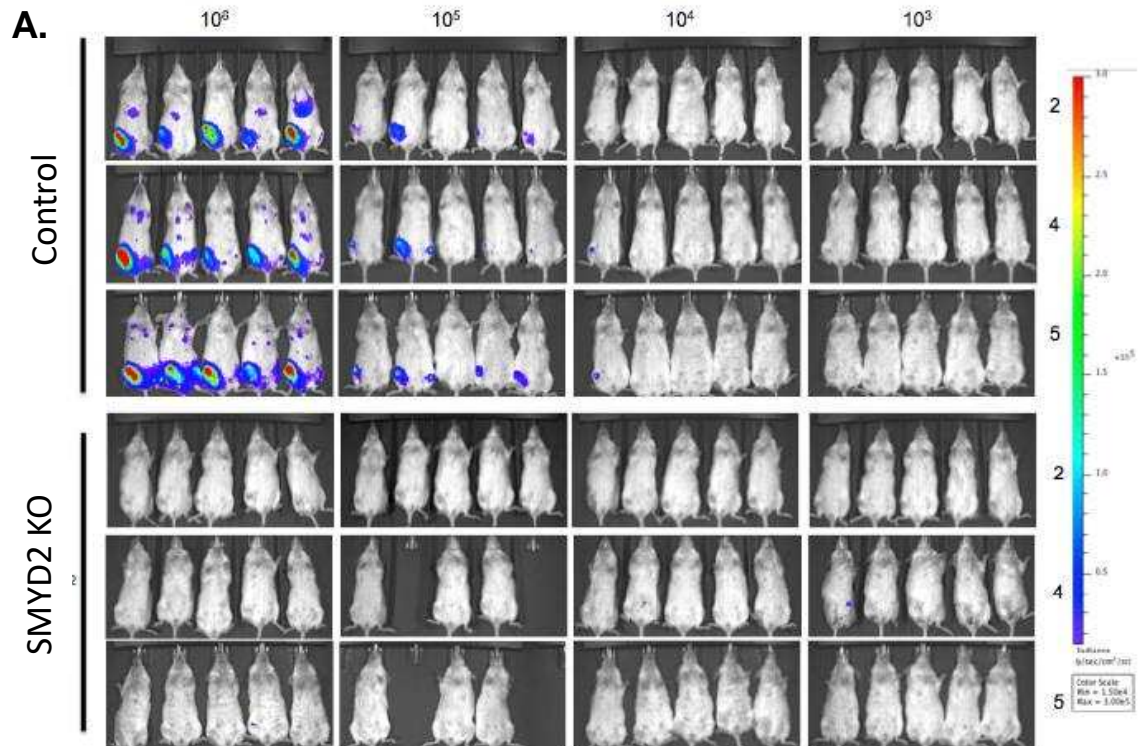


Figure 22: CML-like SMYD2 deleted cells did not result in tumors. (A) In comparison to the control group, SMYD2 cKO-transduced CML cells failed to recapitulate leukemia in the recipient NOD-SCID mice. For tumor formation, 10^3 , 10^4 , 10^5 or 10^6 of non-treated (control) cre-ERT2 ($n=65$) or cre-ERT2 treated with 4-OHT to initiate deletion of SMYD2 ($n= 60$) cells were injected intrafemorally into 6 to 8-week old male NOD/SCID mice. Tumor size was measured by caliper weekly for at least 3 months or until the presence of a tumor diameter $>17\text{mm}$, tumor ulceration or bleeding, when in those cases mice were sacrificed earlier. For examining tumor growth and/or detecting metastasis by bioluminescence imaging, mice were injected with luciferin. The in vivo bioluminescence monitoring was performed in a Xenogen IVIS Lumina II System. **(B)** Is a graphical representation of the survival rate of CML mice injected with 10^6 cells from **(A)**. SMYD2 cKO mice lived almost twice as long as control mice.

B. CONCLUSION

I conclude that SMYD2 contributes to cellular proliferation in hematopoietic malignancies. This was most evident with the absence of SMYD2 in the CML model which impacted cell viability, colony production and tumor formation. These findings support SMYD2 inhibition as a therapeutic means to treating HSC derived cancers. SMYD2 may also be a factor and potential target in the ALL pathway given that colony formation was decreased and the cell cycle was altered. Expression of cell cycle proteins p21 and p19 were affected by the deletion of SMYD2 further supporting its interaction in the p53 pathway. Continued research on the proliferation driving potential of SMYD2 in HSC derived leukemias will likely reveal more connections.

CHAPTER 5 – THE FUNCTION OF SMYD2 IN HEMATOPOIESIS

The SMYDs have demonstrated their propensity for both cellular development and proliferation. When overexpressed, both SMYD2 and SMYD3 have shown to induce tumorigenesis [50, 101, 134-138]. SMYD2, the least characterized of the SMYDs, has been directly linked to immunological tumors when overexpressed and an indicator of poor overall survival [139, 140]. While the localization of SMYD2 in cardiomyocytes is well established, a conditional knockout of SMYD2 showed that it was dispensable for proper embryonic development of the heart [69]. SMYD2 does however methylate two well-known tumor suppressors, p53 [67, 141] and RB1 [65, 66] by which it may regulate cellular proliferation in other systems. Immunological cancers stem from a single pluripotent stem cell, the hematopoietic stem cell (HSC) [88]. From the HSC, all cells that circulate within the bloodstream are produced, including red blood cells, B cells, T cells, macrophages and monocytes.

Here we report our efforts to extend the above findings to the living organism. *SMYD2* was conditionally deleted via *cre/Lox* methodology from the germline of C57BL.6 mice exclusively in hematopoietic progenitors. SMYD2-deficient mice were born healthy and achieved normal lifespans. However, consistent with our findings of Chapter 4, we observed significant blocks in the progression of fetal and bone marrow hematopoietic stem cells to both B lymphocyte and myeloid lineages. While these blocks led to an overall reduction of mature peripheral B cells. These studies further support a model in which SMYD2 is required for normal hematopoiesis.

A. RESULTS

Loss of SMYD2 reduces HSCs

The overall expression of SMYD2 throughout hematopoiesis indicates its potential importance for normal development in the pathway (Figure 9). To determine the effect of HSCs and early progenitors, a conditional knock out of SMYD2 was generated in a murine model. Both an embryonic (*vav* cKO) and an adult inducible (*mx1* cKO) cre-mediated HSC specific promoter were used to delete SMYD2. These cells also possessed an inducible YFP marker to indicate when SMYD2 was deleted.

The *vav* deletion of SMYD2 at the HSC did not prove to be fatal. cKO mice appeared to be as healthy and the same size as control mice and did not encounter a higher disease burden or rate of mortality in comparison to control mice. Litter sizes were average for all mice and the gender distributions were in line with the controls as well. Upon closer inspection of cell populations via flow cytometry, cKO mice did exhibit a depletion of a small subset of the bone marrow hematopoietic stem cell population (**Figure 23**). Despite the loss of this population, the HSCs progressed into the next cell stage to the multipotent progenitor (MPP). The *vav* cKO resulted in increased MPPs contrary to the *mx1* cKO which saw a decrease in those cells. In, the following stage, the lymphoid multipotent progenitor (LMPP), in both models was significantly affected. Again the two deletion models showed opposite trends with the embryonic deletion resulting in increased LMPPs and the *mx1* deletion causing a reduction in the LMPP population. The deletion of SMYD2 shows an early block in hematopoietic stem cells and it may prove to have more severe effects in other cell populations. To determine this, we continued to

look for perturbations in regard to an expansion or depletion of cell proliferation measured by flow cytometry.

SMYD2 increases the population of myeloid and lymphoid progenitors

Downstream of the earliest progenitors, the pathway diverges into one of two very well defined lineages, the myeloid or the lymphoid lines [142]. Each of these are characterized by a committed precursor, either the common myeloid progenitor (CMP) or the common lymphoid progenitor (CLP) [143]. To determine if SMYD2 had a greater impact beyond the HSC, analysis was continued to investigate which committed lineage was the most dependent on SMYD2. Based on the expression of SMYD2 in hematopoiesis (Figure 9), we reasoned that the myeloid lineage was likely to be affected.

The committed progenitors of the myeloid and lymphoid branches, CMP and CLP, respectively, further differentiate to ultimately populate and produce a multitude of mature cells (Figure 6). In the *vav* cKO model, CMPs and CLPs were significantly increased whereas in the *mx1* cKO, the CLPs were significantly decreased and the CMPs were modestly decreased (**Figure 24**). The loss of SMYD2 in the *vav* cKO suggests that further blocks exist downstream of these cells in both lineages while the *mx1* deletion suggests that only lymphocytes would be affected.

SMYD2 deficient CMPs and CLPs contribute to increased pDCs

Previously shown in figure 24, the SMYD2 *vav* cKO resulted in increased populations of both CMPs and CLPs. This is may prove significant in regard to plasmacytoid dendritic cells (pDCs) as they can be derived from either lineage [144].

Dendritic cells, in general, are responsible for taking up antigen circulating in the bloodstream and presenting them to T and B cells in order to illicit an immune response [145, 146]. Their unique shape, upon activation, creates a net type effect to capture antigen as well as to maintain contact and adhesion with T and B cells. Dendritic cells are also highly motile surveying the blood and migrating to locations of concentrated T or B cells primed for activation. There are several subtypes of these antigen presenting cells and we focused primarily at the pDC. The pDCs tend to be associated with lymphocytes based on their resident localization and B cell lineage (B220+) marker [144, 147, 148]. To determine if the resulting increase in both the CMP and the CLP also affected pDCs, flow cytometry was used to investigate the effect on pDCs from both the bone marrow and spleen.

Considering the impact pDCs have in the immune system, their increase could skew the ability of the cells to properly react to antigen. pDCs produce type I interferons (IFNs) which at basal levels help to initiate the immune response. However, higher concentrations of IFN can result in immunosuppression and reduce further signaling. Consequently, the T and B cells, which directly interact with pDCs may be impacted with regard to population size and/or function. Our experiments showed that pDCs were indeed increased in both cKO models (**Figure 25**).

mx1 cKO reduces T cell populations

The gene expression data indicated high expression of SMYD2 through most of T cell differentiation (Figure 9). While SMYD2 did not prove to be vital for T cell development in the *vav* deletion, the immature (double negative) and the CD4+ cells were significantly

decreased by the mx1 SMYD2 deletion. Decreased levels of CD4+ T cells have been associated with CML [149, 150].

B cell progenitors most affected by SMYD2 depletion

B cells mature from a pre-progenitor-B cell through a series of intermediate states until they finally mature and are subsequently activated to antibody secreting plasma cells (**Figure 27**) [151-153]. B cell development starts just downstream of the CLP. From here the lineage begins with a pre-progenitor B cell (pre-pro B), also known as Hardy's fraction A [154]. This cell continues to mature in a linear progression accumulating different cell surface markers as the (v)ariable, (d)iversity, and (j)oining gene (VDJ) chain rearrangement occurs [155]. B220⁺ is the indicator for any dedicated B cell and is expressed from the progenitor B (pro B) cell or Hardy's fraction B and onward. The pro B will eventually enter into the stage of the large pre B where VDJ rearrangement has halted and it begins actively dividing and proliferating. The divided large pre B cell gives rise to smaller nonproliferating small pre B cells which ultimately produce the immature B cell (imm B).

The expression data (Figure 9) indicated that SMYD2 was only present very early in B cell development. Therefore, the deletion of SMYD2 was not expected to have a severe impact on B cells beyond their earliest stages. However, in both the vav and mx1 cKOs, the loss of SMYD2 greatly affected B cell progenitors with the mx1 deletion causing a dramatic loss of cells contrary to an increase in the vav deleted cells (**Figure 28**). Beyond pro-B cells, the vav cKO cells were not further impacted. In contrast, mx1 cre cells exhibited a significant perturbation in the small pre-B cell. The small pre-B cell is

associated with the site of transformation for pre B-ALL. This suggests a potential role for SMYD2 in both early B cell development and the initiation of ALL.

As B cells continue to mature, a vast majority can be found in various splenic localizations. Follicular B cells make up follicles of B cells in the white pulp of the spleen. These cells are primed and organized around dendritic cells for fast activation. Marginal zone B cells reside in the red pulp region of the spleen and do not circulate. These cells are also primed to be recruited to assist in immunity by T cell activation. Marginal zone cells more rapidly differentiate to plasma cells. In these mature cells the deletion of SMYD2 facilitated by *vav* versus *mx1* resulted in differing outcomes. The *mx1* deletion continued its trend of depleted populations from immature spleen cells through transitional 1 B cells. However, the *vav* deletion resulted in only modest increases of cells in the mature, follicular and marginal zone B cells (**Figure 29**).

To test the functionality of mature cells, a B cell specific SMYD2 cKO was generated using *mb1 cre*. The use of this *cre* results in the deletion of SMYD2 prior to the pre-B cell. For specific function of B cells devoid of SMYD2, we immunized *mb1 cKO* and control mice. Their blood sera were analyzed over time to determine if the absence of SMYD2 had an effect on the antibody repertoire produced. IgM, IgA and IgG isotypes were not heavily impacted in the *mb1 cKO* mice (**Figure 30**).

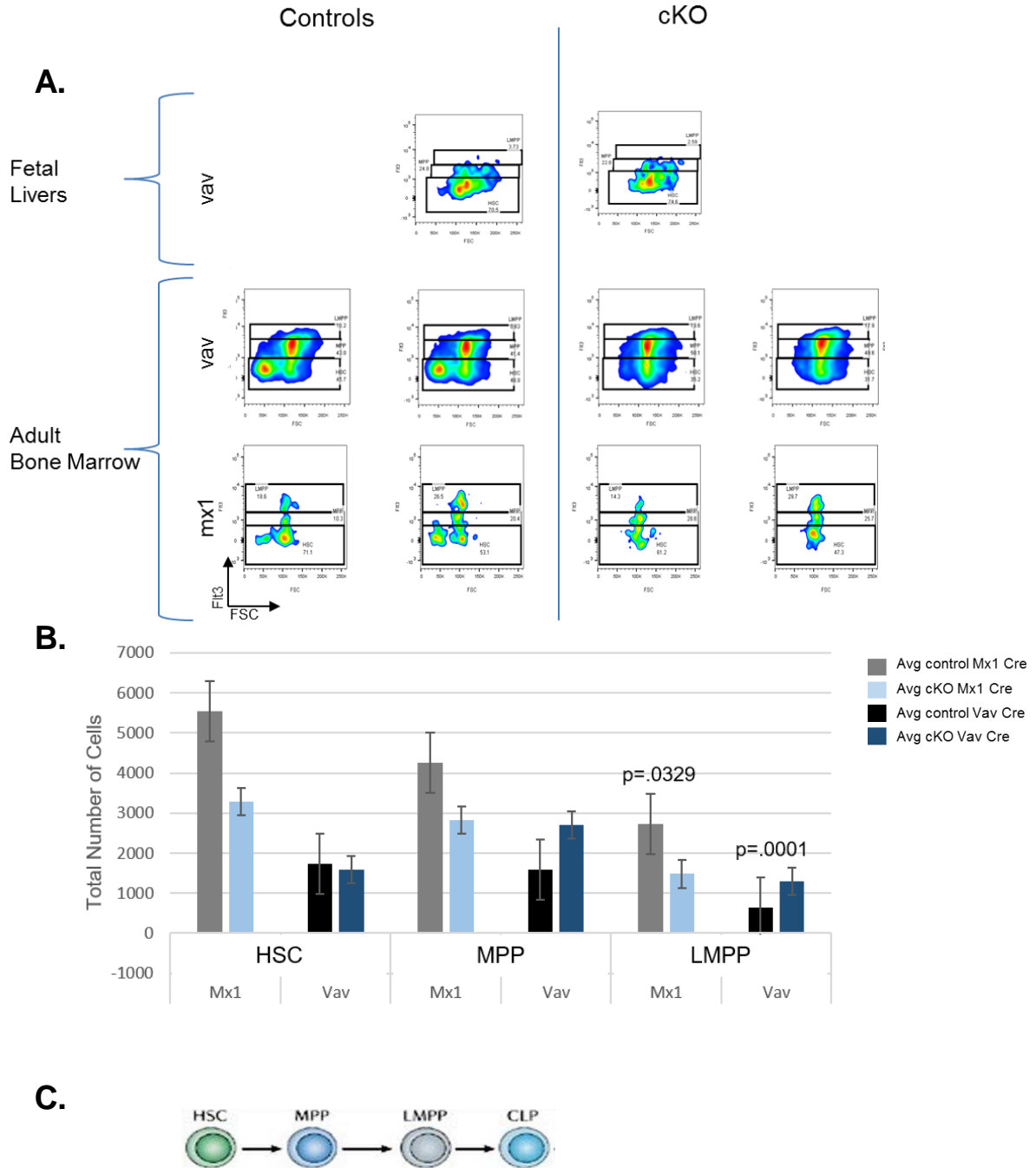


Figure 23: SMYD deficiency results in loss of HSC population in vav and adult cells. (A) Flow cytometric scatter plots of fetal and adult bone marrow. HSC populations from fetal livers were relatively normal (B) A graphical representation of cell numbers from adult bone marrow. Both the vav and mx1 SMYD2 deletions exhibited a loss of a smaller HSC population. In the mx1 cKO model, early cell populations continued a trend of decline. This culminated to a significant decrease of LMPPs. However, in the vav deletion, there was an increase in the MPP cells in addition to a significant increase in LMPP

population. HSC, MPPs and LMPPs share similar transmembrane receptor expression in that they are all lineage negative, Sca-1+ and c-kit high. However, they have varying expression of Flt3 with HSC expressing none, MPPs exhibiting an intermediate level of expression and LMPPs with high expression of Flt3. **(C)** Illustrates the early stages of differentiation of the HSC towards a committed lineage progenitor. The total number of cells was determined by: [(total number of femur/spleen/thymus cells harvested/# of cells collected in a sample via flow cytometry) * (# of cells in a gate)]

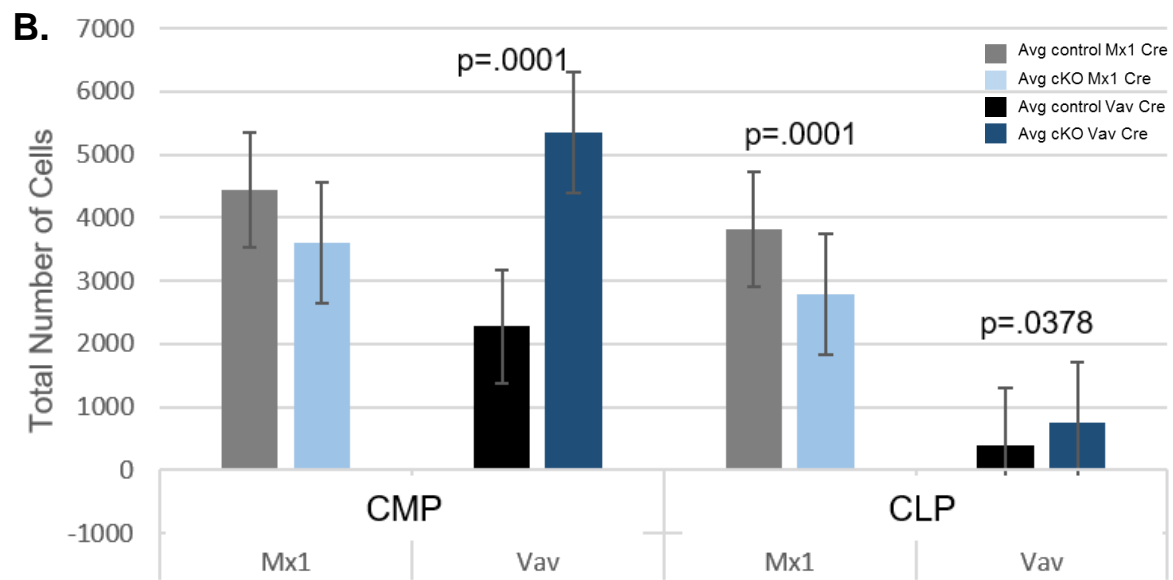
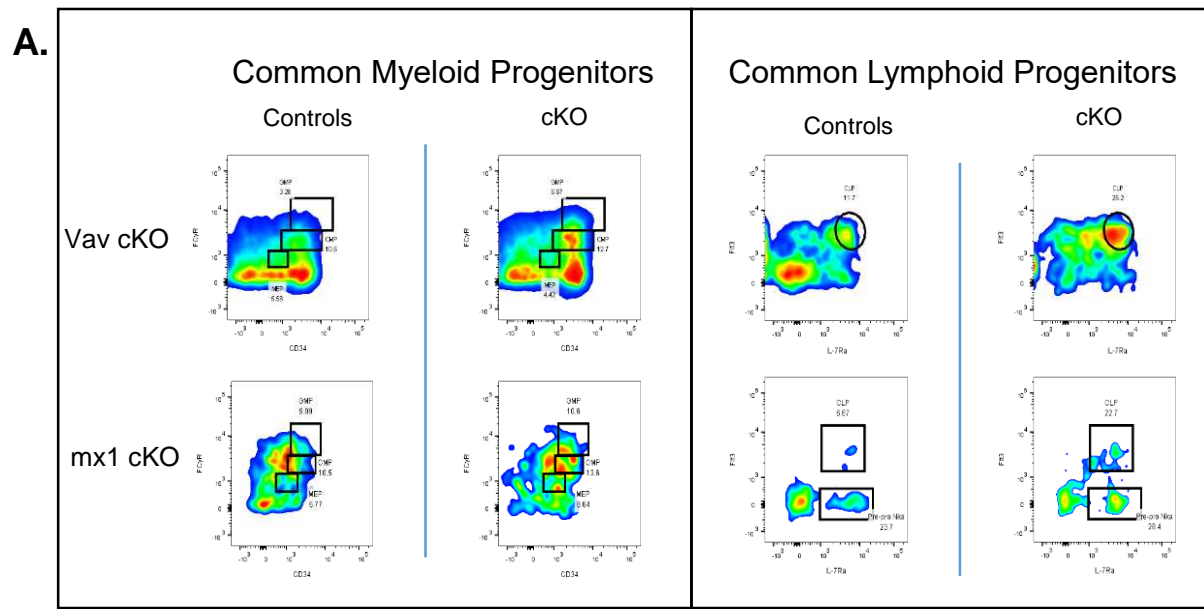


Figure 24: Depletion of SMYD2 affects early lineage progenitors. (A) Scatter plots and **(B)** graphical representations indicated that both the myeloid (CMP) and the lymphoid (CLP) committed progenitors were affected by the loss of SMYD2. The vav cre exhibited drastic increases in both cell types while mx1 cre demonstrated decreased populations, particularly in the CLPs.

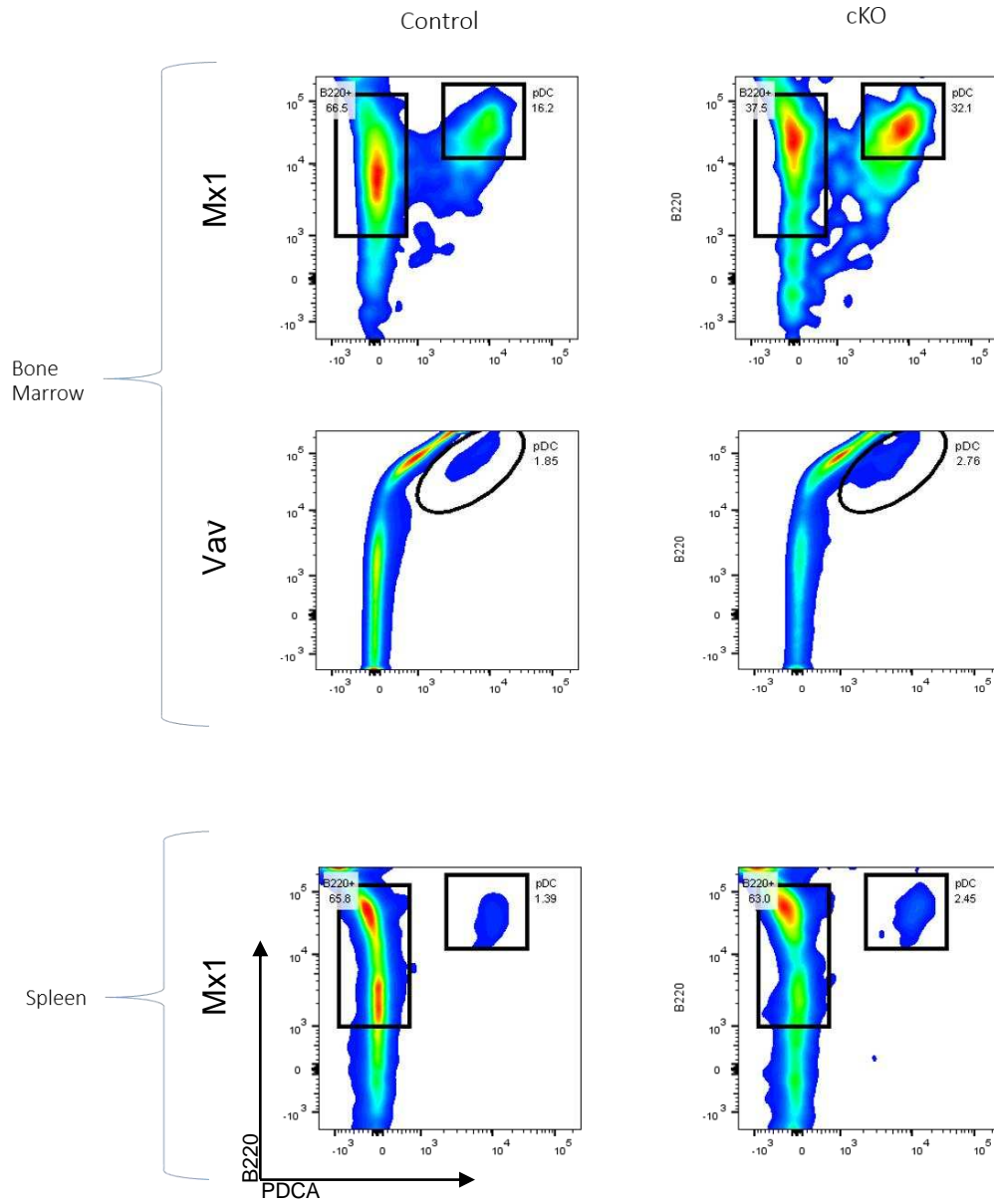


Figure 25: Increase of plasmacytoid dendritic cells (pDCs) in SMYD2 deletion. The populations of pDCs were increased in both HSC promoter deletions of SMYD2.

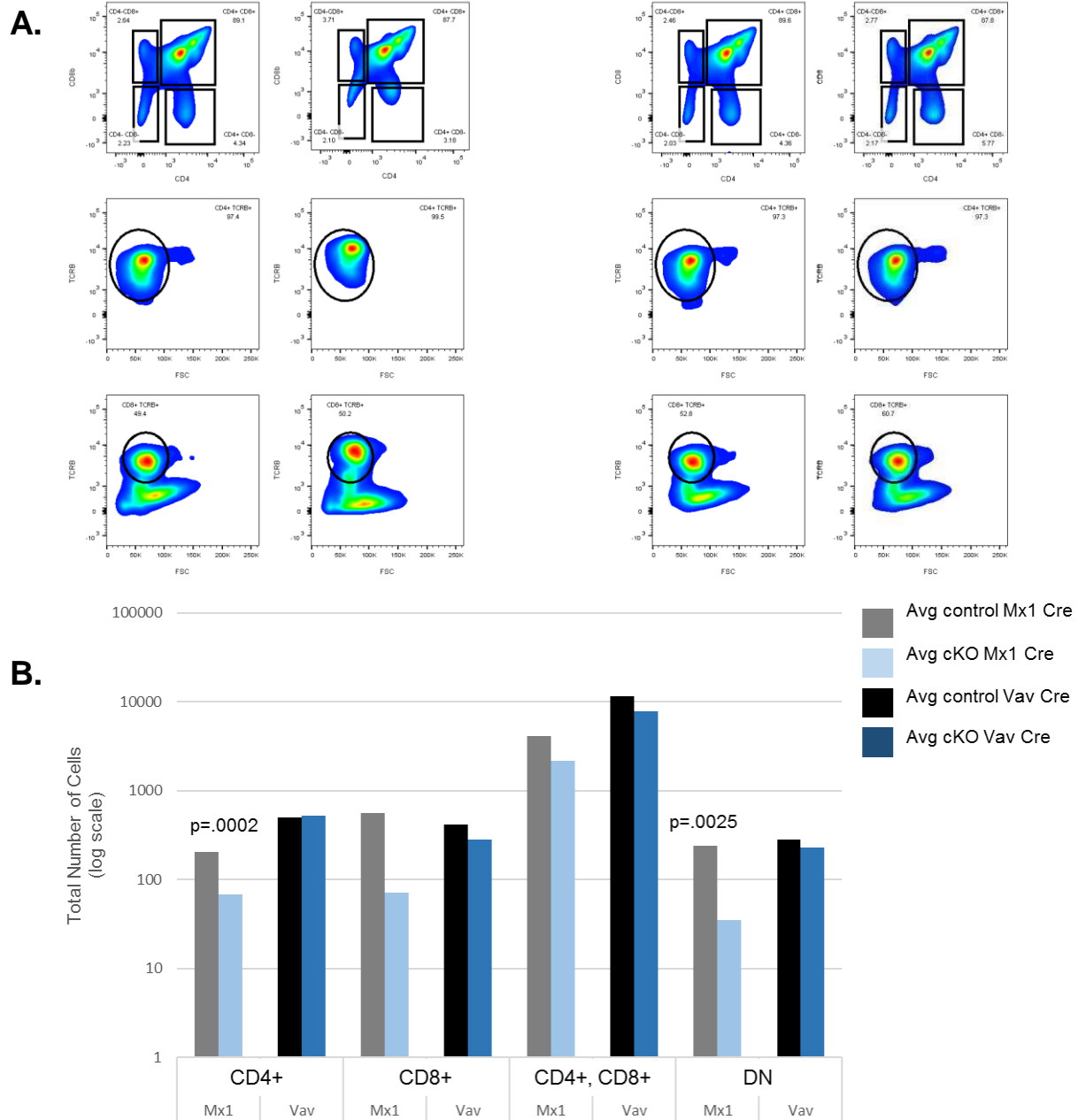
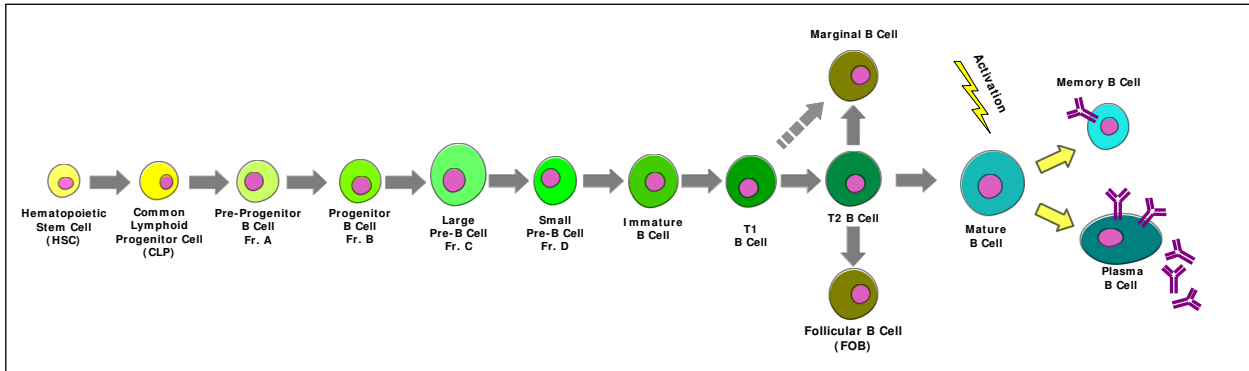


Figure 26: Thymic T-cell populations are only impacted in mx1 cKO. SMYD2 did not prove to be vital for T cell development in the vav cKO. Two of the T cell populations were affected by the mx1 SMYD2 deletion. The immature double negative and the CD4+ cells were significantly decreased.

A.



B.

	<table border="1"> <tr> <td>LOW</td> <td>MID</td> <td>HIGH</td> <td>NOT PRESENT</td> </tr> </table>														LOW	MID	HIGH	NOT PRESENT
LOW	MID	HIGH	NOT PRESENT															
	Hematopoietic Stem Cell (HSC)	Common Lymphoid Progenitor (CLP)	Pre-Progenitor B Cell (Fr. A)	Progenitor B Cell (Fr. B)	Large Pre-B Cell (Fr. C)	Small Pre-B Cell (Fr. D)	Immature B Cell	T1 B Cell	T2 B Cell	Follicular B Cell (FOB)	Marginal B Cell	Mature B Cell	Memory B Cell	Plasma B Cell				
C-KIT	LOW	LOW	NOT PRESENT	NOT PRESENT	NOT PRESENT	NOT PRESENT	NOT PRESENT	NOT PRESENT	NOT PRESENT	NOT PRESENT	NOT PRESENT	NOT PRESENT	NOT PRESENT	NOT PRESENT				
FLT3	LOW	LOW	NOT PRESENT	NOT PRESENT	NOT PRESENT	NOT PRESENT	NOT PRESENT	NOT PRESENT	NOT PRESENT	NOT PRESENT	NOT PRESENT	NOT PRESENT	NOT PRESENT	NOT PRESENT				
B220	NOT PRESENT	NOT PRESENT	NOT PRESENT	HIGH	HIGH	HIGH	HIGH	HIGH	HIGH	HIGH	HIGH	HIGH	HIGH	HIGH				
CD19	NOT PRESENT	NOT PRESENT	NOT PRESENT	HIGH	HIGH	HIGH	HIGH	HIGH	HIGH	HIGH	HIGH	HIGH	HIGH	HIGH				
CD34	LOW	LOW	NOT PRESENT	NOT PRESENT	NOT PRESENT	NOT PRESENT	NOT PRESENT	NOT PRESENT	NOT PRESENT	NOT PRESENT	NOT PRESENT	NOT PRESENT	NOT PRESENT	NOT PRESENT				
CD43	NOT PRESENT	NOT PRESENT	NOT PRESENT	NOT PRESENT	NOT PRESENT	NOT PRESENT	NOT PRESENT	NOT PRESENT	NOT PRESENT	NOT PRESENT	NOT PRESENT	NOT PRESENT	NOT PRESENT	NOT PRESENT				
CD25	NOT PRESENT	NOT PRESENT	NOT PRESENT	NOT PRESENT	NOT PRESENT	NOT PRESENT	NOT PRESENT	NOT PRESENT	NOT PRESENT	NOT PRESENT	NOT PRESENT	NOT PRESENT	NOT PRESENT	NOT PRESENT				
CD20	NOT PRESENT	NOT PRESENT	NOT PRESENT	NOT PRESENT	NOT PRESENT	NOT PRESENT	NOT PRESENT	NOT PRESENT	NOT PRESENT	NOT PRESENT	NOT PRESENT	NOT PRESENT	NOT PRESENT	NOT PRESENT				
CD24	NOT PRESENT	NOT PRESENT	NOT PRESENT	NOT PRESENT	NOT PRESENT	NOT PRESENT	NOT PRESENT	NOT PRESENT	NOT PRESENT	NOT PRESENT	NOT PRESENT	NOT PRESENT	NOT PRESENT	NOT PRESENT				
BAFF	NOT PRESENT	NOT PRESENT	NOT PRESENT	NOT PRESENT	NOT PRESENT	NOT PRESENT	NOT PRESENT	NOT PRESENT	NOT PRESENT	NOT PRESENT	NOT PRESENT	NOT PRESENT	NOT PRESENT	NOT PRESENT				
CD21	NOT PRESENT	NOT PRESENT	NOT PRESENT	NOT PRESENT	NOT PRESENT	NOT PRESENT	NOT PRESENT	NOT PRESENT	NOT PRESENT	NOT PRESENT	NOT PRESENT	NOT PRESENT	NOT PRESENT	NOT PRESENT				
CD23	NOT PRESENT	NOT PRESENT	NOT PRESENT	NOT PRESENT	NOT PRESENT	NOT PRESENT	NOT PRESENT	NOT PRESENT	NOT PRESENT	NOT PRESENT	NOT PRESENT	NOT PRESENT	NOT PRESENT	NOT PRESENT				
CD27	NOT PRESENT	NOT PRESENT	NOT PRESENT	NOT PRESENT	NOT PRESENT	NOT PRESENT	NOT PRESENT	NOT PRESENT	NOT PRESENT	NOT PRESENT	NOT PRESENT	NOT PRESENT	NOT PRESENT	NOT PRESENT				
IGM	NOT PRESENT	NOT PRESENT	NOT PRESENT	NOT PRESENT	NOT PRESENT	NOT PRESENT	NOT PRESENT	NOT PRESENT	NOT PRESENT	NOT PRESENT	NOT PRESENT	NOT PRESENT	NOT PRESENT	NOT PRESENT				
IGD	NOT PRESENT	NOT PRESENT	NOT PRESENT	NOT PRESENT	NOT PRESENT	NOT PRESENT	NOT PRESENT	NOT PRESENT	NOT PRESENT	NOT PRESENT	NOT PRESENT	NOT PRESENT	NOT PRESENT	NOT PRESENT				

Figure 27: Linear development of B cells. (A) B cells mature from a B cell progenitor downstream of the CLP known as the pre-progenitor B cell. After this stage they express B220+, the lineage marker for B cells. B cells enter a proliferative state at the Large pre-B cell and arrest division at the small pre-B stage. Immature B cells migrate out of the bone marrow to other resident organs including the spleen where maturation continues. Mature B cells circulate through the bloodstream and differentiate into plasma cells if activated by antigen. Plasma cells secrete one type of antibody and aid in the adaptive immune response. **(B)** Cell marker expression varies throughout B cell maturation. Cells can be distinguished from one another based on the extracellular markers.

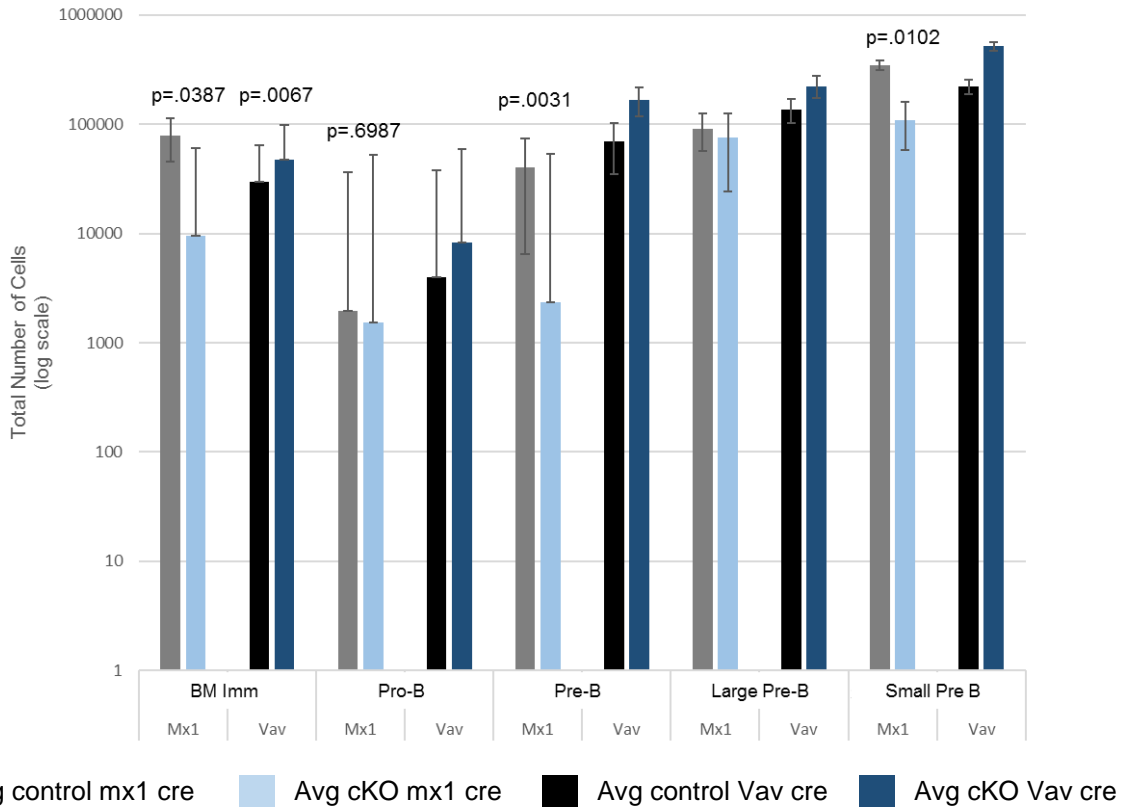


Figure 28: Bone marrow B cell development in the absence of SMYD2. The vav cKO exhibited modest increases of each bone marrow B cell population resulting in an overall significant increase in the total immature bone marrow B cells. The mx1 cKO, however, severely decreased overall immature, and pre-B cells, specifically affecting the small pre B cells. The small pre-B stage is associated with the site of transformation for B-ALL.

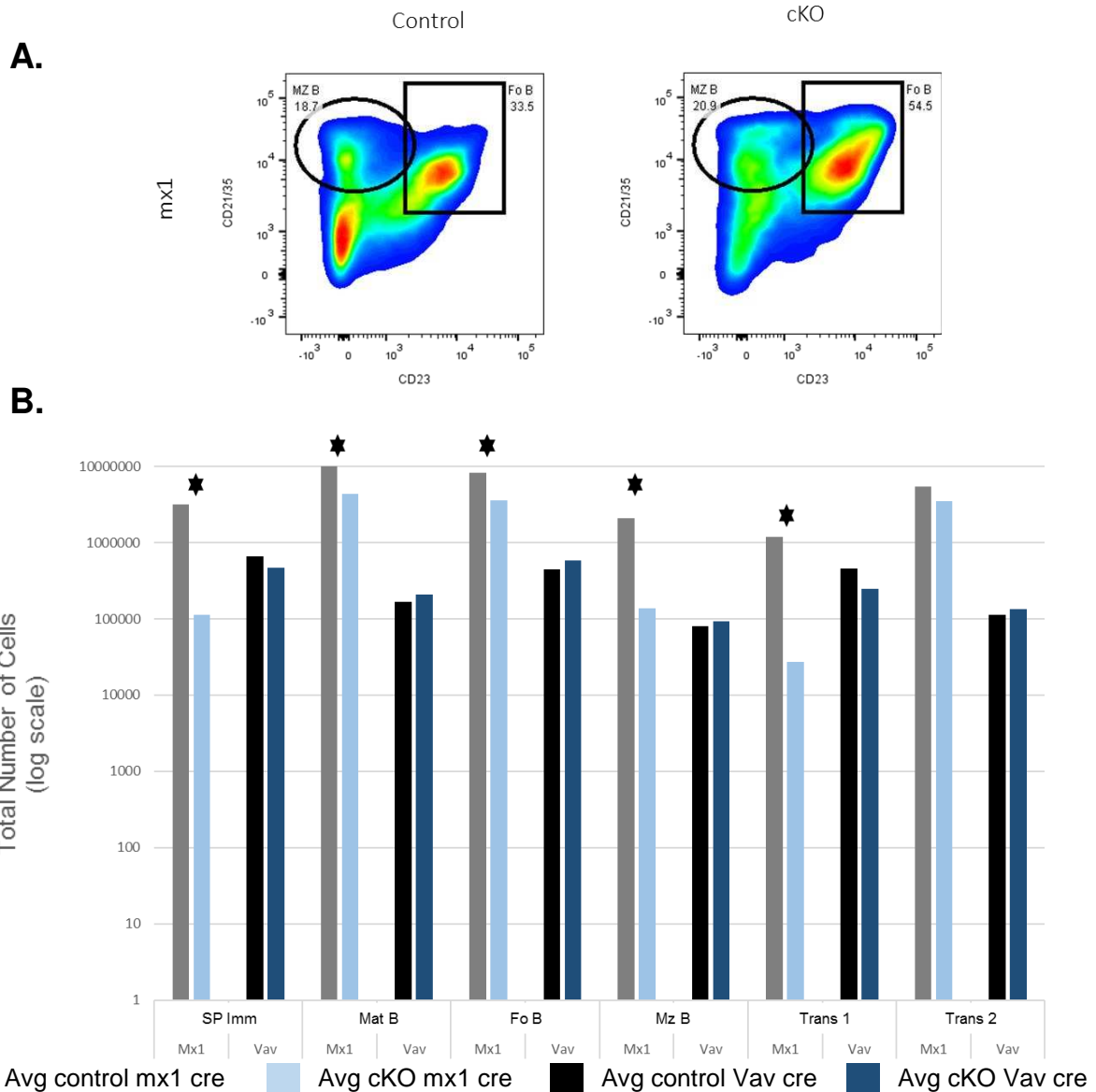


Figure 29: The effect of SMYD2 deletion in mature splenic B cell populations. (A) A scatter plot showing the shift of mature spleen cells to the follicular and marginal zone B cell populations in the mx1 cre. **(B)** Only the mx1 deletion of SMYD2 showed significant changes in the mature B cells. Overall splenic B cells were reduced from immature through transitional 1 B cells. The vav deletion resulted in modest increases of cells in the mature, follicular and marginal zone B cells. * statistical significance $p < 0.005$

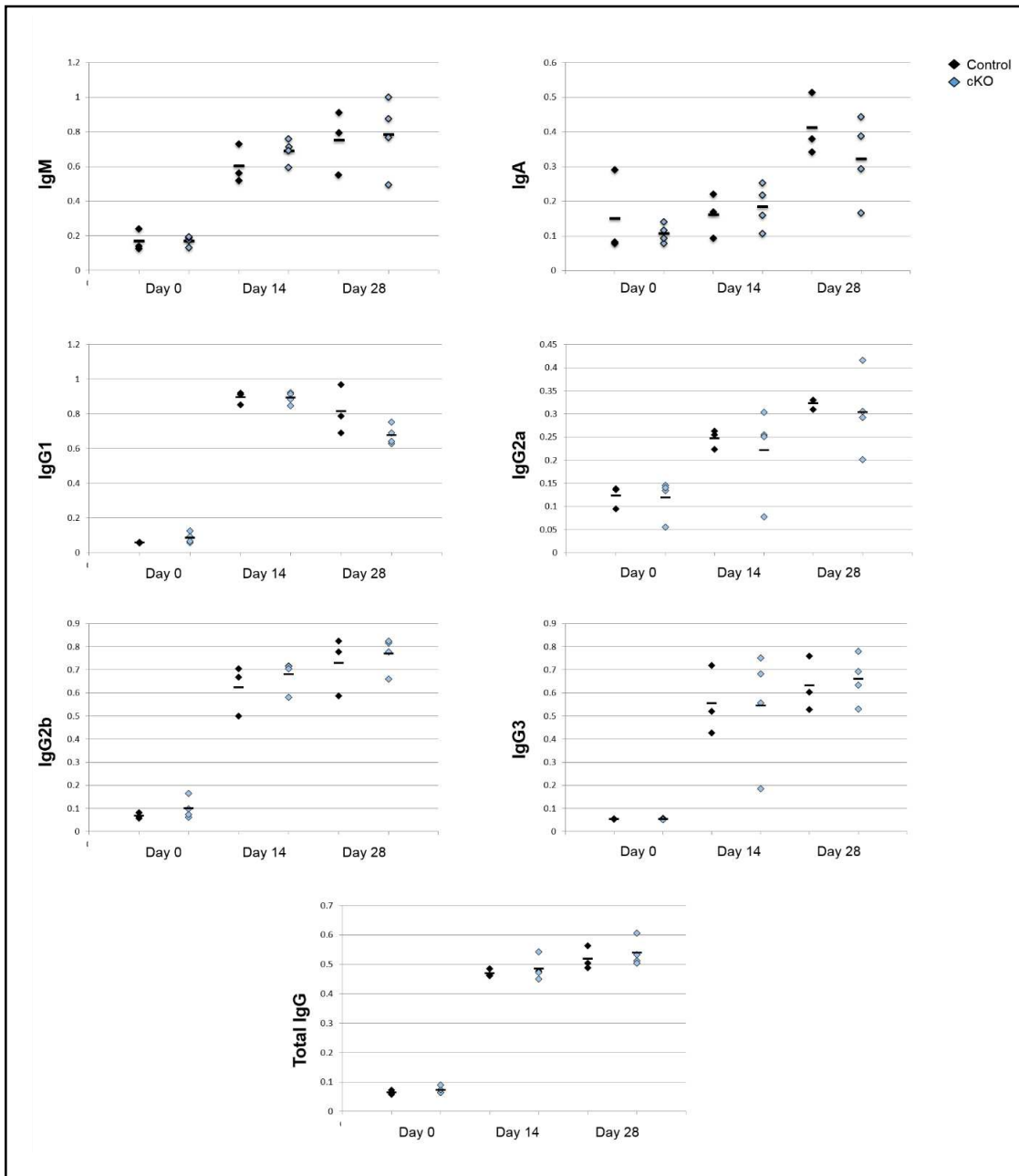


Figure 30: Antibody response in B cell specific (mb1) deletion of SMYD2. Analysis of the antibody production and response to immunization showed little difference between SMYD2 B cell deleted cells and control cells. While the response was robust in both groups, no statistical difference was seen.

B. CONCLUSION

I conclude that SMYD2 is required for proper hematopoietic development. The initial loss of a small HSC population was evident in both deletion models. Aberrations continued in the pathway, of note, in the committed progenitors of both the myeloid and lymphoid lineages. I further propose that SMYD2 plays a role in lymphocyte development. B and T cells were most significantly impacted at their earliest immature progenitors

CHAPTER 6 – DISCUSSION

The ultimate goal of this research was to better understand the function of SMYD2 and SMYD3. Analysis of the SMYD3 structure (**Figure 10**) revealed that a relatively large space near the post-SET domain and N-terminal portion of the CTD along the inner wall of the pocket is decorated by polar residues from the CTD (mainly residues from N324-C333 of helix 4) (**Figure 11**). Conserved clustering suggests that these polar residues might cooperate with the post-SET residues to restrict the histone substrate on both sides of the methyl-lysine. In this context, the CTD could function as a cap necessary to bind substrates effectively and selectively. Consistent with this hypothesis, deletion of CTD helices 1–9 [SMYD3(1–279)] eliminated basal HMTase activity of SMYD3 for histone H4 (**Figure 12A**).

Further investigation of the unanticipated role of the SMYD family's TPR-like CTD in intra-nuclear trafficking may provide insight into the potential for more specific localization of proteins regulated by the TPR-HSP90 interface. Experiments involving HSP90 chaperone inhibitors, such as geldanamycin, together with cells expressing either WT or mutant SMYD3 proteins, might lead to a better understanding of the interplay between these proteins. Significant research, however, still remains in order to fully delineate the influence of HSP90 conformation and activation state on the ability of its C-terminus to interact with TPR and TPR-like motifs, as well as its ability to influence cell localization and nuclear trafficking. Additional experiments which isolate the nuclear localization sequence of SMYD3 and its transporter would also be of value.

The CTD mediated stability of the SMYD3 active site also implies that the CTD is a potential pharmacologic target for the selective knockdown of SMYD3. Most HMTases share a sizable affinity for the methyl donor, S-adenosyl-methionine (SAM), making such a site less desirable as a drug target. Small molecule inhibitors which target the substrate binding site of other HMTases have achieved reasonable potencies and selectivities against those HMTases [46, 47]. That even the most distal portions of the CTD are necessary for basal function, despite predictions of less direct involvement in substrate binding, implies a non-competitive, allosteric means to regulate SMYD3 activity.

The cooperation between HSP90 and SMYDs in oncogenesis presents a novel direction for the clinical management of the resulting malignancies from an HSP90 perspective as well. If its association with SMYD3 is a primary driver of its oncogenic potential, blocking that association could have positive clinical outcomes. HSP90 has been the target of many novel cancer therapeutics which eliminate its chaperone function. Unfortunately, unintended consequences of eliminating the chaperone activity of this broadly expressed protein include off-target toxicities, such as a variety of gastrointestinal side effects [48]. The development of a drug which blocks HSP90-SMYD3 interactions via binding the CTD of SMYD3 may remove transformative avenues of HSP90-driven malignancy without inducing the unintended side effects associated with broad spectrum HSP90 chaperone inhibition. This would still allow basal signaling of SMYD3 in the cytoplasm, thus affecting its nuclear signaling selectively. To ascertain the utility of this approach, development of probe compounds which target SMYD3 and specifically compete with MEEVD binding will be necessary.

Analysis of SMYD2 via three *in vitro* hematopoietic malignant models underscored its potential role in oncogenesis. Further studies of these tumors and examination of tumor suppressor methylation may elucidate the mechanisms by which SMYD2 affects proliferation. SMYD2 is known to methylate residue K370 of p53 hindering its function of mediating apoptosis. The absence of SMYD2 in the cre mediated deletions and the resulting cell death further imply that SMYD2 plays a potential regulatory role of p53. The presence of the constitutively active tyrosine kinase, bcr-abl, may enhance SMYD2 repression of p53 even when not overexpressed. Future experiments analyzing methylation, gene expression and cell viability with an overexpression of SMYD2 in the presence of the transgene will be informative. In addition, *in vivo* overexpression and induced cKO studies without bcr-abl would reveal if inhibition of SMYD2 alone is sufficient to reduce and eliminate HSC tumors.

Considering that much like SMYD3, SMYD2 activity can be enhanced by HSP90 interactions [85, 156, 157], investigating this too in our tumor models would be of value. The bcr-abl construct may heighten the ability of HSP90 to bind to SMYD2 and thereby increase its methylation activity. Experiments aimed toward determining SMYD2 methylation in a system with and without both bcr-abl and HSP90 could prove to be of merit with regard to therapeutic development. Although, as previously mentioned, since targeting HSP90 results in unintended consequences, understanding the many potential mechanisms that contribute to SMYD2 activity is important to its targeted inhibition.

Utilizing our vav and mx1 cre SMYD2 deletion models, we sought to determine the overall role of SMYD2 in hematopoiesis, ultimately investigating potential sites of tumor initiation in this pathway. The deletion of SMYD2 resulted in loss of an initial HSC

population. Thus, SMYD2 may be a factor in stromal signaling that drives HSC differentiation. Further analysis of the variations in cell populations in a SMYD2 overexpression model would be especially telling if the depleted population remained and/or increased. In addition, isolating the HSC and conducting cell cycle analysis would determine if the population lost was of a proliferating or senescent nature. Every aberration observed downstream was likely linked to this initial depleted population of cells.

B cell progenitors were altered due to the deletion of SMYD2. Many lymphomas and leukemias are directly associated with transformations during B cell development and SMYD2 may contribute to those. Although progenitor B cells were affected by the loss of SMYD2, mature B cells exhibited a normal response when stimulated. Considering the known SMYD2 interactions with tumor suppressors p53 and RB1, its role may be better revealed if the system was subject to stressors. DNA damage would provide insight to the potential regulation of p53 and RB1 by SMYD2. Hypoxic, heat and toxic stressors would not only allow analysis of tumor suppressors but also of chaperone proteins expressed under these conditions. Observing these in both an overexpression and knockout model could reveal a clearer picture of the role of SMYD2 in these regulatory pathways.

At the onset of this study, we were unsure if we could trigger the deletion of SMYD2 *in vitro* via our mx1 cre constructs. The *in vivo*, mx1 cre requires multiple injections of a double stranded RNA mimic, PI:PC, which induces an interferon response ultimately activating the cre-recombinase. *In vitro*, we were unsure of how to deliver a proper dosage to elicit the deletion of SMYD2 and therefore, the YFP reporter. Utilizing a co-culture of

OP-9 cells and cytokines, we cultured bone marrow cells toward the B cell lineage and were able to maintain cell viability and effectively knockout SMYD2 (**Figure 31**). This approach could be used to subject cancer cell models to stress both before and after SMYD2 deletion to better understand how and when therapeutics might be most effective.

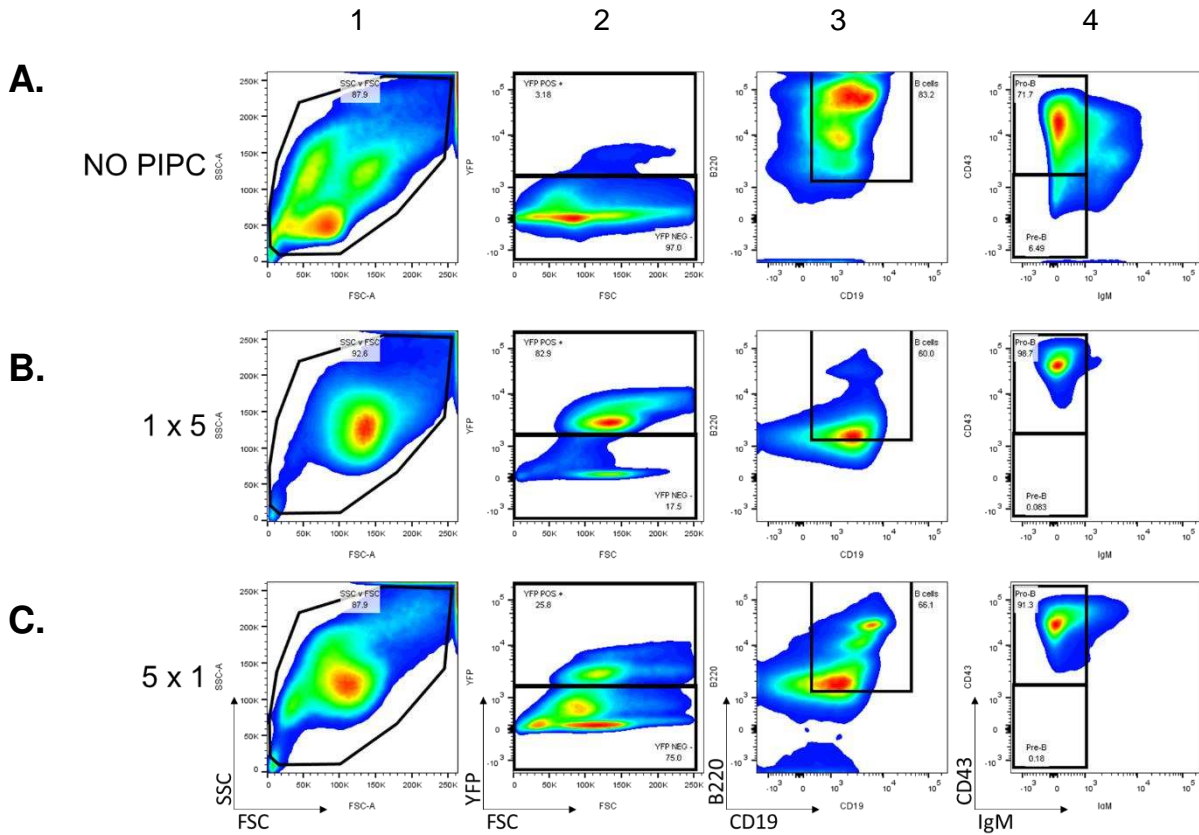


Figure 31. In vitro deletion of SMYD2 with mx1 cre. Mx1 cre bone marrow cells were plated on a co-culture of OP-9 cells with cytokines. PI:PC was either, **(A)** not administered (NO PIPC), **(B)** administered in the same time frame as *in vivo*, once every other day for five days (1 x 5) or **(C)** all at once in one day (5 x 1). Cells were harvested and analyzed by flow cytometry at day 10. Row 1 exhibits the size and granularity of the total cell composition with forward scatter plotted against side scatter. The scatter plots in row 2 show that the slower administration over several days yielded the highest deletion of SMYD2 indicated by presence of YFP (**B. Row 2**). 83% of cells expressed YFP in the **(B)** 1 x 5 dosing versus 25% in **(C. Row 2)** the 5 x 1 dose. Cells progressed towards early pre-B cells normally as indicated in rows 3 and 4.

REFERENCES

1. Grigoryev, S.A., *Nucleosome spacing and chromatin higher-order folding*. Nucleus, 2012. **3**(6): p. 493-9.
2. McGinty, R.K. and S. Tan, *Nucleosome structure and function*. Chem Rev, 2015. **115**(6): p. 2255-73.
3. Czarnota, G.J. and F.P. Ottensmeyer, *Structural states of the nucleosome*. J Biol Chem, 1996. **271**(7): p. 3677-83.
4. Luger, K., et al., *Crystal structure of the nucleosome core particle at 2.8[thinsp]Å resolution*. Nature, 1997. **389**(6648): p. 251-260.
5. Tessarz, P. and T. Kouzarides, *Histone core modifications regulating nucleosome structure and dynamics*. Nat Rev Mol Cell Biol, 2014. **15**(11): p. 703-8.
6. Rivera, C., et al., *Histone lysine methylation and chromatin replication*. Biochim Biophys Acta, 2014. **1839**(12): p. 1433-9.
7. Iwasaki, W., et al., *Contribution of histone N-terminal tails to the structure and stability of nucleosomes()*. FEBS Open Bio, 2013. **3**: p. 363-369.
8. Chi, P., C.D. Allis, and G.G. Wang, *Covalent histone modifications: miswritten, misinterpreted, and miserased in human cancers*. Nature Reviews. Cancer, 2010. **10**(7): p. 457-469.
9. Crea, F., *Histone code, human growth and cancer*. Oncotarget, 2012. **3**(1): p. 1-2.
10. Sneppen, K. and I.B. Dodd, *A simple histone code opens many paths to epigenetics*. PLoS Comput Biol, 2012. **8**(8): p. e1002643.
11. Jenuwein, T. and C.D. Allis, *Translating the histone code*. Science, 2001. **293**(5532): p. 1074-80.
12. Rusk, N., *Writing the histone code*. Nat Methods, 2012. **9**(8): p. 777.
13. DeMicco, A. and C.H. Bassing, *Deciphering the DNA damage histone code*. Cell Cycle, 2010. **9**(19): p. 3845.
14. Jones, B., *Epigenetics: Histones pass the message on*. Nat Rev Genet, 2015. **16**(1): p. 3.
15. Woo, Y.H. and W.H. Li, *Evolutionary conservation of histone modifications in mammals*. Mol Biol Evol, 2012. **29**(7): p. 1757-67.
16. Schnapp, E., *Wrapping up histone regulation*. EMBO Rep, 2015. **16**(11): p. 1409.
17. Bach, S.V. and A.N. Hegde, *The proteasome and epigenetics: zooming in on histone modifications*. Biomol Concepts, 2016. **7**(4): p. 215-27.
18. Struhl, K., *Histone acetylation and transcriptional regulatory mechanisms*. Genes & Development, 1998. **12**(5): p. 599-606.
19. Sterner, D.E. and S.L. Berger, *Acetylation of Histones and Transcription-Related Factors*. Microbiology and Molecular Biology Reviews, 2000. **64**(2): p. 435-459.
20. Brown, C.E., et al., *The many HATs of transcription coactivators*. Trends in Biochemical Sciences. **25**(1): p. 15-19.
21. RUIJTER, A.J.M.d., et al., *Histone deacetylases (HDACs): characterization of the classical HDAC family*. Biochemical Journal, 2003. **370**(3): p. 737-749.

22. Haberland, M., R.L. Montgomery, and E.N. Olson, *The many roles of histone deacetylases in development and physiology: implications for disease and therapy*. Nature reviews. Genetics, 2009. **10**(1): p. 32-42.
23. Cheng, X., *Structure and Function of DNA Methyltransferases*. Annual Review of Biophysics and Biomolecular Structure, 1995. **24**(1): p. 293-318.
24. Cantoni, G.L., *THE NATURE OF THE ACTIVE METHYL DONOR FORMED ENZYMATICALLY FROM L-METHIONINE AND ADENOSINETRIPHOSPHATE*^{1,2}. Journal of the American Chemical Society, 1952. **74**(11): p. 2942-2943.
25. Zhang, Y. and D. Reinberg, *Transcription regulation by histone methylation: interplay between different covalent modifications of the core histone tails*. Genes & Development, 2001. **15**(18): p. 2343-2360.
26. Holliday, R., *DNA methylation and epigenetic inheritance*. Philos Trans R Soc Lond B Biol Sci, 1990. **326**(1235): p. 329-38.
27. Feng, Q., et al., *Methylation of H3-lysine 79 is mediated by a new family of HMTases without a SET domain*. Curr Biol, 2002. **12**(12): p. 1052-8.
28. Shi, Y., et al., *Histone demethylation mediated by the nuclear amine oxidase homolog LSD1*. Cell, 2004. **119**(7): p. 941-53.
29. Felsenfeld, G., *The evolution of epigenetics*. Perspect Biol Med, 2014. **57**(1): p. 132-48.
30. Tschiersch, B., et al., *The protein encoded by the Drosophila position-effect variegation suppressor gene Su(var)3-9 combines domains of antagonistic regulators of homeotic gene complexes*. The EMBO Journal, 1994. **13**(16): p. 3822-3831.
31. Lee, H.W., S. Kim, and W.K. Paik, *S-adenosylmethionine: protein-arginine methyltransferase. Purification and mechanism of the enzyme*. Biochemistry, 1977. **16**(1): p. 78-85.
32. Zagni, C., U. Chiacchio, and A. Rescifina, *Histone Methyltransferase Inhibitors: Novel Epigenetic Agents for Cancer Treatment*. Current Medicinal Chemistry, 2013. **20**(2): p. 167-185.
33. Herz, H.-M., A. Garruss, and A. Shilatifard, *SET for life: biochemical activities and biological functions of SET domain-containing proteins*. Trends in biochemical sciences, 2013. **38**(12): p. 621-639.
34. Dillon, S.C., et al., *The SET-domain protein superfamily: protein lysine methyltransferases*. Genome Biology, 2005. **6**(8): p. 227-227.
35. Peterson, C.L. and M.-A. Laniel, *Histones and histone modifications*. Current Biology. **14**(14): p. R546-R551.
36. Spellmon, N., et al., *Structure and Function of SET and MYND Domain-Containing Proteins*. International Journal of Molecular Sciences, 2015. **16**(1): p. 1406.
37. Gottlieb, P.D., et al., *Bop encodes a muscle-restricted protein containing MYND and SET domains and is essential for cardiac differentiation and morphogenesis*. Nat Genet, 2002. **31**(1): p. 25-32.
38. Brown, M.A., et al., *Identification and characterization of Smyd2: a split SET/MYND domain-containing histone H3 lysine 36-specific methyltransferase that interacts with the Sin3 histone deacetylase complex*. Mol Cancer, 2006. **5**: p. 26.

39. Leinhart, K. and M. Brown, *SET/MYND Lysine Methyltransferases Regulate Gene Transcription and Protein Activity*. Genes (Basel), 2011. **2**(1): p. 210-8.
40. Du, S.J., X. Tan, and J. Zhang, *SMYD proteins: key regulators in skeletal and cardiac muscle development and function*. Anat Rec (Hoboken), 2014. **297**(9): p. 1650-62.
41. Spellmon, N., et al., *Structure and function of SET and MYND domain-containing proteins*. Int J Mol Sci, 2015. **16**(1): p. 1406-28.
42. Jiang, Y., et al., *Crystal structures of histone and p53 methyltransferase SmyD2 reveal a conformational flexibility of the autoinhibitory C-terminal domain*. PLoS One, 2011. **6**(6): p. e21640.
43. Berkholz, J., et al., *skNAC and Smyd1 in transcriptional control*. Experimental Cell Research, 2015. **336**(2): p. 182-191.
44. Sims, R.J., 3rd, et al., *m-Bop, a repressor protein essential for cardiogenesis, interacts with skNAC, a heart- and muscle-specific transcription factor*. J Biol Chem, 2002. **277**(29): p. 26524-9.
45. Franklin, S., et al., *The chromatin binding protein Smyd1 restricts adult mammalian heart growth*. American Journal of Physiology - Heart and Circulatory Physiology, 2016.
46. Du, S.J., X. Tan, and J. Zhang, *SMYD Proteins: Key Regulators in Skeletal and Cardiac Muscle Development and Function*. The Anatomical Record, 2014. **297**(9): p. 1650-1662.
47. Phan, D., et al., *BOP, a regulator of right ventricular heart development, is a direct transcriptional target of MEF2C in the developing heart*. Development, 2005. **132**(11): p. 2669-78.
48. Ehler, E. and M. Gautel, *The sarcomere and sarcomerogenesis*. Adv Exp Med Biol, 2008. **642**: p. 1-14.
49. Van Aller, G.S., et al., *Smyd3 regulates cancer cell phenotypes and catalyzes histone H4 lysine 5 methylation*. Epigenetics, 2012. **7**(4): p. 340-3.
50. Hamamoto, R., et al., *Enhanced SMYD3 expression is essential for the growth of breast cancer cells*. Cancer Sci, 2006. **97**(2): p. 113-8.
51. He, C., et al., *High expression of trimethylated histone H3 lysine 4 is associated with poor prognosis in hepatocellular carcinoma*. Hum Pathol, 2012. **43**(9): p. 1425-35.
52. Wang, S.Z., et al., *Knockdown of SMYD3 by RNA interference inhibits cervical carcinoma cell growth and invasion in vitro*. BMB Rep, 2008. **41**(4): p. 294-9.
53. Giakountis, A., et al., *Smyd3-associated regulatory pathways in cancer*. Seminars in Cancer Biology.
54. Hamamoto, R., et al., *SMYD3 encodes a histone methyltransferase involved in the proliferation of cancer cells*. Nat Cell Biol, 2004. **6**(8): p. 731-40.
55. Hamamoto, R., et al., *SMYD3 encodes a histone methyltransferase involved in the proliferation of cancer cells*. Nat Cell Biol, 2004. **6**(8): p. 731-740.
56. Qu, L., et al., *Decreased expression of the Nkx2.8 gene correlates with tumor progression and a poor prognosis in HCC cancer*. Cancer Cell International, 2014. **14**: p. 28-28.

57. Yu, C., et al., *The tumor-suppressor gene Nkx2.8 suppresses bladder cancer proliferation through upregulation of FOXO3a and inhibition of the MEK/ERK signaling pathway*. *Carcinogenesis*, 2012. **33**(3): p. 678-86.
58. Lin, C., et al., *Nkx2-8 downregulation promotes angiogenesis and activates NF-kappaB in esophageal cancer*. *Cancer Res*, 2013. **73**(12): p. 3638-48.
59. Xu, J.Y., et al., [*Experimental research of therapeutic effect on hepatocellular carcinoma of targeting SMYD3 gene inhibition by RNA interference*]. *Zhonghua Wai Ke Za Zhi*, 2006. **44**(7): p. 481-4.
60. Xu, J.Y., et al., [*Inhibition of SMYD3 gene expression by RNA interference induces apoptosis in human hepatocellular carcinoma cell line HepG2*]. *Ai Zheng*, 2006. **25**(5): p. 526-32.
61. Chen, L.B., et al., *Silencing SMYD3 in hepatoma demethylates RIZ1 promoter induces apoptosis and inhibits cell proliferation and migration*. *World J Gastroenterol*, 2007. **13**(43): p. 5718-24.
62. Xu, J.Y., et al., [*Suppression of SMYD3 expression in HepG2 cell by shRNA interference*]. *Zhonghua Gan Zang Bing Za Zhi*, 2006. **14**(2): p. 105-8.
63. Abu-Farha, M., et al., *The tale of two domains: proteomics and genomics analysis of SMYD2, a new histone methyltransferase*. *Mol Cell Proteomics*, 2008. **7**(3): p. 560-72.
64. Huang, J., et al., *Repression of p53 activity by Smyd2-mediated methylation*. *Nature*, 2006. **444**(7119): p. 629-32.
65. Cho, H.S., et al., *RB1 methylation by SMYD2 enhances cell cycle progression through an increase of RB1 phosphorylation*. *Neoplasia*, 2012. **14**(6): p. 476-86.
66. Saddic, L.A., et al., *Methylation of the retinoblastoma tumor suppressor by SMYD2*. *J Biol Chem*, 2010. **285**(48): p. 37733-40.
67. Wang, L., et al., *Structure of human SMYD2 protein reveals the basis of p53 tumor suppressor methylation*. *J Biol Chem*, 2011. **286**(44): p. 38725-37.
68. Sajjad, A., et al., *Lysine methyltransferase Smyd2 suppresses p53-dependent cardiomyocyte apoptosis*. *Biochim Biophys Acta*, 2014. **1843**(11): p. 2556-62.
69. Diehl, F., et al., *Cardiac deletion of Smyd2 is dispensable for mouse heart development*. *PLoS One*, 2010. **5**(3): p. e9748.
70. Ahmed, H., et al., *An Integrative Proteomic Approach Identifies Novel Cellular SMYD2 Substrates*. *J Proteome Res*, 2016. **15**(6): p. 2052-9.
71. Finkelstein, D.B. and S. Strausberg, *Identification and expression of a cloned yeast heat shock gene*. *J Biol Chem*, 1983. **258**(3): p. 1908-13.
72. Koyasu, S., et al., *Two mammalian heat shock proteins, HSP90 and HSP100, are actin-binding proteins*. *Proc Natl Acad Sci U S A*, 1986. **83**(21): p. 8054-8.
73. Meng, X., et al., *Cloning of chicken hsp90 beta: the only vertebrate hsp90 insensitive to heat shock*. *Biochem Biophys Res Commun*, 1993. **190**(2): p. 630-6.
74. Pearl, L.H. and C. Prodromou, *Structure and in vivo function of Hsp90*. *Curr Opin Struct Biol*, 2000. **10**(1): p. 46-51.
75. Pearl, L.H. and C. Prodromou, *Structure and mechanism of the Hsp90 molecular chaperone machinery*. *Annu Rev Biochem*, 2006. **75**: p. 271-94.

76. Borkovich, K.A., et al., *hsp82 is an essential protein that is required in higher concentrations for growth of cells at higher temperatures*. Mol Cell Biol, 1989. **9**(9): p. 3919-30.
77. Versteeg, S., A. Mogk, and W. Schumann, *The Bacillus subtilis htpG gene is not involved in thermal stress management*. Mol Gen Genet, 1999. **261**(3): p. 582-8.
78. Whitesell, L. and S.L. Lindquist, *HSP90 and the chaperoning of cancer*. Nat Rev Cancer, 2005. **5**(10): p. 761-72.
79. Pratt, W.B., et al., *Role of molecular chaperones in steroid receptor action*. Essays Biochem, 2004. **40**: p. 41-58.
80. Steinmetz, A.C., J.P. Renaud, and D. Moras, *Binding of ligands and activation of transcription by nuclear receptors*. Annu Rev Biophys Biomol Struct, 2001. **30**: p. 329-59.
81. Pearl, L.H., *Hsp90 and Cdc37 -- a chaperone cancer conspiracy*. Curr Opin Genet Dev, 2005. **15**(1): p. 55-61.
82. Shao, J., et al., *Functional dissection of cdc37: characterization of domain structure and amino acid residues critical for protein kinase binding*. Biochemistry, 2003. **42**(43): p. 12577-88.
83. Calderwood, S.K., et al., *Heat shock proteins in cancer: chaperones of tumorigenesis*. Trends Biochem Sci, 2006. **31**(3): p. 164-72.
84. Erlejman, A.G., et al., *Regulatory role of the 90-kDa-heat-shock protein (Hsp90) and associated factors on gene expression*. Biochim Biophys Acta, 2014. **1839**(2): p. 71-87.
85. Abu-Farha, M., et al., *Proteomic analyses of the SMYD family interactomes identify HSP90 as a novel target for SMYD2*. J Mol Cell Biol, 2011. **3**(5): p. 301-8.
86. Lee, D.Y., et al., *Role of Protein Methylation in Regulation of Transcription*. Endocrine Reviews, 2005. **26**(2): p. 147-170.
87. Johnson, C.N., N.L. Adkins, and P. Georgel, *Chromatin remodeling complexes: ATP-dependent machines in action*. Biochemistry and Cell Biology, 2005. **83**(4): p. 405-417.
88. Orkin, S.H. and L.I. Zon, *Hematopoiesis: an evolving paradigm for stem cell biology*. Cell, 2008. **132**(4): p. 631-44.
89. Steinman, R.A., *Cell cycle regulators and hematopoiesis*. Oncogene. **21**: p. 3403-3413.
90. Dilly, S.A. and C.J. Jagger, *Bone marrow stromal cell changes in haematological malignancies*. J Clin Pathol, 1990. **43**(11): p. 942-6.
91. Lisovsky, M. and V.G. Savchenko, *Defect of stromal microenvironment in long term bone marrow cultures of patients with acute and chronic myelogenous leukemias*. Leuk Lymphoma, 1995. **19**(1-2): p. 145-52.
92. Tabe, Y., et al., *Role of stromal microenvironment in nonpharmacological resistance of CML to imatinib through Lyn/CXCR4 interactions in lipid rafts*. Leukemia, 2012. **26**(5): p. 883-92.
93. Duhrsen, U. and D.K. Hossfeld, *Stromal abnormalities in neoplastic bone marrow diseases*. Ann Hematol, 1996. **73**(2): p. 53-70.
94. Kelly, L.M. and D.G. Gilliland, *Genetics of myeloid leukemias*. Annu Rev Genomics Hum Genet, 2002. **3**: p. 179-98.

95. Chalandon, Y. and J. Schwaller, *Targeting mutated protein tyrosine kinases and their signaling pathways in hematologic malignancies*. *Haematologica*, 2005. **90**(7): p. 949-68.
96. Rieger, M.A. and T. Schroeder, *Hematopoiesis*. Cold Spring Harbor Perspectives in Biology, 2012. **4**(12).
97. NIH, N.C.I. *Childhood Acute Lymphoblastic Leukemia Treatment (PDQ®)*. 2013; Available from: <http://www.cancer.gov/cancertopics/pdq/treatment/childALL/HealthProfessional/page1>.
98. Juric, D., et al., *Differential gene expression patterns and interaction networks in BCR-ABL-positive and -negative adult acute lymphoblastic leukemias*. *J Clin Oncol*, 2007. **25**(11): p. 1341-9.
99. Geng, H., et al., *Integrative epigenomic analysis identifies biomarkers and therapeutic targets in adult B-acute lymphoblastic leukemia*. *Cancer Discov*, 2012. **2**(11): p. 1004-23.
100. Jootar, S., et al., *Bone marrow derived mesenchymal stem cells from chronic myeloid leukemia t(9;22) patients are devoid of Philadelphia chromosome and support cord blood stem cell expansion*. *Leuk Res*, 2006. **30**(12): p. 1493-8.
101. Komatsu, S., et al., *Overexpression of SMYD2 relates to tumor cell proliferation and malignant outcome of esophageal squamous cell carcinoma*. *Carcinogenesis*, 2009. **30**(7): p. 1139-46.
102. Seita J, S.D., Rossi DJ, Bhattacharya D, Serwold T, Inlay MA, Ehrlich LI, Fathman JW, Dill DL, Weissman IL., *Gene Expression Commons: an open platform for absolute gene expression profiling*. *PLoS One*, 2012.
103. Fathman, J.W., et al., *Upregulation of CD11A on hematopoietic stem cells denotes the loss of long-term reconstitution potential*. *Stem Cell Reports*, 2014. **3**(5): p. 707-15.
104. Berger, S.L., *The complex language of chromatin regulation during transcription*. *Nature*, 2007. **447**(7143): p. 407-12.
105. Taverna, S.D., et al., *How chromatin-binding modules interpret histone modifications: lessons from professional pocket pickers*. *Nature structural & molecular biology*, 2007. **14**(11): p. 1025-1040.
106. Foreman, K.W., et al., *Structural and Functional Profiling of the Human Histone Methyltransferase SMYD3*. *PLoS ONE*, 2011. **6**(7): p. e22290.
107. Kunizaki, M., et al., *The lysine 831 of vascular endothelial growth factor receptor 1 is a novel target of methylation by SMYD3*. *Cancer Res*, 2007. **67**(22): p. 10759-65.
108. Silva, F.P., et al., *Enhanced methyltransferase activity of SMYD3 by the cleavage of its N-terminal region in human cancer cells*. *Oncogene*, 2008. **27**(19): p. 2686-92.
109. Tsuge, M., et al., *A variable number of tandem repeats polymorphism in an E2F-1 binding element in the 5' flanking region of SMYD3 is a risk factor for human cancers*. *Nat Genet*, 2005. **37**(10): p. 1104-7.
110. Wang, H., et al., *Association of the variable number of tandem repeats polymorphism in the promoter region of the SMYD3 gene with risk of esophageal*

- squamous cell carcinoma in relation to tobacco smoking.* Cancer Sci, 2008. **99**(4): p. 787-91.
111. Brown, M.A., et al., *Hsp90--from signal transduction to cell transformation.* Biochem Biophys Res Commun, 2007. **363**(2): p. 241-6.
 112. Jarosz, D.F. and S. Lindquist, *Hsp90 and environmental stress transform the adaptive value of natural genetic variation.* Science, 2010. **330**(6012): p. 1820-4.
 113. Sollars, V., et al., *Evidence for an epigenetic mechanism by which Hsp90 acts as a capacitor for morphological evolution.* Nat Genet, 2003. **33**(1): p. 70-4.
 114. Trepel, J., et al., *Targeting the dynamic HSP90 complex in cancer.* Nat Rev Cancer, 2010. **10**(8): p. 537-49.
 115. Sirinupong, N., et al., *Structural insights into the autoinhibition and posttranslational activation of histone methyltransferase Smyd3.* J Mol Biol, 2011. **406**(1): p. 149-59.
 116. Xu, S., et al., *Structural and biochemical studies of human lysine methyltransferase Smyd3 reveal the important functional roles of its post-SET and TPR domains and the regulation of its activity by DNA binding.* Nucleic Acids Res, 2011. **39**(10): p. 4438-49.
 117. Veraksa, A., J. Kennison, and W. McGinnis, *DEAF-1 function is essential for the early embryonic development of Drosophila.* Genesis, 2002. **33**(2): p. 67-76.
 118. Spadaccini, R., et al., *Structure and functional analysis of the MYND domain.* J Mol Biol, 2006. **358**(2): p. 498-508.
 119. Liu, Y., et al., *The tetramer structure of the Nervy homology two domain, NHR2, is critical for AML1/ETO's activity.* Cancer Cell, 2006. **9**(4): p. 249-60.
 120. Blatch, G.L. and M. Lassel, *The tetratricopeptide repeat: a structural motif mediating protein-protein interactions.* Bioessays, 1999. **21**(11): p. 932-9.
 121. Sanchez, E.R., *Hsp56: a novel heat shock protein associated with untransformed steroid receptor complexes.* J Biol Chem, 1990. **265**(36): p. 22067-70.
 122. Wu, B., et al., *3D structure of human FK506-binding protein 52: implications for the assembly of the glucocorticoid receptor/Hsp90/immunophilin heterocomplex.* Proc Natl Acad Sci U S A, 2004. **101**(22): p. 8348-53.
 123. Owens-Grillo, J.K., et al., *A model of protein targeting mediated by immunophilins and other proteins that bind to hsp90 via tetratricopeptide repeat domains.* J Biol Chem, 1996. **271**(23): p. 13468-75.
 124. Ratajczak, T. and A. Carrello, *Cyclophilin 40 (CyP-40), mapping of its hsp90 binding domain and evidence that FKBP52 competes with CyP-40 for hsp90 binding.* J Biol Chem, 1996. **271**(6): p. 2961-5.
 125. Jiang, Y., et al., *Structural insights into estrogen receptor alpha methylation by histone methyltransferase SMYD2, a cellular event implicated in estrogen signaling regulation.* J Mol Biol, 2014. **426**(20): p. 3413-25.
 126. Lee, B.J., et al., *Rules for nuclear localization sequence recognition by karyopherin beta 2.* Cell, 2006. **126**(3): p. 543-58.
 127. Buchner, J., *Hsp90 & Co. - a holding for folding.* Trends Biochem Sci, 1999. **24**(4): p. 136-41.
 128. Luo, X.G., et al., *Effects of SMYD3 overexpression on transformation, serum dependence, and apoptosis sensitivity in NIH3T3 cells.* IUBMB Life, 2009. **61**(6): p. 679-84.

129. Kim, H., et al., *Requirement of histone methyltransferase SMYD3 for estrogen receptor-mediated transcription*. J Biol Chem, 2009. **284**(30): p. 19867-77.
130. Cock-Rada, A.M., et al., *SMYD3 promotes cancer invasion by epigenetic upregulation of the metalloproteinase MMP-9*. Cancer Res, 2012. **72**(3): p. 810-20.
131. Patki, J.M. and S.S. Pawar, *HSP90: chaperone-me-not*. Pathol Oncol Res, 2013. **19**(4): p. 631-40.
132. Luo, X.G., et al., *SET and MYND domain-containing protein 3 decreases sensitivity to dexamethasone and stimulates cell adhesion and migration in NIH3T3 cells*. J Biosci Bioeng, 2007. **103**(5): p. 444-50.
133. National Academy of Sciences. Science, 1960. **132**(3438): p. 1488-1501.
134. Reynoird, N., et al., *Coordination of stress signals by the lysine methyltransferase SMYD2 promotes pancreatic cancer*. Genes Dev, 2016. **30**(7): p. 772-85.
135. Piao, L., et al., *The histone methyltransferase SMYD2 methylates PARP1 and promotes poly(ADP-ribosyl)ation activity in cancer cells*. Neoplasia, 2014. **16**(3): p. 257-64, 264 e2.
136. Komatsu, S., et al., *Overexpression of SMYD2 contributes to malignant outcome in gastric cancer*. Br J Cancer, 2015. **112**(2): p. 357-64.
137. Tsai, C.H., et al., *SMYD3-Mediated H2A.Z.1 Methylation Promotes Cell Cycle and Cancer Proliferation*. Cancer Res, 2016.
138. Ohtomo-Oda, R., et al., *SMYD2 overexpression is associated with tumor cell proliferation and a worse outcome in human papillomavirus-unrelated nonmultiple head and neck carcinomas*. Hum Pathol, 2016. **49**: p. 145-55.
139. Sakamoto, L.H., et al., *SMYD2 is highly expressed in pediatric acute lymphoblastic leukemia and constitutes a bad prognostic factor*. Leuk Res, 2014. **38**(4): p. 496-502.
140. Xu, G., et al., *The histone methyltransferase Smyd2 is a negative regulator of macrophage activation by suppressing interleukin 6 (IL-6) and tumor necrosis factor alpha (TNF-alpha) production*. J Biol Chem, 2015. **290**(9): p. 5414-23.
141. Fan, J.D., et al., *The selective activation of p53 target genes regulated by SMYD2 in BIX-01294 induced autophagy-related cell death*. PLoS One, 2015. **10**(1): p. e0116782.
142. Bigas, A. and C. Waskow, *Blood stem cells: from beginning to end*. Development, 2016. **143**(19): p. 3429-3433.
143. MacLean, A.L., C. Lo Celso, and M.P. Stumpf, *Stem Cell Population Biology: Insights from Haematopoiesis*. Stem Cells, 2016.
144. Manz, M.G., et al., *Dendritic cell potentials of early lymphoid and myeloid progenitors*. Blood, 2001. **97**: p. 3333-3341.
145. Heath, W.R. and F.R. Carbone, *Cross-presentation, dendritic cells, tolerance and immunity*. Annu. Rev. Immunol., 2001. **19**: p. 47-64.
146. Steinman, R.M., *The dendritic cell system and its role in immunogenicity*. Annu. Rev. Immunol., 1991. **9**: p. 271-296.
147. Izon, D., *A common pathway for dendritic cell and early B cell development*. J. Immunol., 2001. **167**: p. 1387-1392.
148. Liu, Y.J., et al., *Dendritic cell lineage, plasticity and cross-regulation*. Nature Immunol., 2001. **2**: p. 585-589.

149. Li, Y., et al., *Decreased level of recent thymic emigrants in CD4+ and CD8+T cells from CML patients*. J Transl Med, 2010. **8**: p. 47.
150. Li, Y., et al., *Restricted TRBV repertoire in CD4+ and CD8+ T-cell subsets from CML patients*. Hematology, 2011. **16**(1): p. 43-9.
151. Jongstra, J. and V. Misener, *Developmental maturation of the B-cell antigen receptor*. Immunol Rev, 1993. **132**: p. 107-23.
152. Schwartz, R.S. and B.D. Stollar, *Heavy-chain directed B-cell maturation: continuous clonal selection beginning at the pre-B cell stage*. Immunol Today, 1994. **15**(1): p. 27-32.
153. Milstein, C. and M.S. Neuberger, *Maturation of the immune response*. Adv Protein Chem, 1996. **49**: p. 451-85.
154. Hardy, R.R., et al., *B-cell commitment, development and selection*. Immunol Rev, 2000. **175**: p. 23-32.
155. Wagner, S.D. and M.S. Neuberger, *Somatic hypermutation of immunoglobulin genes*. Annu Rev Immunol, 1996. **14**: p. 441-57.
156. Voelkel, T., et al., *Lysine methyltransferase Smyd2 regulates Hsp90-mediated protection of the sarcomeric titin springs and cardiac function*. Biochim Biophys Acta, 2013. **1833**(4): p. 812-22.
157. Hamamoto, R., et al., *SMYD2-dependent HSP90 methylation promotes cancer cell proliferation by regulating the chaperone complex formation*. Cancer Lett, 2014. **351**(1): p. 126-33.

LIST OF ABBREVIATIONS

ABBREVIATION	MEANING	PAGE
AGM	Aorta, gonad, mesonephros	9
ALL	Acute lymphoblastic leukemia	11
BLP	B cell lineage progenitor	20
CD	Cluster of differentiation	20
CD4+ CD69-	(referring to cell markers on T cells)	20
CD4+ CD69+	(referring to cell markers on T cells)	20
CD8+ CD69-	(referring to cell markers on T cells)	20
CD8+ CD69+	(referring to cell markers on T cells)	20
cKO	Conditional knockout	14
CLP	Common lymphoid progenitor	12
CML	Chronic myeloid leukemia	12
CMP	Common myeloid progenitor	12
DN1	Double negative 1 (referring to T cells)	20
DN3	Double negative 3 (referring to T cells)	20
DN4	Double negative 4 (referring to T cells)	20
DP CD69-	Double positive (referring to T cells)	20
DP CD69+	Double positive (referring to T cells)	20
EP	Erythroid progenitor	20
Ery	Erythrocyte	20
Flt3	<i>fms-like</i> tyrosine kinase 3	10
Fo B	Follicular B cell	20
gGMP	Pre granulocyte/macrophage progenitor	20
GMLP	Granulocyte/macrophage-lymphoid progenitor	10
GMP	Granulocyte/macrophage progenitor	20
GRAN	Granulocytes	20
H(x)-K(x)	Histone(x)-Lysine(x)	3
HAT	Histone acetyltransferase	9
HDAC	Histone deacetyltransferase	2
HKMT	Histone lysine methyltransferase	2
HMTases	Histone methyltransferases	40
HSC	Hematopoietic stem cell	9
IFN	Interferon	78
IL-3	Interleukin 3	10
IL-7	Interleukin 7	10
Imm B	Immature B cell	20
iNK	Natural Killer	20
LMPP	Lymphoid primed multipotent progenitor	10

ABBREVIATION	MEANING	PAGE
LSD1	Lysine demethylase	3
MACRO	Macrophage	20
Mat B	Mature B cell	20
Me 1/2/3	Mono/di/tri methylation	3
Megak	Megakaryocyte	20
MEP	Megakaryocyte/erythroid progenitor	10
MKP	Megakaryocyte progenitor	20
MLL	Mixed lineage leukemia	66
mNK	Natural Killer	20
MONO	Monocytes	20
MP	Monocyte progenitor	20
MPP	Multipotent progenitor	10
MT	Methyltransferase	3
MYND	Myeloid-Nervy-DEAF1	4
Mz B	Marginal zone B cell	20
New B	Immature B cell	20
pCFU	Pre colony forming units	20
PCR	Polymerase chain reaction	24
pDC	Plasmacytoid dendritic cell	77
Plt	Platelets	20
pMEP	Pre megakaryocyte/erythroid progenitor	20
Pre-B	Pre B cell	10
Pre-B-ALL	Pre B cell acute lymphoblastic leukemia	11
Pre-pro B	Pre progenitor B cell	11
Pro-B	Progenitor B cell	19
RB1	Retinoblastoma	6
RBC	Red blood cells	9
SAM	S-adenylsilmethionine	4
sCMP	Common myeloid progenitor	11
SET	Suppressor of variegation, enhancer of zeste and trithorax	4
skNAC	Skeletal nascent polypeptide-associated complex alpha	5
SMYD	SET and MYND domain containing protein	4
T1 B	Transitional B cell 1	20
T2 B	Transitional B cell 2	20
TPR	Tetratricopeptide repeat	8
VDJ	Variable, diversity, and joining genes	79